

Structural and functional analysis of the GTPase
Activating Protein of the small guanine nucleotide
binding protein Rap1

Inaugural-Dissertation
zur
Erlangung des Doktorgrades
der Mathematisch-Naturwissenschaftlichen Fakultät
der Universität zu Köln

Vorgelegt von
Dipl. Biol.
Oliver Daumke
aus Freiburg

Köln 2004

Die vorliegende Arbeit wurde im Zeitraum Februar 2001 bis März 2004 in der Abteilung I - Strukturelle Biologie - am Max-Planck-Institut für molekulare Physiologie in Dortmund unter der Anleitung von Prof. Dr. Alfred Wittinghofer angefertigt.

1. Berichterstatter: Prof. Dr. Helmut W. Klein
2. Berichterstatter: Prof. Dr. Jonathan C. Howard
3. Berichterstatter: Prof. Dr. Alfred Wittinghofer

Mündliche Prüfung: 18. Mai 2004

Index

1	Abstract	1
2	Introduction	2
2.1	Guanine nucleotide binding proteins	2
2.1.1	The molecular switch	2
2.1.2	Overview of the GTPase superclass	3
2.1.3	Biochemical and structural features of small GNBPs	5
2.1.4	The hydrolysis reaction	8
2.1.5	The Ras signal transduction pathway	9
2.1.6	The Rap GNBPs	10
2.2	GTPase Activating Proteins	12
2.2.1	RasGAP and the arginine finger	13
2.2.2	RhoGAPs	14
2.2.3	G α proteins and regulators of G protein signalling	15
2.2.4	Other GAPs with an arginine finger	16
2.2.5	ArfGAP	18
2.2.6	RanGAP – catalysis without an arginine finger	19
2.2.7	The signal recognition particle and its receptor	20
2.3	GTPase activating proteins of the Rap1GAP family	22
2.3.1	Rap1GAP	22
2.3.2	Signal-induced proliferation-associated protein 1 (Spa-1)	23
2.3.3	E6TP-1	24
2.3.4	Tuberin	24
2.3.5	Biochemistry of the Rap1-Rap1GAP system	25
2.4	Objectives of this work	26
3	Materials and Methods	27
3.1	Materials	27
3.1.1	Chemicals	27
3.1.2	Enzymes	27
3.1.3	Kits	27
3.1.4	Microorganisms	27
3.1.5	Media and antibiotics	28
3.1.6	Buffers	28
3.2	Molecular biology methods	29
3.2.1	Agarose gels	29
3.2.2	Isolation of plasmid DNA	29
3.2.3	Polymerase chain reaction (PCR)	29
3.2.4	DNA digestion	29

3.2.5	Ligation	29
3.2.6	Competent cells	29
3.2.7	Transformation	30
3.2.8	Bacteria storage	30
3.2.9	Site specific mutagenesis	30
3.2.10	DNA sequencing	30
3.2.11	Constructs	31
3.2.12	Point mutants	31
3.3	Biochemical methods	32
3.3.1	Sequence alignment	32
3.3.2	SDS-PAGE	32
3.3.3	Determination of protein concentration	32
3.3.4	Matrix assisted laser desorption ionisation (MALDI)	32
3.3.5	Test expression	32
3.3.6	Protein overexpression and preparation of soluble bacteria extract	33
3.3.7	Rap1GAP purification	33
3.3.8	Purification of other GST fusion proteins	34
3.3.9	Assignment of degradation bands	34
3.3.10	Partial digest	35
3.3.11	Purification of Rap1B C'	35
3.3.12	Rap1-Aedans preparation	36
3.3.13	Nucleotide exchange	36
3.3.14	Nucleotide detection using reversed-phase HPLC	36
3.3.15	Radioactive charcoal assay	37
3.3.16	Fast kinetics using stopped-flow measurement	38
3.3.17	CD spectrometry	39
3.4	Crystallographic methods	40
3.4.1	Crystallisation	40
3.4.2	Data collection and processing	41
3.4.3	Phase determination	42
3.4.4	Refinement	44
3.4.5	Figure preparation	46
4	Results	47
4.1	Initial characterisation of Rap1GAP	47
4.1.1	Expression	47
4.1.2	Biochemical characterisation of Rap1GAP	47
4.1.3	Arginine mutants	49
4.1.4	Lysine and glutamine mutants	50
4.2	The Rap1GAP structure	53
4.2.1	Purification	53
4.2.2	Degradation and partial digest	53
4.2.3	High throughput cloning	54
4.2.4	Crystallisation	55
4.2.5	Structure determination	57
4.2.6	Topology	60

4.2.7	Description of the dimer.....	63
4.2.8	The catalytic centre	65
4.3	The hydrolysis mechanism of Rap1GAP	69
4.3.1	Dimerisation and Rap1GAP function.....	69
4.3.2	Involvement of both domains in the GAP mechanism	70
4.3.3	Role of helix stabilisation for Rap1GAP function.....	72
4.3.4	The catalytic residue.....	73
4.3.5	Binding to a transition state analogue of GTP hydrolysis.....	76
4.3.6	Other important residues in Rap1GAP	77
4.3.7	Role of the carboxamide for GAP activity.....	78
4.3.8	Implications for Tuberous sclerosis	80
5	Discussion.....	83
5.1	Dimerisation and role of two domains in Rap1GAP	83
5.2	Interacting partners of Rap1GAP	85
5.3	The novel GAP mechanism.....	88
5.4	Proposed model of the Rap1GAP-Rap1 complex	90
5.5	Implications for Tuberous Sclerosis and cancer	93
5.6	Evolution of the Rap1GAP system	95
6	References	97
7	Appendix	111
7.1	Abbreviations.....	111
7.2	Deduction of equations.....	113
7.2.1	Determination of k_{on} and k_{off} via k_{obs}	113
7.2.2	Fluorescence titration	115
8	Zusammenfassung	117
	Danksagung.....	119
	Teilpublikationen dieser Arbeit.....	121
	Erklärung	122
	Lebenslauf	123

1 Abstract

Rap1GAP is the founding member of a family of GTPase activating proteins (GAPs) for the small guanine nucleotide binding protein (GNBP) Rap1, which show no sequence homology to GAPs of other small GNBP. Rap1 does not have a catalytic glutamine residue which is essential for the intrinsic and GAP mediated GTP hydrolysis of all other small GNBP. In this thesis, the structure and the mechanism of GAP catalysed GTP hydrolysis are examined.

Most GAPs provide a catalytic arginine residue to the GNBP to complement the incomplete catalytic machinery. However, site-directed mutagenesis revealed that Rap1GAP does not employ a catalytic arginine. To understand the novel reaction mechanism, the structure of Rap1GAP was determined by X-ray crystallography to a maximal resolution of 2,9 Å. Initial phases were obtained by selenomethionine substituted crystals and a SIRAS phasing protocol. The structure was built and refined to an $R_{\text{cryst}} = 23,4\%$ and an R_{free} of 27,6%.

Two Rap1GAP dimers were observed in the asymmetric unit, consistent with gel filtration experiments in which also dimerisation was observed. A Rap1GAP monomer consists of two domains. Both domains show a mixed α - β fold and were named dimerisation and catalytic domain, respectively. Surprisingly, the catalytic domain has structural similarity to the G domain of GNBP itself suggesting a common evolutionary origin. No structural similarity to any other GAP was observed. By site-directed mutagenesis, it was shown that dimerisation is not required for GAP function. However, both domains are necessary for full catalytic activity. Mutations around a highly invariant helix, the putative interaction helix, dramatically reduced GAP activity. Using a single-turnover fluorescence reporter assay it could be conclusively proven that Rap1GAP employs a catalytic asparagine from the interaction helix to stimulate GTP hydrolysis in Rap1. In the absence of this asparagine side-chain Rap1GAP was completely inactive but could still bind to Rap1•GTP. In contrast to the wild-type, the Rap1GAP^{N290A} mutant can not associate with a transition state mimic of Rap1 GTP hydrolysis. Thus, Rap1GAP is the first example of a GAP which provides a catalytic asparagine for catalysis. Based on the analysis of various mutants, a model for the interaction of Rap1GAP with Rap1 is proposed.

The results of this thesis have implications for the disease Tuberous sclerosis. Loss of function mutations in the Rap1GAP homologue Tuberin are associated with this disease and can be rationalised in the view of this work.

2 Introduction

2.1 Guanine nucleotide binding proteins

2.1.1 The molecular switch

Guanine nucleotide binding proteins (GNBPs) are involved in a wide range of cellular processes including protein synthesis, sensual perception, vesicular transport and signal transduction cascades leading to cell proliferation and cell differentiation. Most GNBPs regulate these processes rather than provide energy for mechano-chemical work or chemical synthesis. Typically, GNBPs exist in an active GTP bound conformation and in an inactive GDP bound state (Bourne et al., 1990), therefore acting as a molecular switch (Figure 1). The GTP bound state has high affinity for interacting proteins which are referred to as effector molecules whereas the GDP bound state has low affinity and poorly interacts. In turn, the effectors are relocalised to their specific subcellular sites by this interaction or their activity is modulated.

To reach the active state, GDP has to be released and a new GTP molecule has to be bound. Since this reaction is intrinsically too slow to regulate cellular processes it can be accelerated by the action of guanine nucleotide exchange factors (GEFs). GEFs catalyse nucleotide dissociation and allow GTP which is more abundant in the cell to bind. Also the intrinsic GTPase reaction of GNBPs is slow. For efficient inactivation, the intrinsic reaction can be drastically stimulated by the action of GTPase activating proteins (GAPs).

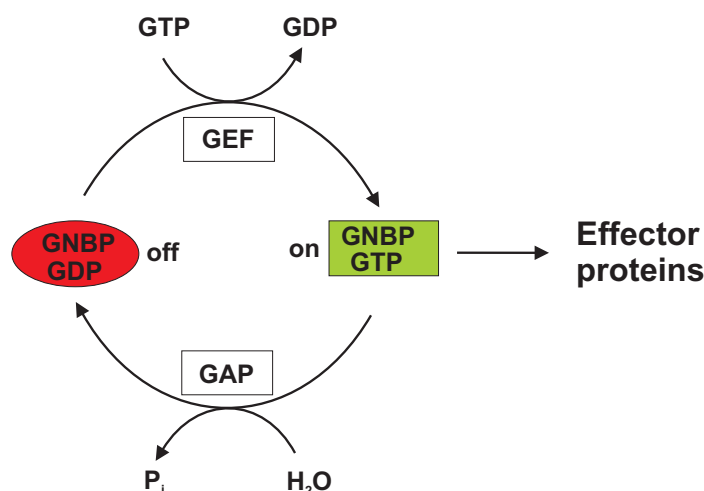


Figure 1. The molecular switch of guanine nucleotide binding proteins. For explanation see text.

2.1.2 Overview of the GTPase superclass

Nucleotide binding proteins appear in a number of different folds (Vetter and Wittinghofer, 1999) including the di-nucleotide binding (Rossmann) fold, the protein and histidine kinase fold and the mono-nucleotide binding fold (P-loop containing nucleotide triphosphate (NTP) hydrolases). P-loop containing NTP hydrolases share the most abundant protein fold in most organisms and comprise 10 to 18% of all gene products (Koonin et al., 2000). This family can be divided in at least seven further lineages one of which is the GTPase superclass (Leipe et al., 2002).

The GTPase superclass was recently classified anew based on sequence and structure alignments of all available bacterial and eukaryotic GNBPs (Leipe et al., 2002). Two major branches could be identified which were named the TRAFAC (translation factor-related) and the SIMBI class (signal recognition particle, MinD and BioD). The best known members of the SIMBI class are the signal recognition particle GTPase (Ffh in bacteria) and the α -subunit of the signal recognition particle receptor (FtsY in bacteria) (Freyman et al., 1997). They exist in bacteria and eukaryotes and are involved in co-translational cellular targeting of nascent secretory and membrane proteins. The TRAFAC class contains most notably the translation factor superfamily, the Myosin-kinesin and the Ras-like superfamily.

Initiation factors IF2 (eIF5B in eukaryotes), eIF2 γ (in some bacteria SelB) and elongation factors EF-Tu and EF-G are the four members of the translation factor superfamily that appear ubiquitously in bacteria and eukaryotes (Leipe et al., 2002). eIF2 γ forms a ternary complex with GTP and Met-tRNA_i^{Met} and mediates with other initiation factors the binding of tRNA_i^{Met} to the ribosome (reviewed in Sonenberg and Dever, 2003). GTP hydrolysis in eIF2 γ is triggered in a reaction which requires among others initiation factor IF2/eIF5B. EF-Tu is a three-domain protein that forms a ternary complex with aminoacyl-tRNA and controls incorporation of the correct amino acids into the peptide chain (reviewed in Ogle et al., 2003). The five-domain protein EF-G catalyses translocation of tRNAs on the ribosome. The origin of other factors involved in protein biosynthesis, e.g. the release factors, differs in the three kingdoms of life (Leipe et al., 2002).

The eukaryotic cellular motor ATPases kinesin and myosin were grouped in the myosin-kinesin superfamily of TRAFAC GTPases. It has been argued that these proteins have evolved from an ancestral GTPase at the onset of eukaryotic evolution and have lost later their specificity towards GTP (Leipe et al., 2002). Members of the

dynamain family which are involved in the budding of clathrin-coated vesicles (Urrutia et al., 1997), and the GB1 family including GBPs (Prakash et al., 2000), are also grouped in this superfamily.

Heterotrimeric G-proteins appear exclusively in eukaryotes and more than 20 members are known (Sprang, 1997). They are activated by cell-surface receptors of the seven-transmembrane-helix class and regulate intracellular effectors such as adenylyl-cyclase or phospholipase C β .

Members of the Ras superfamily exist predominantly in eukaryotes. The exact classification of this superfamily varies (Bourne et al., 1990; Garcia-Ranea and Valencia, 1998; Leipe et al., 2002). The group of 20-25 kD GNBPs with Ras as most prominent member was called the small GNBPs. They were first grouped as a separate superfamily composed of the Ras, Rab, Rho, Ran and Arf/Sar1 family (Garcia-Ranea and Valencia, 1998), albeit it was recently suggested that the family of hetero-trimeric GNBPs should also be included in this superfamily (Leipe et al., 2002). More than 100 small GNBPs have been identified in eukaryotes (reviewed in Takai et al., 2001). Ras family members mainly regulate gene expression, whereas GNBPs of the Rho/Rac family control gene expression and cytoskeletal reorganisation. Members of the Ran family regulate nucleo-cytoplasmic transport during G₁, S, G₂ and among others microtubule organisation during M phase. Rab and Arf GNBPs control intracellular vesicle trafficking. A dendrogram showing the evolutionary relation between the small GNBPs is depicted in Figure 2.

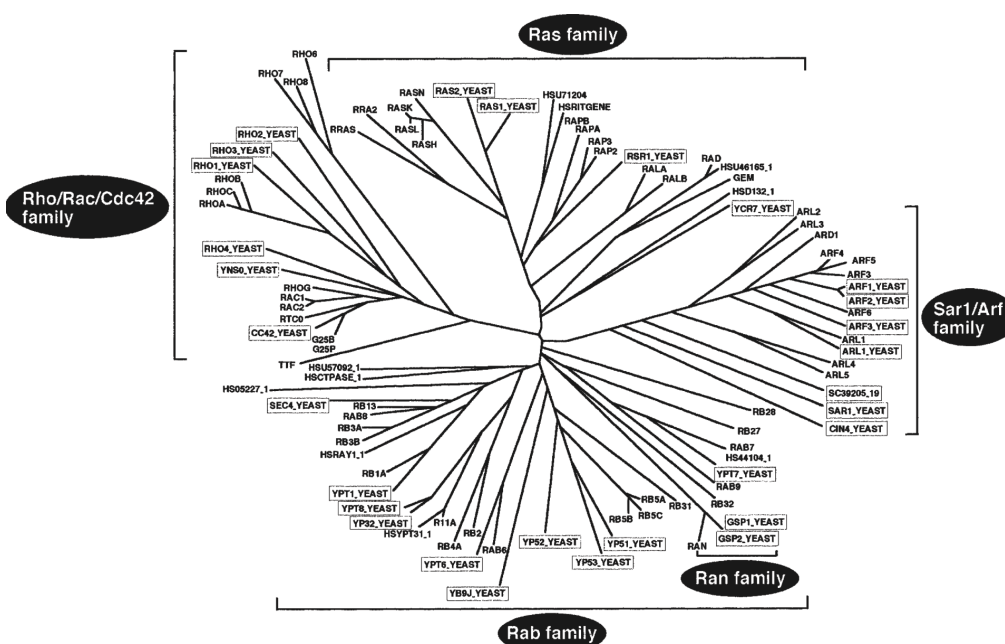


Figure 2. Dendrogram of the family of small GNBPs (from Takai et al., 2001)

2.1.3 Biochemical and structural features of small GNBPs

Ras consists of 189 amino acids and is the best characterised small GNPB (Wittinghofer and Waldmann, 2000). It is considered a paradigm for the complete family and its biochemical features are often representative for the other small GNBPs as well.

Ras is located in the plasma membrane by means of a farnesyl and a palmitoyl anchor which is required for its function *in vivo*. As most other small GNBPs, it has an extremely high affinity for both GDP and GTP with a K_D in the picomolar range (Wittinghofer and Waldmann, 2000). No other standard nucleotide binds to Ras with a comparable affinity showing the high specificity for guanine nucleotides. The β -phosphate is required for high affinity binding since guanosin monophosphate (GMP) has a 10^6 -fold reduced affinity in comparison to GDP/GTP. The binding affinity strongly depends on the presence of magnesium ions. When magnesium ions are absent, the dissociation rate constant (k_{off}) increases by many hundredfold with a concomitant increase in the equilibrium dissociation constant (K_D) (John et al., 1988). Available crystal structures demonstrate that Ras shares a common structural core - the G domain fold - with the complete class of TRAFAC GTPases (Leipe et al., 2002; Sprang, 1997). The G domain fold comprises approximately 200 residues and consists of a six stranded mixed β -sheet surrounded by five α -helices (Figure 3). The most highly conserved elements in this domain are the five polypeptide loops that form the guanine nucleotide-binding site called G1 through G5 (Figure 3, Bourne et al., 1991).

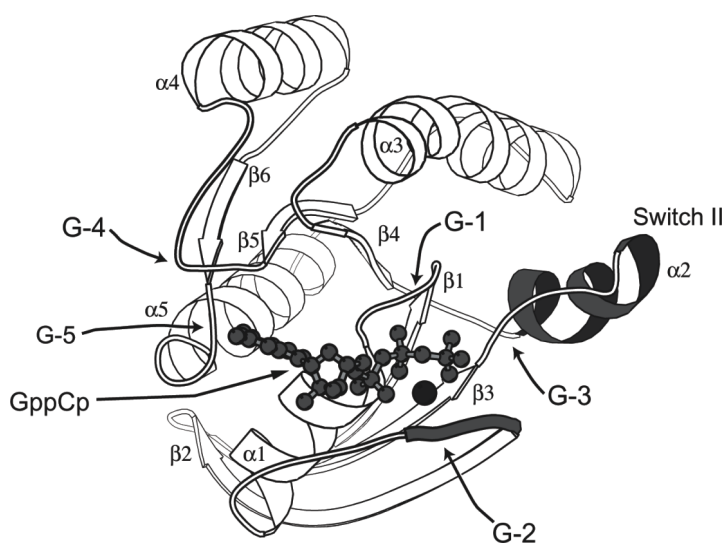


Figure 3. Structure of the Ras protein in the GppCp·Mg bound form with the conserved elements and G-box regions labelled (from Sprang, 1997).

Two elements in GNBPs have been shown to undergo major conformational changes upon GTP hydrolysis, the switch I and switch II region (reviewed in Vetter and Wittinghofer, 2001). Conformational changes in switch I (amino acids 32-40 in Ras) are mediated mainly by the conserved threonine T35 of motif G2, conformational changes in switch II (amino acids 61-67 in Ras) by the conserved glycine G60 of motif G3. Due to the interaction of these residues with the γ -phosphate, the switches become stabilised in the GTP bound form. In contrast, the switches are rather mobile in the GDP bound form (Figure 5).

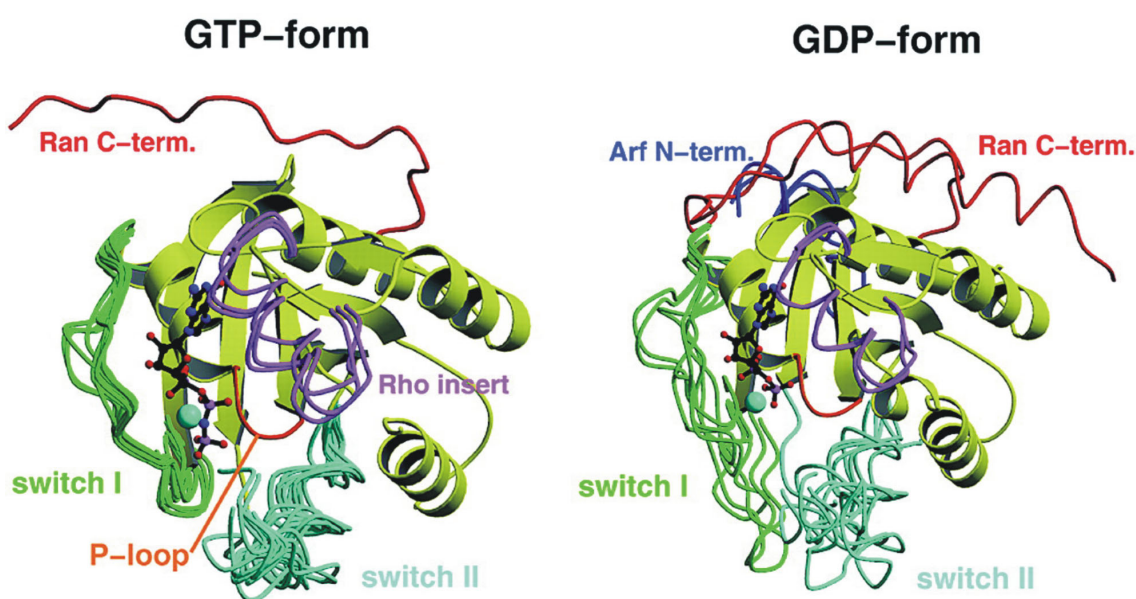


Figure 5. Superposition of selected Ras-related proteins in the GDP and the GTP bound form. Whereas in the GTP bound form, all switches are stabilised in a similar conformation, they are much more flexible in the GDP bound form and show divergent conformations. Extra elements in the structures of Rho, Arf and Ran are highlighted (from Vetter and Wittinghofer, 2001).

The switches are the main determinants for binding of effector molecules. In the case of Ras, switch I was shown to bind to an 80 residues Ras Binding Domain (RBD) of effectors (Nassar et al., 1995; Huang et al., 1998; Vetter et al., 1999; Pacold et al., 2000). Although there is no sequence homology among the RBDs of different effectors, all examined RBDs show a ubiquitin-like fold. The RBD and Ras•GTP interact via an interprotein β -sheet. Besides some main chain interactions, most contacts are mediated by hydrophilic side chains. RBDs from different proteins, however, use different residues for interaction (Joneson et al., 1996).

2.1.4 The hydrolysis reaction

The intrinsic GTPase reaction of small GNBPs is slow, for Ras in the range of $0,02 \text{ min}^{-1}$, and is strictly dependent on the presence of divalent cations (Wittinghofer and Waldmann, 2000). A water molecule close to the γ -phosphate and in hydrogen bond distance to glutamine Q61 is considered to be the attacking nucleophile, and mutations of this glutamine to most other amino acids dramatically reduce the intrinsic GTP hydrolysis (Der et al., 1986; Krenzel et al., 1990; Prive et al., 1992). Based on NMR studies with various Ras mutants and by determining intrinsic GTP hydrolysis reaction rates at various pH, a substrate assisted catalysis was proposed in which the γ -phosphate itself activates the attacking water molecule by abstracting a hydrogen atom (Schweins et al., 1995; Schweins et al., 1997). Both the less charged γ -phosphate and the more reactive nucleophile (the hydroxide ion) were suggested to promote catalysis. The role of glutamine Q61 is thought to be the positioning of the attacking water molecule in vicinity of the γ -phosphate.

A continuum of possible transition states of the GTP hydrolysis reaction ranging from purely dissociative to purely associative can be described (Figure 6) (Maegley et al., 1996). The dissociative transition state is dominated by bond cleavage, so that the bond to the leaving group is fully broken and the bond to the incoming nucleophile is barely formed. To maintain charge, this leads to a loss of negative charge on the terminal phosphoryl group during the transition (Figure 6) and to an increase in charge at the β -phosphate, especially at the β - γ bridging oxygen. On the other hand in the associative transition state, there is a large amount of bond formation to the incoming nucleophile but only a small amount of bond cleavage to the leaving group. To maintain charge, this will result in an increase in negative charge on the terminal phosphoryl group (Admiraal and Herschlag, 1995).

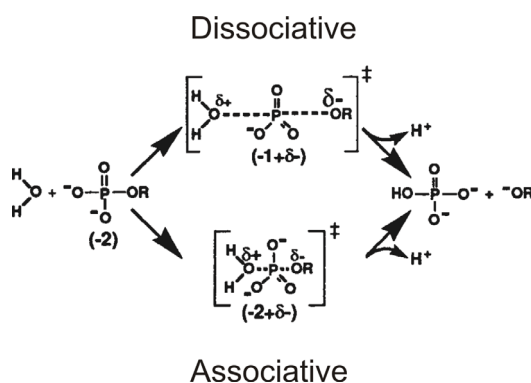


Figure 6. Associative versus dissociative mechanism (from Maegley et al., 1996). For explanation see text.

In solution, GTP hydrolysis seems to proceed via a dissociative transition state (Admiraal and Herschlag, 1995). It is however controversially discussed whether in the protein environment the transition state has a dissociative or associative character (Maegley et al., 1996; Cepus et al., 1998; Allin and Gerwert, 2001; Schweins et al., 1995; Scheffzek et al., 1997; Glennon et al., 2000; Seewald et al., 2002).

2.1.5 The Ras signal transduction pathway

The *Ras* gene was originally identified as the active principle of sarcoma viruses and was called an oncogene (reviewed in Takai et al., 2001). Later, it was realised that cellular counterparts exist in mammals.

In humans, three isoforms of Ras exist, H-Ras, N-Ras and K-Ras with a molecular weight of 21 kD which differ mainly at the C-terminus. From studies in *Drosophila* and *C. elegans* Ras was recognised as a central component in signal transduction pathways linking activation of cell surface receptors to gene expression in the nucleus (reviewed in Pawson and Saxton, 1999; Wittinghofer and Waldmann, 2000). Growth factors such as EGF or PDGF bind to the extracellular domain of specific receptor tyrosine kinases. This leads to receptor dimerisation and subsequent transphosphorylation of tyrosine residues in the cytoplasmic part of the receptor. Phosphorylated tyrosines in a sequence specific context are recognised by proteins possessing specialised phospho-tyrosine binding domains, e.g. *SH2* (*src* homology 2) domains. In this way, the adapter protein Grb2 binds via its SH2 domain to phosphorylated growth factor receptor. SOS, an exchange factor for Ras and associated with Grb2, is thereby recruited to the membrane where it promotes GDP-GTP exchange on Ras. Ras in the GTP bound form activates several effectors of which the best characterised is the protein kinase Raf. Raf phosphorylates the protein kinase MEK which activates the protein kinase ERK. Finally, ERK phosphorylates a class of transcription factors, the ternary complex factors, which associate with a second class of transcription factors, the serum response factors. The resulting protein complex initiates transcription by binding to a conserved promoter element, the serum response element which is present in a variety of genes, e.g. many transcription factors. The Ras signal is terminated by the action of GAPs targeted to the intracellular part of the receptor and by dissociation of the SOS-Grb complex upon phosphorylation by ERK.

Ras acts also in different pathways. It is activated by G-protein coupled receptors and cytoplasmic tyrosine kinases (Weiss and Littman, 1994), and it also triggers different pathways, e.g. by activating PI-3-Kinase or the nucleotide exchange factor for the small GNBPs Ral, RalGEF.

Point mutations of Ras at either position 12, 13 or 61 render the protein unable to hydrolyse GTP, even in the presence of GAP (Trahey and McCormick, 1987; Downward, 1998) thus leading to constitutively active Ras. These mutations were found in human tumours (e.g. Almoguera et al., 1988) indicating that a constitutive active Ras pathway leads to malignant transformation. It is now estimated that 30% of all human tumours carry activated forms of the *Ras* gene. Thus, the Ras pathway is an important target for cancer therapy (Wittinghofer and Waldmann, 2000).

2.1.6 The Rap GNBPs

Rap1 was identified by low stringency hybridisation of various cDNA libraries with *Ras* cDNA (Pizon et al., 1988) and, at the same time as *K-rev1* in a screen for cDNAs which revert the phenotype of *K-Ras* transformed fibroblast (Kitayama et al., 1989). With more than 50% sequence identity, Rap1 is the closest relative of Ras, especially Switch I is highly conserved. Unlike Ras, it is modified by a geranyl-geranyl anchor rather than a farnesyl anchor.

Rap1 homologues are found in all vertebrates, in *Drosophila* and in yeast (reviewed in Bos et al., 2001). The yeast homologue Bud1 is involved in selecting the new budding site by recruiting and activating effectors to the selected region in the cell (Park et al., 2002). In *Drosophila*, maternal and zygotic *Rap1* expression is essential for development of the embryo, imaginal disc development and oogenesis (Asha et al., 1999). *Drosophila* Rap1 was shown to be enriched at adherens junctions, particularly between newly divided sister cells, and to regulate the position of these junctions thereby regulating cell adhesion (Knox and Brown, 2002).

Four isoforms of *Rap* exist in humans, namely Rap1a, Rap1b, Rap2a and Rap2b. Most work has been done on Rap1a and Rap1b, which share more than 90% sequence identity, and in most experimental approaches, no discrimination between Rap1a and Rap1b (from here Rap1) has been made (Bos et al., 2001).

Rap1 in human was shown to be ubiquitously expressed. In fibroblast, it is located in the mid-Golgi compartment and early and late endosomes (Beranger et al., 1991; Pizon et al., 1994). However, in platelets and neutrophils, it translocates from

granules to the plasma membrane upon GTP loading caused by a variety of different stimuli (Franke et al., 1997). In malignant oral keratinocytes, it was recently demonstrated to translocate from a perinuclear distribution to the nucleus upon GTP loading. Rap1 is thus, besides Ran, the only other small GNBPs which is present in the nucleus (Mitra et al., 2003). By fluorescent resonance energy transfer studies it was established that activation of Rap1 in COS cells takes place at internal perinuclear membranes rather than at the plasma membrane (Mochizuki et al., 2001).

Based on the striking similarity of the Ras and Rap1 switch I region, Rap1 interaction with Ras effectors was analysed (e.g. Nassar et al., 1996). All Ras effectors examined are able to interact with the GTP bound form of Rap1 as well. However, this interaction does not activate all the effectors, as shown for the Raf-Kinase isoform, Raf-1 (Shirouzu et al., 1998). In line with the suppression of K-Ras action in fibroblasts and the recent finding that Rap1•GTP can inhibit cell proliferation in keratinocytes (Mitra et al., 2003), this suggested initially that Rap1 has an antagonistic role in Ras signalling by sequestering mutual effectors in an inactive state.

However, many lines of evidence suggest now that Rap1 is also able to activate signal transduction pathways independently of Ras. When micro-injected into *Swiss3T3* fibroblasts, Rap1 is able to induce DNA synthesis and morphological changes (Altschuler and Ribeiro-Neto, 1998). In fibroblasts, Rap1 activation fails to interfere with Ras-dependent ERK activation (Zwartkuis et al., 1998). In *PC12* cells, the Raf-isoform B-Raf is activated by Rap1•GTP and activates ERK, independently of Ras action (Vossler et al., 1997; Kao et al., 2001). B-Raf and likewise Ral-GEF activity are also stimulated in vitro by Rap1•GTP (Ohtsuka et al., 1996).

The best characterised role of Rap1, however, is the activation of integrin mediated cell-adhesion referred to as inside-out signalling (Katagiri et al., 2000; Reedquist et al., 2000; Sebzda et al., 2002; de Bruyn et al., 2002). A new Rap1 effector molecule, RAPL, was identified which mediates this effect by linking Rap1 to the integrin LFA-1 (Katagiri et al., 2002). This relocalisation is accompanied by an increase in integrin-mediated cell adhesion.

Furthermore, Rap1 was shown to be involved in the process of learning and memory (Morozov et al., 2003), in the development of leukaemia (Ishida et al., 2003), in angiogenesis and cerebrovascular diseases (Sahoo et al., 1999).

Activation of Rap1 can be observed upon a wide variety of stimuli, e.g. activation of tyrosine kinases, hetero-trimeric G-protein-coupled receptors and cell-adhesion molecules (McLeod et al., 1998; Posern et al., 1998; M'Rabet et al., 1998; York et al., 1998; Zwartkruis et al., 1998). Common second messengers such as cyclic AMP, Ca^{2+} and diacylglycerol (DAG) are involved in transducing extracellular signals to Rap1 (Bos et al., 2001). This activation is mediated by a variety of Rap1 specific GEFs. C3G was the first RapGEF to be identified (Gotoh et al., 1995). Analogous to the *Ras* exchange factor SOS, it is recruited to the membrane by an SH2 containing adapter protein Crk and allows consequently GDP-GTP exchange of membrane bound Rap1 (Okada et al., 1998). Another class of GEFs are the recently identified Epacs which are directly activated by cyclic AMP (de Rooij et al., 1998; Kawasaki et al., 1998a). CalDAG-GEFs can be activated by Ca^{2+} influx or by diacylglycerol (Kawasaki et al., 1998b). A fourth group of RapGEFs are the PDZ-GEFs which may be responsible for signal amplification (de Rooij et al., 1999). It was suggested that PDZ-GEFs are recruited by Rap1•GTP via their RBDs to the membrane and catalyse further GDP-GTP exchange in Rap1 (Gao et al., 2001b). The Rap1 signal is terminated by GTP hydrolysis in Rap1 which can be stimulated by the action of GTPase activating proteins (see below).

2.2 GTPase Activating Proteins

The intrinsic GTPase reaction of most GNBPs is too slow to regulate signal transduction processes in a meaningful time frame (reviewed in Vetter and Wittinghofer, 2001). Thus, GTP hydrolysis can be accelerated by GTPase Activating Proteins (GAPs) which typically down-regulate GNBPs in the range of a few seconds (Scheffzek et al., 1998). The slow intrinsic GTPase activity of EF-Tu is for example dramatically stimulated by the mRNA charged 70S ribosome (reviewed in Ogle et al., 2003). GTP hydrolysis in $G\alpha$ proteins can be stimulated by a family of proteins called regulators of G protein signalling (RGS) (Tesmer et al., 1997). Furthermore, GAPs specific for the Ras, Rho, Rab, Ran and Arf family members were discovered. GAPs for one family of small GNBPs show generally, albeit not always, sequence homology to each other. However, GAPs of different families share no sequence homology. Many GAPs have a modular architecture to fulfil various other functions in the cell.

2.2.1 RasGAP and the arginine finger

RasGAP was discovered when it was found that Ras•GTP microinjected in cells was rapidly converted into Ras•GDP (Trahey and McCormick, 1987). The protein responsible for this activity was identified and is now known as p120GAP. A fragment comprising 334 amino acids (GAP-334) was shown to be sufficient for catalysis. The structure of GAP-334 showed a helical, elongated protein with a central domain of 218 amino acids that is conserved among all RasGAPs (Scheffzek et al., 1996). Later, the structure of a complex of RasGAP and Ras•GDP was solved (Scheffzek et al., 1997) in the presence of aluminium fluoride which along with GDP/ADP is a mimic of the transition state of many phosphoryl transferring enzymes (Figure 7, Chabre, 1990).

GAP-334 interacts predominantly with the switch regions and the P-loop of Ras. An exposed loop of RasGAP containing the highly conserved arginine R789 complements the catalytic site of Ras, and the guanidium group of arginine R789 interacts with the β -phosphate and with AlF_3 (Figure 8). Additionally, the main-chain carbonyl oxygen of arginine R789 makes a hydrogen bond to the side-chain amide group of the catalytic glutamine Q61 in Ras thereby stabilising its position. Since arginine R789 is located in a flexible loop and points into the active site, it has been called the 'arginine finger' (Scheffzek et al., 1998).

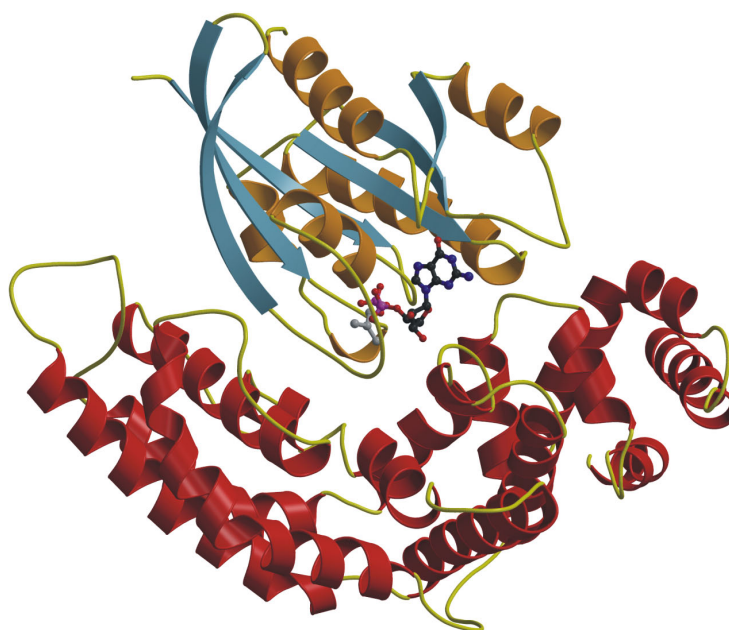


Figure 7. Structure of RasGAP in complex with Ras•GDP•AlF₃ (PDB accession code 1WQ1). RasGAP is shown in red, Ras in orange and blue.

The principles of GTPase stimulation of GAP are thought to be the stabilisation of glutamine Q61 leading to correct positioning of the attacking water molecule and the provision of positive charge by the arginine residue involved in stabilising the transition state.

This structure also helped to explain why mutations in glycine G12 of Ras interfere with the activation by GAPs. Glycine G12 is within van-der-Waals distance of the catalytic glutamine of Ras and the catalytic arginine of RasGAP and any mutation interferes sterically with the arrangement of these residues in the transition state.

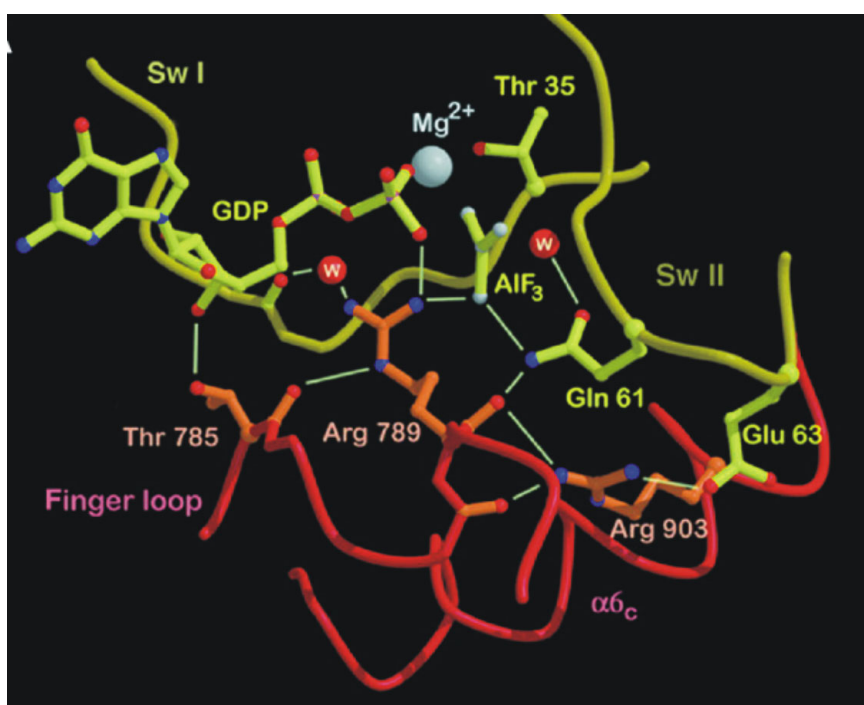


Figure 8. The active site of the RasGAP•Ras•GDP•AlF₃ complex showing important elements of catalysis (from Scheffzek et al., 1997).

2.2.2 RhoGAPs

Numerous GAPs specific for Rho/Rac/Cdc42 have been described and several structures have been solved (Barrett et al., 1997; Rittinger et al., 1997a; Rittinger et al., 1997b; Nassar et al., 1998). Similar to GAPs for Ras, these proteins are purely helical (Figure 9). Based on their similar three-dimensional architecture, it was proposed that RhoGAPs and RasGAPs have a common evolutionary origin although no obvious sequence similarity is observed (Rittinger et al., 1998).

The structure of the RhoGAP•Rho•GDP•AlF₃ complex revealed that the mechanism of GTPase stimulation involves - as in the case of RasGAP – the introduction of a catalytic arginine from the GAP and stabilisation of the catalytic glutamine in Rho (Rittinger et al., 1997b).

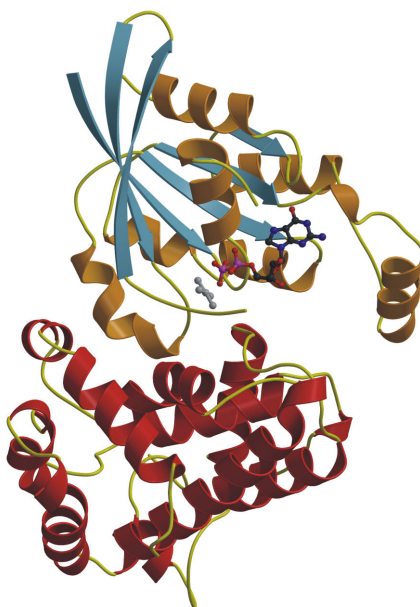


Figure 9. Structure of RhoGAP in complex with Rho•GDP•AlF₄⁻ (PDB accession code 1AM4). RhoGAP is in coloured in red, Rho in orange and blue.

2.2.3 G α proteins and regulators of G protein signalling

G α proteins transduce signals from seven-helix-transmembrane receptors to downstream targets. The crystal structure of G $\alpha_{t\alpha}$ in the GTP γ S bound state showed that these proteins have a Ras-like G domain fold with a helical insertion shortly behind the switch I region (Noel et al., 1993). The structure of a G α protein bound to GDP and aluminium fluoride revealed that the mechanism of GTP hydrolysis involves stabilisation of the attacking water molecule by a catalytic glutamine (homologous to glutamine Q61 in Ras) and by a threonine from the helical domain (Coleman et al., 1994). Strikingly, the GTPase reaction was highly dependent on an arginine residue supplied by the helical domain which makes a hydrogen bond to aluminium fluoride mimicking the transition state of GTP hydrolysis. This arginine residue provided by G α in cis (from G α itself) is the functional equivalent of the arginine finger of RasGAP and RhoGAP which is provided in trans (from a second molecule).

Regulator of G protein signalling (RGS) proteins accelerate the intrinsic reaction of $G\alpha$ proteins but do not share sequence homology to any other GAPs (Druey et al., 1996). They bind with modest affinity to the GTP bound forms of $G\alpha$ and with high affinity to the $GDP\cdot AlF_4^-$ bound form and stimulate GTP hydrolysis by at least 50-fold. The structure of RGS4 bound to $G_{i\alpha 1}\cdot GDP\cdot AlF_4^-$ showed that RGS proteins are helical, bind to the switch regions of $G\alpha$ and stabilise them (Figure 10; Tesmer et al., 1997). However, they do not contribute catalytic residues to the active site of $G\alpha$ except one asparagine residue which stabilises the catalytic glutamine of $G\alpha$. It was suggested that this asparagine could assist in the positioning of the hydrolytic water molecule.

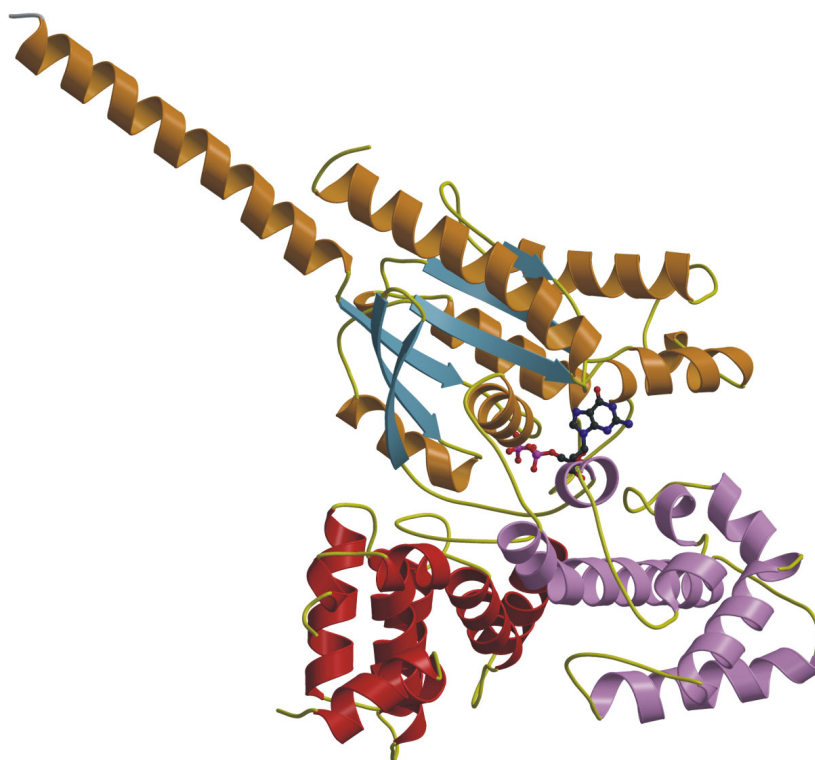


Figure 10. Complex structure of RGS4 bound to $G_{i\alpha 1}\cdot GDP\cdot AlF_4^-$ (PDB code 1AGR). $G_{i\alpha 1}$ is shown in orange and blue, its helical insert domain in purple and RGS4 in red.

2.2.4 Other GAPs with an arginine finger

RabGAPs comprise a family of GAPs for the small GNBPs Rab (Ypt in yeast) involved in vesicle trafficking. The structure of the yeast GAP Gyp1 revealed a fully α -helical protein (Figure 11A) albeit with a different fold than GAPs for Ras, Rho and $G\alpha$

proteins (Rak et al., 2000). By mutational analysis, an arginine was identified which is critical for the catalytic activity (Albert et al., 1999). However, the exact mode of interaction between RabGAP and Rab is currently unknown, since no structure of a RabGAP-Rab complex has been described yet.

Some bacterial toxins such as ExoS from *Pseudomonas aeruginosa*, SptP from *S. typhimurium* and YopE from *Yersinia sp.* are introduced in eukaryotic cells and act as Rho-specific GAPs to reorganise the cell's cytoskeleton (Goehring et al., 1999; Fu and Galan, 1999; Pawel-Rammingen et al., 2000). The structure of the GAP domain of ExoS (130 residues, from here on ExoS) in complex with Rac•GDP•AlF₄⁻ was solved (Figure 11B; Wurtele et al., 2001). It revealed that ExoS has a helical fold with a small two-stranded β -sheet. No structural homology was observed to any other known GAP structure. However, the mechanism of GTPase stimulation is similar to other GAPs since ExoS also provides an arginine finger into the active site of Rac. Similarly, the structure of SptP in complex with Rac1•GDP•AlF₃ revealed that SptP provides a catalytic arginine to Rac1 (Stebbins and Galan, 2000). It was suggested that bacterial GAPs and RhoGAPs have most likely evolved independently.

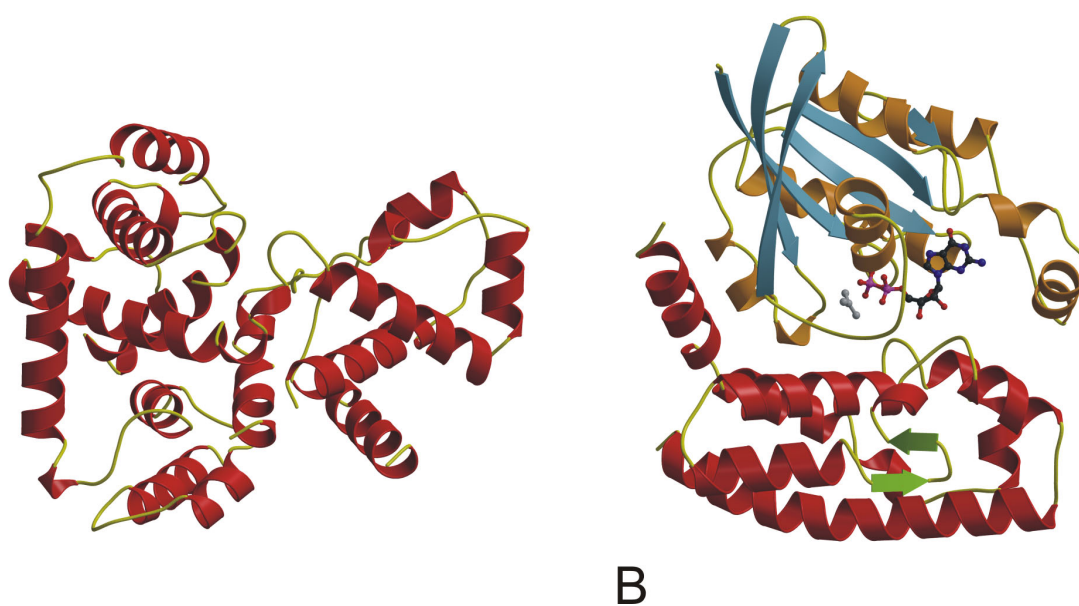


Figure 11. A) Ypt GAP (PDB code 1FKM) is a purely helical protein with no structural homology to other GAPs. B) The GAP domain of ExoS (in red and green) in complex with Rac•GDP•AlF₄⁻ (orange and blue) (PDB code 1HE1).

2.2.5 ArfGAP

Arf is a small GNPB which is involved in vesicle trafficking in eukaryotic cells (for review see Spang, 2002). Arf in the GDP bound state translocates from the cytosol to the membrane and is activated by Arf specific exchange factors (Renault et al., 2003). Arf in its GTP bound form associates with the membrane and recruits a seven-subunit complex called coatamer. This process is followed by budding of a vesicle containing Arf and the coatamer complex. When the membrane curvature of the vesicle increases, the activity of ArfGAP also present in this complex is stimulated dramatically, leading to GTP hydrolysis and Arf•GDP dissociation (Bigay et al., 2003). The catalytic domain of the ArfGAPs family comprises 140 residues including a zinc finger motif (Cukierman et al., 1995). The structure of the ArfGAP domain including four C-terminal ankyrin repeats (Mandiyani et al., 1999) and of the ArfGAP domain in complex with Arf•GDP (Goldberg, 1999) was solved. It revealed that the zinc finger of ArfGAP – consisting of four strands and one helix – is embedded in an irregular array of six α -helices and one β -strand (Figure 12). Clearly, no structural similarity to any GAPs of another GNPB family was observed.

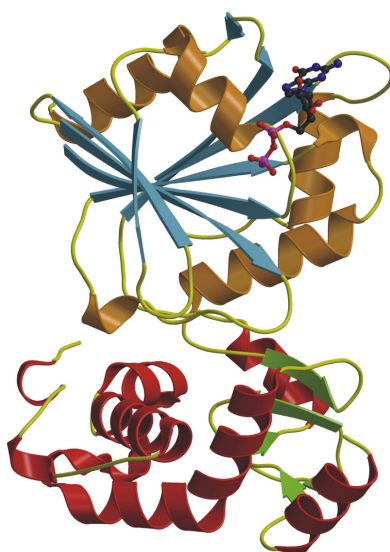


Figure 12. Crystal structure of ArfGAP (in red and green) in complex with Arf•GDP coloured in orange and blue (pdb coordinates provided by J.Goldberg). ArfGAP binds to Arf at a position far away from the nucleotide binding site.

Mutagenesis studies in ArfGAP revealed an arginine residue whose mutation to alanine dramatically reduced the GAP activity (Mandiyani et al., 1999). However, the structure of the complex showed that ArfGAP binds to a region of switch II of Arf which is at least 15 Å away from the nucleotide binding site. It was therefore

proposed that the GTPase reaction is not stimulated by a catalytic residue but rather by rearranging switch II of Arf leading to a better positioning of the catalytic glutamine in switch II. In further experiments it was shown, that upon addition of coatomer to Arf•GTP and ArfGAP, the GTPase reaction was a further 1000-fold stimulated. This suggests that the coatomer itself is involved in the GAP reaction and that an arginine finger is provided by the coatomer (Goldberg, 1999).

Sar1 is an Arf related protein which is involved in the formation of so-called COPII coated vesicles on the endoplasmic reticulum (Pasqualato et al., 2002). COPII consists of Sar1 and two large heterodimeric complexes Sec23/24 and Sec13/31 (Barlowe et al., 1994).

Sar1 has a histidine residue at the equivalent position of the catalytic glutamine in most other small GNBPs, and the intrinsic GTP hydrolysis of Sar1 is very slow. However, GTP hydrolysis can be stimulated by the Sec23 subunit which does not show sequence similarity to other GAPs (Yoshihisa et al., 1993). The crystal structure of Sec23 in complex with Sar1•GppNHp revealed that Sec23 provides a catalytic arginine into the active site of Sar1, and that the catalytic histidine of Sar1 positions the attacking water molecule (Bi et al., 2002). This reaction employing a catalytic histidine for positioning of the attacking water is unique for small GNBPs but might be similar for EF-Tu (Cool and Parmeggiani, 1991; Berchtold et al., 1993; Vogeley et al., 2001; Mohr et al., 2002).

2.2.6 RanGAP – catalysis without an arginine finger

RanGAPs stimulate the GTPase reaction of the small GGBP Ran (Seewald et al., 2002) which is involved in nuclear transport. A third protein, RanBP, binds to Ran and increases its affinity for RanGAP (Seewald et al., 2003). RanGAPs consist of a modular architecture with a 330-350 residue leucine-rich repeat (LRR) domain followed by an acidic region of approximately 40 residues (Hillig et al., 1999). The LRRs appear in proteins with various function, e.g. in the ribonuclease A inhibitor or *Drosophila* Toll-like receptor (Kobe and Deisenhofer, 1995). A single LRR forms a β - α hairpin consisting of a β -strand, a loop and an α -helix roughly parallel to the β -strand. The structure of yeast RanGAP showed that eleven LRR repeats form a crescent shaped molecule (Hillig et al., 1999). RanGAP does not have any structural similarity to the purely helical GAPs of Ras and Rho.

The complex between RanGAP, RanBP and Ran in the presence of a GTP analogue and in the presence of GDP and aluminium fluoride was solved (Figure 13; Seewald et al., 2002). Surprisingly, the only arginine in the vicinity of the active site was bent away from the γ -phosphate or the aluminium fluoride, and it was previously shown that this arginine is not important for catalysis (Hillig et al., 1999). This led to the proposal that RanGAP mediates GTP hydrolysis without an arginine finger. It was suggested that the basic machinery of fast GTP hydrolysis is provided exclusively by Ran and that binding of RanGAP leads to correct positioning of the catalytic glutamine in Ran.

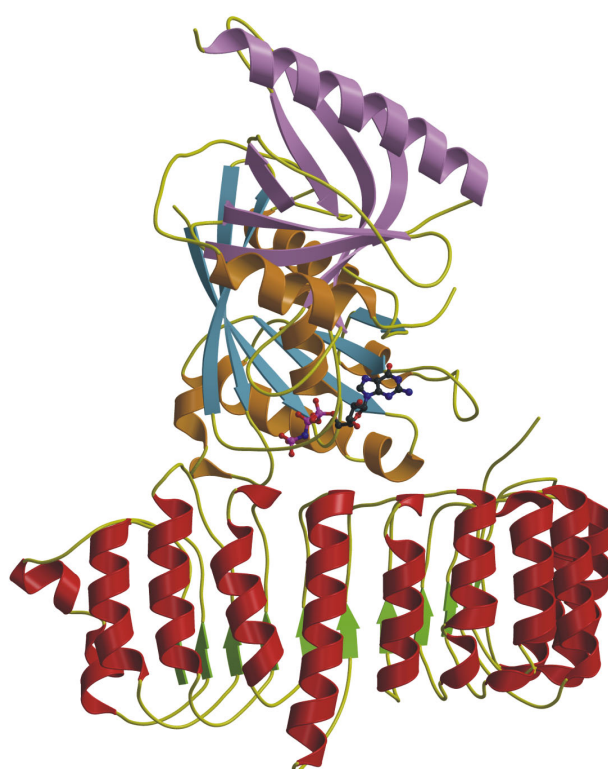


Figure 13. Structure of RanGAP in complex with Ran•GDP•AlF₃ and RanBP1 (PDB code 1K5D). RanGAP is shown in green and red, Ran in yellow and blue and RanBP1 in purple.

2.2.7 The signal recognition particle and its receptor

The signal recognition particle (SRP) and its receptor (SR) target newly synthesised proteins destined for secretion or membrane integration to the endoplasmic reticulum (Keenan et al., 2001). Both SRP and SR are conserved across all kingdoms of life. In prokaryotes, SRP consists of a single 48 kD GTPase called Ffh and a 110 nucleotide 4,5S RNA, whereas SR consists of the GTPase called FtsY. When both proteins are

loaded with GTP, they can bind to each other leading to a reciprocal stimulation of their GTPase activities, GTP hydrolysis and concomitant dissociation of the complex. Very recently, the mechanism of this reciprocal stimulation was elucidated by solving the structure of the complex between the two GTPases in the presence of a non-hydrolysable GTP analogue (Egea et al., 2004; Focia et al., 2004). The two GTPases form a quasi symmetric heterodimer, and the two nucleotides are aligned in a nearly symmetrical composite active site (Figure 14). In each chain, a catalytic aspartate was identified which is thought to activate the attacking nucleophilic water molecule in cis. Additionally, an arginine and a glutamine residue are provided from both molecules into the active site and interact in cis and possibly in trans with the β - and γ -phosphate groups. Strikingly, the 3' OH group of each GTP molecule contacts the γ -phosphate group of the opposing GTP molecule and reduces the negative charge on the γ -phosphate. This hydroxyl group was shown to be essential for association, reciprocal activation and catalysis (Egea et al., 2004).

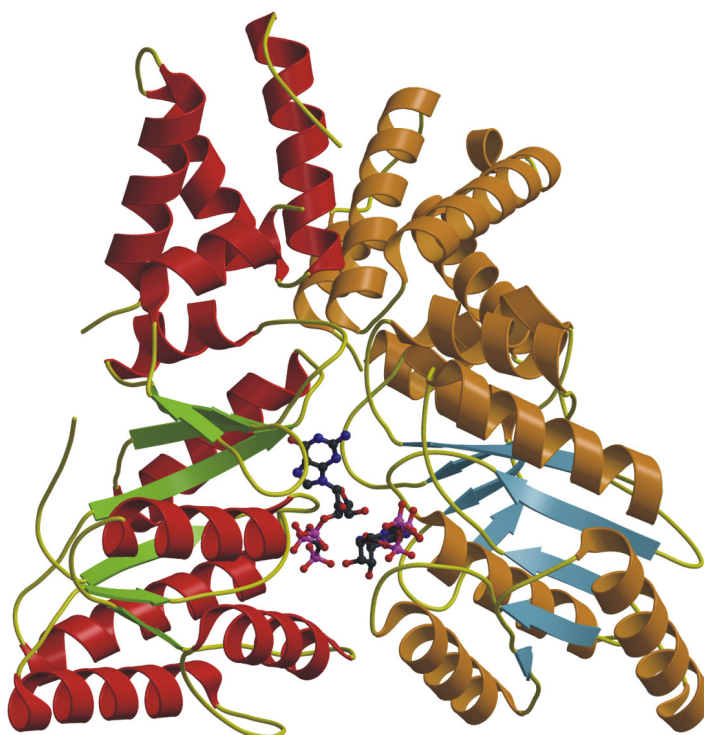


Figure 14. Ribbon type presentation of the SRP and SR heterodimer both in the GppNHp bound form (PDB code 1OKK). The nucleotides are buried in a common active site. SRP is shown in green and red, SR in orange and blue.

2.3 GTPase activating proteins of the Rap1GAP family

2.3.1 Rap1GAP

Rap1GAP (formerly GAP3) was isolated as a soluble and a membrane-associated isoform from cytosolic brain extract (Kikuchi et al., 1989; Polakis et al., 1991) which specifically stimulate GTP hydrolysis in Rap1, and to a smaller extent in Rap2 (Janoueix-Lerosey et al., 1992). The protein responsible for this activity was sequenced and the corresponding gene was cloned from a human brain cDNA (Rubinfeld et al., 1991). It turned out to encode a polypeptide of 663 amino acids with a molecular weight of 73 kD which in human is expressed most abundantly in brain, foetal tissue, undifferentiated cells and certain tumour cell lines. By deletion analysis it was shown that a protein fragment consisting of amino acids 75-416 is necessary and sufficient to retain full GAP activity (Rubinfeld et al., 1992). This fragment did not show any sequence similarity to GAPs of other small GNBPs. However, homologous sequences have been identified in the human genes *Spa1* (Hattori et al., 1995), *E6TP1/SpaR/SpaL* (Gao et al., 1999; Roy et al., 1999) and *Tsc2* (Figure 15; Tuberous Sclerosis Consortium, 1993). Homologues of these genes are found in all higher organisms.

Rap1GAP was shown to be regulated by protein degradation and relocalisation from cytosol to the membrane. It is phosphorylated *in vivo* at four distinct sites which are located C-terminally of the catalytic fragment (Polakis et al., 1992; Rubinfeld et al., 1992). Recently, it was demonstrated that in thyroid cells phosphorylation of Rap1GAP by GSK3 β is associated with proteasome-mediated degradation (Tsygankova et al., 2004).

A splice isoform of Rap1GAP, RapGAPII, is expressed in heart, liver, kidney and cerebrum and contains an N-terminal GoLoco motif which specifically binds to the α -subunits of the G_i family of heterotrimeric G-proteins (Mochizuki et al., 1999; Kimple et al., 2002). Upon stimulation of G_i , RapGAPII translocates from the cytosol to the membrane, followed by a decrease of Rap1•GTP and an activation of the ERK pathway, thus linking G_i and Rap1 signalling pathways. Rap1GAP was also shown to bind to the GTP bound form of $G_{\alpha z}$ (Meng et al., 1999) accompanied by a decrease of cellular Rap1•GTP (Meng and Casey, 2002) and to the GDP bound form of $G_{\alpha 0}$ accompanied by an increase of cellular Rap1•GTP (Jordan et al., 1999).

Another possible interaction partner of Rap1GAP is the cytoskeleton-anchoring protein AF-6 (Su et al., 2003) which was earlier described as a putative Rap1 effector (Linnemann et al., 1999; Boettner et al., 2000). It was proposed that the interaction is mediated by the PDZ domain of AF-6 which should bind to an internal VVF motif of Rap1GAP located in the catalytic domain (Su et al., 2003).

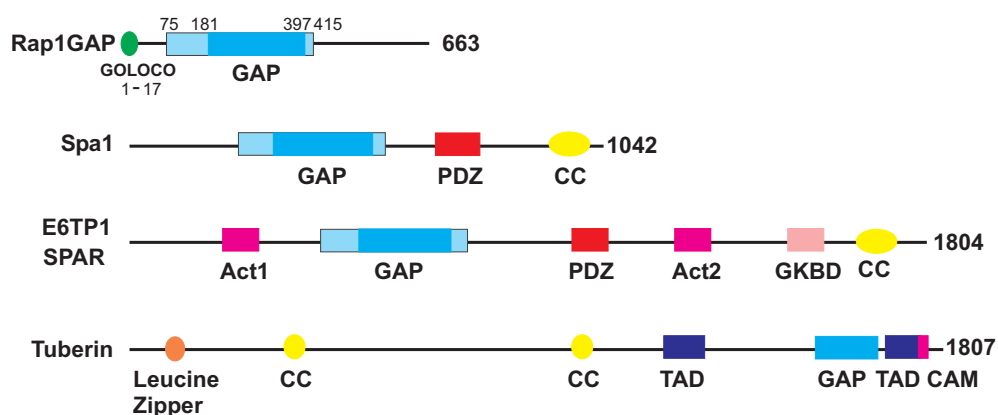


Figure 15. Schematical view of the Rap1GAP family showing the domain structure of the involved proteins. Abbreviations used here: CC: coiled coil, Act: actin regulatory domain, GKBD: guanylate kinase-like binding domain, TAD: Transcription activation domain CAM: Calmoduline binding domain. The GoLoco domain is present in RapGAPII but not Rap1GAP. This figure was kindly provided by P. Chakrabarti.

2.3.2 Signal-induced proliferation-associated protein 1 (Spa-1)

Spa-1 encoding a 130 kD protein was identified as a gene which was little expressed in a quiescent murine lymphoid cell line but was induced upon interleukin-2 stimulation (Hattori et al., 1995). The corresponding protein contains the Rap1GAP domain, a PDZ domain involved in protein-protein interaction and a C-terminally located coiled-coil region (Figure 15). In human, *Spa-1* is most abundantly expressed in lymphoid tissues such as thymus, spleen but not in tissues expressing *Rap1GAP* such as brain, kidney and pancreas (Kurachi et al., 1997). Baculo-virus expressed *Spa-1* showed specific GAP activity towards Rap1 and Rap2 (Kurachi et al., 1997). As for Rap1GAP, AF-6 was described as possible interaction partner (Su et al., 2003). Recently, *Spa-1* was shown to be a tumour-suppressor gene since *Spa-1* knockout mice developed a spectrum of myeloid disorders that resembled human chronic myelogenous leukaemia (Ishida et al., 2003). Furthermore, it was demonstrated that the increased Rap1•GTP levels caused by *Spa-1* deletion were responsible for increased cell proliferation of hematopoietic progenitors.

2.3.3 E6TP-1

E6TP1 (E6 targeted protein 1) was identified as a 200 kD protein which is targeted to proteasome-mediated degradation by the papilloma virus protein E6 (Gao et al., 1999). Degradation of E6TP1 was correlated with the ability of E6 to immortalise mammary epithelial cells (Gao et al., 2001a), thus establishing the role of *E6TP1* as a tumour suppressor gene. The 1804 residue protein is widely expressed in tissues and in-vitro cultured cell lines. Like Spa-1, it contains a Rap1GAP homology domain (residues 489–819), a PDZ domain and a coiled-coil region (Figure 15). Additionally, it has two actin binding domains (Pak et al., 2001). GAP activity towards Rap1 and Rap2 was demonstrated (Singh et al., 2003).

SPAR/SPAL is the rat homologue of E6TP1 and was found to form a complex with PSD-95 and NMDA receptors in neurons. This complex has a crucial role for establishing dendritic spines (Pak et al., 2001) which are postsynaptic protrusions where glutamate-mediated neuronal transmission takes place (Meyer and Brose, 2003). Phosphorylation of SPAR1 by serum-inducible kinase leads to its degradation accompanied by loss of the dendritic spine (Pak and Sheng, 2003). Thus, SPAR is a critical component in the formation of neuronal activity albeit the role of Rap1 regulation is unclear to date.

2.3.4 Tuberin

Tuberous sclerosis (Tsc) is an autosomal dominant inherited disease with a prevalence of 1 in 6000 births characterised by benign tumours called hamartomas in a variety of tissues, as well as rare malignancies (reviewed in Manning and Cantley, 2003; Li et al., 2004). Other symptoms include mental retardation and epilepsy. This disease is caused by loss of function mutations in either of the two tumour suppressor genes *Tsc1* and *Tsc2* encoding Hamartin (130 kD) and Tuberin (200 kD), respectively (Tuberous Sclerosis Consortium, 1993; van Slegtenhorst et al., 1998). In vivo, Tuberin and Hamartin form a heterodimer which is thought to stabilise the two proteins. This complex functions in the insulin/mTOR pathway to inhibit cell growth and proliferation (Potter et al., 2002; Tee et al., 2002).

Tuberin was shown to have sequence homology to a C-terminal fragment of the Rap1GAP domain, and in-vitro GAP activity towards the small GNBPs Rap1 and Rab5 was reported (Wienecke et al., 1995; Xiao et al., 1997). However, it is evident now that Tuberin acts in vivo as a GAP towards the small GNBPs RheB (Tee et al.,

2003; Garami et al., 2003; Castro et al., 2003; Zhang et al., 2003). It is currently unclear how RheB in the GTP bound form can activate the downstream effector kinase mTOR.

2.3.5 Biochemistry of the Rap1-Rap1GAP system

A catalytic glutamine (glutamine Q61 in Ras) is crucial for the intrinsic and GAP stimulated GTP hydrolysis of $G\alpha$, Ras, Rho, Rab and Ran GNBPs. In contrast, Rap1 does not have a catalytic glutamine but a threonine at the equivalent position. As a result, the intrinsic GTP hydrolysis rate of Rap1 is 10-fold slower than for Ras but can be reconstituted by exchanging threonine T61 for a glutamine (Frech et al., 1990). Furthermore, threonine T61 is not required for the intrinsic and GAP stimulated GTP hydrolysis in Rap1 (Maruta et al., 1991). It is therefore anticipated that the mechanism of hydrolysis is different between Rap1 and the other GNBPs.

Glycine G12 mutations in Ras and other GNBPs render the protein inactive to GAPs since any side-chain at position 12 would interfere with the positioning of the arginine finger and the catalytic glutamine (see above). However, the G12V mutant of Rap1 can still be down-regulated by Rap1GAP, albeit with an 8-fold reduced rate (Brinkmann et al., 2002). This again indicates that Rap1GAP stimulates GTP hydrolysis in a completely different way than all other GAPs.

A fluorescence assay was developed to monitor a single turnover reaction cycle of the Rap1GAP catalysed reaction in Rap1 (Kraemer et al., 2002). It was proposed that the rate limiting step of the reaction was not GTP hydrolysis but the release of inorganic phosphate, similarly as already proposed for RasGAP-Ras system (Allin et al., 2001).

2.4 Objectives of this work

All available data indicated that the Rap1GAP stimulated reaction is fundamentally different from all other GAP systems described hitherto (see above). Therefore, this new mechanism was explored by biochemical and structural analysis.

In a first step, the reaction should be characterised and residues important for catalysis should be identified. Consequently, the structure of one member of the Rap1GAP family should be solved. It was expected that Rap1GAP has a completely novel GAP fold since no sequence similarities to any other GAP could be detected. Based on the structure and the available biochemical data, the catalytic centre should be identified and further characterised by mutational and biochemical analysis. This work also aimed to understand the molecular basis for diseases such as Tuberous sclerosis since single point mutations in the Rap1GAP domain of Tuberin were described in Tuberous sclerosis patients. However, the role of these mutations in disease was unclear and could be unravelled by understanding the involved reaction mechanism.

3 Materials and Methods

3.1 Materials

3.1.1 Chemicals

Chemicals from the following companies were used: Amersham-Pharmacia (Freiburg), Baker (Deventer, Niederlande), Fluka (Neu-Ulm), GERBU (Gaiberg), Merck (Darmstadt), Pharma-Waldhof (Düsseldorf), Qiagen (Hilden), Riedel-de-Haen (Seelze), Roche (Mannheim), Roth (Karlsruhe), Serva (Heidelberg) und Sigma-Aldrich (Deisenhofen).

3.1.2 Enzymes

DNAase-I	Roche (Mannheim)
Pfu DNA polymerase	New England Biolabs (Schwalbach)
Restriction enzymes	New England Biolabs (Schwalbach)
T4 DNA ligase	New England Biolabs (Schwalbach)
Trypsin, α -chymotrypsin	Sigma (Deisenhofen)
Thrombin	Serva (Heidelberg)

3.1.3 Kits

QIAprep Spin Miniprep Kit	Qiagen (Hilden)
QIAquick Gel Extraction Kit	Qiagen (Hilden)
BigDye Terminator Sequencing Kit	Applied Biosystems (Langen)
λ -DNA standard	Invitrogen (Karlsruhe)
Wide Range, SDS7 protein marker	Sigma (Deisenhofen)

3.1.4 Microorganisms

<i>E. coli</i> CK600K	<i>supE</i> , <i>hsdM</i> ⁺ , <i>hsdR</i> ⁻ , <i>kanR</i> (Hoffmann-Berling, Heidelberg)
<i>E. coli</i> TG1	<i>K12</i> , <i>supE</i> , <i>hsd</i> Δ 5, <i>thi</i> , Δ (<i>lac-proAB</i>), <i>F'</i> [<i>traD36</i> , <i>proAB</i> ⁺ , <i>lacI</i> ^q , <i>lacZ</i> Δ M15] (Promega)

E. coli BL21 (DE3) *B, F, hsdSB (rB⁻, mB⁻), gal, dcm, ompT, λ(DE3)* (Novagen)

E. coli BL21 (DE3) *F⁻ ompT hsdSB(rB⁻ mB⁻) gal dcm (DE3) pRARE2 (CmR)*
Rosetta (Novagen) *pRARE* containing the tRNA genes *argU, argW, ileX, glyT, leuW, proL, metT, thrT, tyrU, and thru*

3.1.5 Media and antibiotics

Luria-Bertani (LB) 10 g/l Bactotryptone, 10 g/l NaCl, 5 mM NaOH, 5 g/l yeast extract

Terrific Broth (TB) 12 g/l BactoTryptone, 24 g/l Bacto-yeast-extract, 4 g/l glycerol,
17 mM KH₂PO₄, 72 mM K₂HPO₄

Standard I 25 g/l standard-I powder (Merck, Darmstadt)

SeMet-Medium was prepared according to Van Duyne et al. (1993). It is a minimal medium which contains 50 mg/l seleno-L-methionine (Calbiochem-Novabiochem, Schwalbach), no methionine, a high concentration (250 mg/l) of the amino acids Val, Leu, Ile, Lys, Thr, Phe to suppress bacterial methionine biosynthesis and 50 mg/ml of the other amino acids.

Antibiotics from GERBU (Gaiberg) were used in the concentration 100 mg/l.

3.1.6 Buffers

PBS 140 mM NaCl; 2,7 mM KCl; 10,1 mM Na₂HPO₄; 1,8 mM KH₂PO₄

3.2 Molecular biology methods

3.2.1 Agarose gels

Agarose gels were prepared and run according to standard procedures (Sambrook, 1989).

3.2.2 Isolation of plasmid DNA

DNA was isolated using QIAprep Spin Miniprep Kit from Qiagen (Hilden) according to the manufacturer's protocol.

3.2.3 Polymerase chain reaction (PCR)

Amplification of DNA fragments was carried out using *Pfu* polymerase (New England Biolabs, Schwalbach) or *Pwo* polymerase (Roche, Mannheim) according to standard procedures (Sambrook, 1989). Fragments were digested (see 3.2.3) and purified using QIAquick Gel Extraction Kit (Hilden) according to the manufacturer's protocol.

3.2.4 DNA digestion

DNA was digested using enzymes from New England Biolabs (Schwalbach) according to the manufacturer's protocol.

3.2.5 Ligation

Vector and insert DNA were quantified in agarose gels using digested λ -marker (New England Biolabs, Schwalbach) as a reference. 10 ng of vector was ligated with a six fold molar excess of insert overnight at 8 °C using T4 ligase (Roche, Mannheim) according to the manufacturer's protocol.

3.2.6 Competent cells

Competent cells were prepared according to Chung et al. (1989). 200 ml LB medium was inoculated with 2 ml preculture and grown at 37 °C until an OD₆₀₀ of 0,4. Bacteria were incubated for 20 min on ice, pelleted for 5 min at 1200 x g (4 °C), resuspended in 20 ml ice-cold sterile TSS buffer (85% LB medium without NaOH,

10% PEG 8000, 5% DMSO, 50 mM MgCl₂, pH 6,5), flash frozen and stored at -80 °C.

3.2.7 Transformation

The heat shock method was used according to the standard protocol (Sambrook, 1989). Ligated DNA was transformed in *E. coli* TG-1, amplified and isolated. The isolated DNA was transformed in *BL21 (DE3)* expression bacteria.

3.2.8 Bacteria storage

30% glycerol was added to an overnight culture and bacteria stocks were stored at -80 °C.

3.2.9 Site specific mutagenesis

Site specific mutagenesis was carried out using the QuickChange kit (Stratagene, Amsterdam) according to the manufacturer's protocol.

3.2.10 DNA sequencing

DNA sequencing was done according to Sanger et al. (1992) using the Big Dye terminator kit (Applied Biosystems, Langen). A sequencing reaction contained 10 µl DNA Qiaprep solution (see 3.2.2), 4 µl terminator mix, 3 pmol sequencing primer in a volume of 20 µl. The sequencing PCR and DNA precipitation was carried out according to the manufacturer's protocol. Analysis of the sequencing products was done in house on a ABI PRISM 3700 DNA Analyzer (Applied Biosystems, Langen).

3.2.11 Constructs

Construct	Remark
<i>ptac Rap1B C</i> ¹⁻¹⁶⁶	Provided by D. Kühlmann
<i>pGEX 4T1 hsRap1GAP</i> ⁷⁵⁻⁴¹⁵	Provided by P. Stege, expressed protein soluble and active
<i>pGEX 4T1 hsRap1GAP</i> ⁸⁶⁻⁴⁰⁵	Expressed GST-fusion not cleavable by thrombin
<i>pGEX 4T1 hsRap1GAP</i> ⁷⁵⁻⁴⁰⁵	Expressed protein prepared in big amounts, initial crystallisation trials
<i>pGEX 4T1 hsRap1GAP</i> ¹⁷⁸⁻⁴⁰⁵	Expressed protein insoluble
<i>pGEX 4T1 hsRap1GAP</i> ¹⁸⁸⁻³⁸⁸	Provided by D. Kühlmann, expressed protein precipitated upon removal of GST
<i>pGEX 4T1 hsRap1GAP</i> ¹⁸³⁻³⁹⁸	Expressed protein could be prepared and GST cleaved in big amounts
<i>pGEX 4T1 hsRap1GAP</i> ¹⁷¹⁻⁴⁰⁵	Expressed protein insoluble
<i>pGEX 4T1 dmRap1GAP</i> ²³⁴⁻⁵⁴¹	Expressed GST-fusion soluble but precipitated upon removal of GST
<i>pGEX 4T1 dmRap1GAP</i> ²¹⁵⁻⁵⁵⁵	Expressed protein insoluble
<i>pGEX 4T1 dmRap1GAP</i> ²³⁴⁻⁵⁴¹	Expressed protein insoluble
<i>pGEX 4T1 dmRap1GAP</i> ²³⁴⁻⁵⁵⁵	Expressed protein insoluble
<i>pGEX 4T1 dmRap1GAP</i> ²¹⁵⁻⁵⁴¹	Expressed protein insoluble
<i>pGEX 4T1 dmRap1GAP</i> ³⁴³⁻⁵⁵⁵	Expressed protein insoluble
<i>pGEX 4T1 dmRap1GAP</i> ³⁴³⁻⁵⁴¹	Expressed protein insoluble
<i>pGEX 4T1 dicRap1GAP</i> ⁹¹³⁻¹²¹²	Provided by Dr. Faix, expressed protein insoluble
<i>pGEX 4T1 hsSpa-1</i> ²⁰⁵⁻⁵⁵⁷	Expressed protein insoluble
<i>pGEX 4T1 hsSpa-1</i> ²⁰⁵⁻⁵⁴⁹	Expressed protein insoluble
<i>pGEX 4T1 hsE6TP1</i> ⁴⁸⁵⁻⁸²⁴	Expressed protein insoluble
<i>pGEX 4T1 hsE6TP1</i> ⁴⁷⁷⁻⁸²⁴	Expressed protein insoluble
<i>pGEX 4T1 hsTuberin</i> ¹²⁰⁸⁻¹⁷⁸⁴	Provided by Eva Kostinova, expressed protein degraded upon purification
<i>pGEX 4T1 hsTuberin</i> ¹³⁴⁶⁻¹⁷⁸⁴	Provided by Eva Kostinova, expressed protein degraded upon purification
<i>pGEX 4T1 hsTuberin</i> ¹⁵³²⁻¹⁷⁶⁰	Expressed protein degraded upon purification
<i>pGEX 4T1 hsTuberin</i> ¹⁴⁹⁸⁻¹⁷⁶⁰	Expressed protein degraded upon purification

3.2.12 Point mutants

Construct	Point Mutants
<i>pGEX4T1 Rap1GAP</i> ⁷⁵⁻⁴¹⁵	Wild-type, R91A, R128A, R132A, K194A, R286A, Q204A, R388A were provided by P. Stege
<i>pGEX4T1 Rap1GAP</i> ⁷⁵⁻⁴¹⁵	(F100E, L173E), E207A, R240A, H267A, H287A, N290A, N290I, N290K, D291A, F313A, R339A

3.3 Biochemical methods

3.3.1 Sequence alignment

Sequences were aligned using the ClustalW algorithm (Thompson et al., 1994) and manually refined using Genedoc (Nicholas et al., 1997).

3.3.2 SDS-PAGE

Separation of proteins of different molecular weight was performed according to Laemmli (1970) using denaturing, discontinuous SDS-polyacrylamide gel electrophoresis (SDS-PAGE).

3.3.3 Determination of protein concentration

Protein concentration was determined according to Bradford (1976) using the Biorad protein assay (Biorad). The solution was calibrated using bovine serum albumin.

3.3.4 Matrix assisted laser desorption ionisation (MALDI)

The molecular weight of newly isolated proteins, digested protein bands and heavy atom protein derivatives was determined by matrix assisted laser desorption ionisation (MALDI). A concentrated protein solution was diluted with water and 1:1 mixed with matrix (for proteins > 10 kD: saturated sinapinic acid in acetonitrile, 0,2% TFA; for peptides < 10 kD: saturated a-cyano-4-hydroxy cinnamic acid in acetonitrile, 0,2% TFA water). Data were acquired on a Voyager DE Pro (Applied Biosystems).

3.3.5 Test expression

To test expression and solubility of proteins expressed from pGEX vectors, vectors containing the desired insert were transformed in expression bacteria (*BL21-DE3* and *BL21-DE3 Rosetta*). A 50 ml bacteria culture in TB medium was induced at on OD₆₀₀ of ~0,4 with 500 µM IPTG and grown at 37 °C overnight. Two other cultures were induced with 50 µM and 200 µM IPTG and grown at 18 °C overnight.

To test expression, 1 ml of the overnight culture was pelleted, resuspended in water and analysed using SDS-PAGE. To test the solubility, 1 ml bacteria culture was

pelleted, resuspended in 100 μ l BugBuster solution (Novagen) and lysed for 5 min on ice. The solution was centrifuged at 25000 X g for 10 min at 4 °C. Fractions of 5 and 10 μ l of the supernatant were analysed by SDS-PAGE. Alternatively, 20 ml bacteria were pelleted and resuspended in 1 ml buffer of choice. Cells were broken by 1 min sonification on ice using a Sonifier 450 (Branson Ultrasonics, Danbury, USA) at 50% duty cycle. After 30 min centrifugation at 4 °C and 25000 x g, various amounts of the supernatant were analysed via SDS-PAGE.

3.3.6 Protein overexpression and preparation of soluble bacteria extract

Proteins were overexpressed using the parameters described in Table 1.

Table 1 Expression constructs and expression conditions

Plasmid	<i>E. coli</i> strain	Medium	Antibiotics	Induction at OD ₆₀₀	[IPTG] / μ M	T / °C	Expression time / h
Ptac Rap1B C'	CK600K	Standard I	Amp, Kan	0,8	500	30	24
pGEX4T1 Rap1GAP	BI21DE3	TB	Amp	0,2	50	18	24
pGEX4T1 Rap1GAP SeMet	BI21DE3	SeMet medium	Amp	0,2	50	18	48
All other pGEX vectors	BI21DE3	TB	Amp	0,2	50	18	24

Upon expression, bacteria were pelleted at 4000 x g, resuspended in buffer containing 100 μ M phenylmethylsulfonylfluoride (PMSF) as protease inhibitor and frozen at -20 °C. Cells were thawed, 20 mg/l DNase I (stock 20 g/l in 1 M MgCl₂) and 100 μ M PMSF was added and the cells incubated for 30 min on ice. Cells were broken using a micro fluidizer (Microfluidics, Newton, USA). Insoluble material was removed by centrifuging at 100.000 x g for 45 min, and the supernatant used for further purification.

3.3.7 Rap1GAP purification

Rap1GAP⁷⁵⁻⁴¹⁵, selenomethionine substituted Rap1GAP⁷⁵⁻⁴¹⁵, Rap1GAP⁷⁵⁻⁴¹⁰ and all Rap1GAP mutants were purified as GST-fusion according to Brinkmann et al. (2002)

with a subsequent gel filtration. The first buffers contain ATP, potassium and magnesium ions to remove bound GroEL.

Bacteria were broken in PBS, 5 mM MgCl₂, 5 mM DTE, 1 mM ATP, 100 μM PMSF (see 3.3.5). The cell supernatant was applied to a GST-column (25 ml, Amersham, Freiburg) equilibrated with PBS, 5 mM MgCl₂, 5 mM DTE, 1 mM ATP and excessively washed with at least 500 ml of the same buffer. The buffer was exchanged to PBS, 5 mM DTE or 50 mM Hepes (pH 7,5), 100 NaCl, 2 mM CaCl₂, 5 mM DTE. GST was cleaved by addition of 300 units thrombin (Serva) and overnight incubation. Rap1GAP was eluted with PBS, 5 mM DTE or 50 mM Hepes (pH 7,5), 100 NaCl, 2 mM CaCl₂, 5 mM DTE. The protein was concentrated (30 mg/ml) using an Amicon concentrator (10 kD cutoff) and further purified on a Sephadex200 gel filtration using 20 mM Hepes (pH 7,5), 100 mM NaCl, 5 mM DTE as running buffer. Rap1GAP eluted in two peaks from gel filtration, the first one containing bound chaperone and eluting in the exclusion volume, the second eluting as protein with an apparent molecular weight of 100 kD and containing pure Rap1GAP. Protein from the second peak was pooled, concentrated and twice washed with 20 mM Hepes (pH 7,5), 5 mM DTE using Amicon concentrators (10 kD cutoff) to remove NaCl. The protein was finally concentrated to 60 mg/ml and flash frozen.

3.3.8 Purification of other GST fusion proteins

All GST-fusions were prepared as described in 3.3.7 with the following modification. The running buffer was 50 mM Hepes (pH 7,5), 100 mM NaCl, 5 mM DTE. GST was cleaved in 50 mM Hepes (pH 7,5), 100 mM NaCl, 5 mM DTE, 2 mM CaCl₂.

3.3.9 Assignment of degradation bands

Rap1GAP⁷⁵⁻⁴¹⁵ and Rap1GAP⁷⁵⁻⁴⁰⁵ showed specific degradation bands after incubation for few days at 8 °C.

To locate these fragments, peptide masses were determined by MALDI (3.3.4). Rap1GAP⁷⁵⁻⁴¹⁵ yielded fragments of 24,4 kD and 14,4 kD mass adding up to the mass of 39 kD of Rap1GAP. Rap1GAP⁷⁵⁻⁴⁰⁵ yielded fragments of 23,4 kD and 14,4 kD mass indicating that the 24,4 kD fragment is C-terminally located.

3.3.10 Partial digest

Rap1GAP was partially digested to find a smaller, compact folded Rap1GAP fragment. The reaction buffer was chosen according to the protease employed (Table 2). The reaction (100 μ l) containing 100 μ g Rap1GAP was started at 20 °C by adding the indicated amount of protease. After 0 min, 5 min, 10 min, 15 min, 20 min, 30 min, 60 min, 120 min, 240 min and 1000 min, 10 μ l aliquots were transferred in SDS sample buffer and immediately flash frozen. Aliquots were analysed by SDS-PAGE. Tested proteases are depicted in Table 2.

Table 2 Proteases with the chosen reaction buffer.

Protease	Reaction buffer	Final conc.	Temp
α -Chymotrypsin	50 mM Tris (pH 8)	8 μ g / ml	25 °C
Trypsin	50 mM Tris (pH 8)	2 μ g / ml	15 °C
Aminopeptidase	50 mM Tris (pH 8)	3 μ g / ml	25 °C
Carboxypeptidase	50 mM Tris, 50 μ M ZnCl ₂ pH 6,5	4 μ g / ml	30 °C
Elastase	50 mM Tris (pH 8,9)	8 μ g / ml	30 °C
Papain	50 mM MES, pH 6,5	4 μ g / ml	25 °C

3.3.11 Purification of Rap1B C'

C-terminally truncated Rap1B (Rap1B C') was purified according to Tucker et al. (1986). Bacteria were broken in 32 mM Tris (pH 7,5), 100 μ M PMSF, 2 mM EDTA (see 3.3.6).

The cell supernatant was applied on a Q-sepharose column equilibrated with 0,5 x buffer C. The column was excessively washed with 0,5 x buffer C and bound proteins were eluted using a salt gradient (0-300 mM NaCl) in 0,5 x buffer C. Fractions containing Rap1B C' were identified using SDS-PAGE and pooled. Protein was precipitated by slowly adding solid ammonium sulfate (3M final concentration). Precipitated protein was pelleted by centrifugation for 60 min at 16000 x g and resuspended in buffer D. Rap1B C' was further purified on a Sephadex75 gel filtration column equilibrated with buffer D. Fractions containing Rap1B C' were pooled and concentrated using an Amicon concentrator (10kD cutoff).

Buffer C 64 mM Tris, 10 mM MgCl₂, pH 7,6 (HCl), 5 mM DTE

Buffer D 1 x Puffer C, 200 μ M GDP, 0,4 M NaCl, 5 mM DTE

3.3.12 Rap1-Aedans preparation

Rap1-Aedans•GTP wild-type was a gift of Astrid Krämer and was prepared according to Kraemer et al. (2002). Rap1-Aedans^{T61Q} was a gift of Partha Chakrabarti. In this method, a surface-exposed cysteine is modified by a haloacetamides (here 1,5-laedans) which is an environmentally sensitive fluorophore and acts as an indicator of protein binding.

The Rap1B C^{A86C} and Rap1B C^{A86C,T61Q} mutants were prepared as described in 3.3.11. DTE interferes with the labelling reaction. Thus, DTE was exchanged with a buffer containing 2 mM ascorbate using ultrafiltration with an Amicon concentrator (10 kD cutoff). The protein was diluted to 100 µM and incubated with a 3-fold excess of 1,5-laedans for 12 h at 4 °C. The reaction was stopped by buffer exchange with standard buffer containing DTE. Products were analysed by mass spectrometry. The protein was flash frozen and stored at -80 °C.

3.3.13 Nucleotide exchange

Nucleotide exchange was performed according to Tucker et al. (1986). This method uses EDTA which binds Mg²⁺ ions leading to an increase in the dissociation rate of the nucleotide. The nucleotide can then be exchanged by an excess of freshly added nucleotide.

200 µM Rap1B C' in 50 mM Hepes (pH 7,5), 100 mM NaCl was incubated with 15 mM EDTA, 150 mM ammonium sulfate and 10 mM nucleotide (stock 100 mM nucleotide in 1 M Hepes, pH 7,5) for 60 min at room temperature or overnight at 4 °C. The exchange reaction was stopped by adding 30 mM MgCl₂. Non-bound nucleotide was removed by washing the protein several times with an Amicon concentrator (10 kD cutoff) at 4 °C. To confirm successful nucleotide exchange, the nucleotide concentration was determined (see 3.3.14) and compared to the protein concentration (see 3.3.3). The protein was flash frozen and stored at -80 °C.

3.3.14 Nucleotide detection using reversed-phase HPLC

This method was carried out according to Lenzen et al. (1995). The principle of nucleotide separation is the interaction between the hydrophobic static phase and the ion pair of nucleotide and tetrabutylammonium in the mobile phase. Depending on

the number of phosphates, a variable number of tetrabutylammonium ions are bound by the nucleotide which increases the retention time on the column.

The sample was applied on a HPLC system Gold 166 (Beckman, Palo Alto, USA) and separated via a reversed-phase column ODS Hypersil C18 (Bischoff, Leonberg). Denatured proteins were adsorbed at a nucleosil-100-C18 precolumn. The running buffer contained 10 mM tetrabutylammoniumbromide, 100 mM potassium phosphate (pH 6,5) with 7,5% acetonitrile. Nucleotide peaks were detected by measuring adsorption at 254 nm and quantified by integration. The column was calibrated by standard nucleotide solutions.

3.3.15 Radioactive charcoal assay

This assay detects radioactive inorganic phosphate and was carried out according to Leupold et al. (1983). Charcoal is suspended in phosphoric acid and a reaction sample containing the GNBP loaded with [γ - 32 P] labelled GTP is added. The GNBP immediately denatures due to the acidic pH and binds with the nucleotide to the charcoal. Free radioactive phosphate will not bind since the charcoal is already saturated with phosphate. Upon removal of the charcoal by centrifugation, it can be quantified by scintillation counting. To determine initial rates of Rap1GAP stimulated GTP hydrolysis in Rap1, not more than 30% of Rap1•[γ - 32 P]GTP must have reacted. GTP was partially exchanged with [γ - 32 P]GTP by incubating 1,5 mM Rap1•GTP (see 3.3.11) with 20 μ Ci of [γ - 32 P]GTP (800 Ci/mmol, Amersham-Pharmacia) in the presence of 12 mM EDTA for 30 min on ice. The exchange reaction was stopped by adding 25 mM MgCl₂.

Initial rates were determined using 100 nM Rap1GAP and increasing concentrations of Rap1•[γ - 32 P]GTP at 25 °C in standard buffer (here 30 mM Tris (pH 7,5), 2 mM MgCl₂, 5 mM DTE). At different time points, 10 μ l aliquots of the reaction were withdrawn, added to 390 μ l charcoal solution (5% (w/v) Norit in 20 mM H₃PO₄) and vortexed. To determine end points of GTP hydrolysis, all Rap1•GTP was hydrolysed by addition of a highly concentrated Rap1GAP solution, and a last aliquot was taken. Upon centrifugation, the radioactivity of a 200 μ l aliquot of the charcoal supernatant was subjected to scintillation counting. Initial rates were evaluated by linear regression fitting, and K_m and k_{cat} were determined by fitting the initial rates to Michaelis-Menten equation using the program Grafit5 (Erythacus software).

3.3.16 Fast kinetics using stopped-flow measurement

This method was carried out according to Kraemer et al. (2002) to examine fast reaction kinetics using an SX18MV-Stopped-flow-apparatus (Applied Photophysics, Leatherhead, U.K.). Dansylated protein was excited with monochromatic light ($\lambda = 350$ nm, band width = 6,4 nm) and emission was followed using a cut-off filter ($\lambda > 408$ nm). For every time course, 1000 data points were measured.

3.3.16.1 Initial reaction assays

The reaction buffer was 50 mM Hepes (pH 7,5), 100 mM NaCl, 5 mM MgCl₂. 2 μ M Rap1-Aedans•GTP was 1:1 mixed with 50 μ M Rap1GAP in a stopped-flow apparatus and the fluorescence was followed. All traces shown are the average of at least three (in most cases five) individual measurements.

3.3.16.2 Displacement reaction

The reaction buffer was 50 mM Hepes (pH 7,5), 100 mM NaCl, 5 mM MgCl₂. 2 μ M Rap1-Aedans•GTP and 20 μ M Rap1GAP^{N290A} were mixed with 200 μ M non-labelled Rap1•GTP and the fluorescence monitored over 20 sec.

3.3.16.3 AIF₃ Binding assay

Rap1-Aedans was incubated with a catalytic amount of Rap1GAP at 20 °C for 120 min to convert it in the GDP bound form. For stopped-flow measurements, 2 μ M Rap1-Aedans•GDP in 50 mM Hepes (pH 7,5), 100 NaCl, 5 MgCl₂, 500 μ M AlCl₃, 5 mM NaF was rapidly mixed with 50 μ M of the corresponding Rap1GAP construct and the fluorescence monitored over 500 sec.

3.3.16.4 Data processing

The fluorescence was normalised by dividing all data points by the initial value. To determine observed rate constants (k_{obs}), individual traces were fitted to a monoexponential equation using the program Grafit 5 (Erithacus Software Limited). To determine association (k_{on}) and dissociation (k_{off}) rate constants, k_{obs} rates were plotted against the Rap1GAP concentration and the data points fitted to a linear fit equation in which the slope corresponds to the k_{on} and the intercept to the k_{off} rate (see Appendix).

To determine the affinity constant by equilibrium titration, the maximal amplitudes of the k_{obs} rate were plotted against the concentration of Rap1GAP and the data non-linearly fitted (see Appendix).

3.3.17 CD spectrometry

CD spectra were taken at a Jasco J-710 CD Spectrometer (Japan Spectroscopic Co. Ltd., Tokyo, Japan) in a 100 μm quartz cuvette with a band width of 1 nm, 1 nm step width, and 2 sec integration time. All spectra were 10 times accumulated. Data evaluation was done according to the Provenchor and Glockner method (Lobley et al., 2002)

3.4 Crystallographic methods

3.4.1 Crystallisation

For initial crystallisation trials, Rap1GAP was rapidly thawed and diluted to 20 mg/ml using 20 mM Hepes (pH 7,5), 5 mM DTE.

All crystallisation trials were carried out using the hanging drop method. 1 ml of reservoir solution containing buffer, salt and precipitant was temperature equilibrated and put in 24-well cell culture linbro plate (Linbro, Flow Laboratories Inc., USA). The hanging drop consisted of 1 - 4 μ l protein solution and 1 - 4 μ l reservoir solution. Since Rap1GAP was very susceptible to protease impurities, all crystallisation trials were carried out at 4 °C and 12 °C.

To reduce radiation damage, crystals were transferred in a cryo-solution and flash cooled in liquid nitrogen according to Hope (1988). Since Rap1GAP crystals were rather sensitive to osmotic changes, crystals were transferred in several steps in the cryo-solution thereby slowly increasing the cryo-protectant.

Initial tiny needles appearing after 14 days were obtained using Crystal Screen II from Hampton (Hampton Research, Laguna Hills, USA). The needles could be optimised in size using streak seeding and the following condition: T = 4 °C, [Rap1GAP] = 60 mg/ml, 550 mM ammonium sulfate, 30 mM citrate (pH 5,6), 240 mM potassium sodium tartrate. However, these needles did not diffract X-rays at all.

A second condition resulting in spherulites was found at 12 °C using the PEG-Ion screen from Hampton and a C-terminally truncated Rap1GAP construct (75-405). This condition could be improved to obtain tiny needles: [Rap1GAP] = 40 mg/ml, 8% PEG 2000 MME, 100 mM lithium acetate, T = 12 °C. Using the same condition but switching back to the Rap1GAP⁷⁵⁻⁴¹⁵ construct resulted in small 3-dimensional crystals. Crystal size could be improved by using the previously described fully active Rap1GAP^{75-415,Q204A} mutant which also showed a 3-fold higher amount of soluble protein than wild-type. The optimal crystallisation condition resulting in crystals with dimensions 400 x 100 x 50 μ m³ after 4 days were: [Rap1GAP^{Q204A}] = 45 mg/ml, 9% PEG2000 MME, 230 mM lithium acetate, 7% MPD with at least 4 μ l drops, T = 12 °C. The best cryo-condition found for this crystal form was 8% PEG 2000 MME, 20% MPD, 20 mM HEPES (pH 7,5), 5 mM DTE in which the crystals had to be slowly transferred in three steps over 30 min.

Since these crystals displayed a rather poor diffraction quality, bad reproducibility and a very large unit cell, it was decided to search for a new crystal form. Using similar conditions but re-screening 50 different salts, a new crystal form was discovered. Crystals with the final size of 300x100x50 μm^3 appearing after 7 days were finally obtained with the following reservoir conditions: [Rap1GAP] = 20 mg/ml, 9% PEG 2000 MME, 100-200 mM MgSO_4 , 5-7% MPD, 100 mM Hepes (pH 7,1). The optimal cryo-condition found for these crystals was 20% PEG 2000 MME, 100 mM MgSO_4 , 5% MPD, 100 mM Hepes (pH 7,1).

Mercury substituted crystals could be obtained by incubating crystals for 30 min in cryo-solution containing 1 mM HgCl_2 . Incorporation of mercury was confirmed by dissolving crystals in sinapinic acid matrix and by MALDI analysis as described in 3.3.4.

3.4.2 Data collection and processing

All frozen crystals were first tested at 100 K on a copper rotating X-ray anode with an osmic mirror ($\lambda = 1,5419 \text{ \AA}$, 50 kV, 100 mA, 0,1 mm collimator). The final datasets were obtained at beamline ID14-EH1 at the European synchrotron radiation facility (ESRF, Grenoble, France) at a wavelength of 0,934 \AA . An ADSC Q105 CCD-detector was used. For the native and the selenomethionine substituted crystal, the detector distance was 270 mm and the oscillation range 0,6°. 207 frames were collected for the native crystal and 423 frames for the selenomethionine substituted crystal. The quality of the dataset was validated by calculating R_{symm} which compares symmetry related reflections according to Equation 1.

$$R_{\text{symm}} = \frac{\sum_{hkl} \sum_i |I_i - \langle I \rangle|}{\sum_{hkl} \sum_i |I_i|} \quad \text{Equation 1}$$

h, k, l - indices of independent reflections with the average intensity $\langle I \rangle$
 I_i - intensities of independent reflections.

Data were processed using XDS/XSCALE package (Kabsch, 1993).

Based on the volume of the asymmetric unit and the molecular weight of the protein, the number of molecules in the asymmetric unit can be estimated (Matthews, 1968). The Matthew coefficient V_M is derived by Equation 2.

$$V_M = \frac{V}{M \cdot W \cdot Z} \quad \text{Equation 2}$$

MW: Molecular weight of the monomer in Dalton
 V: Volume of the asymmetric unit in Å³
 Z: Number of molecules in the asymmetric unit

The average Matthew coefficient of a protein crystal is 2,5 Å³/Da corresponding to a solvent content of 50% (Matthews, 1968). The solvent content x_s of a crystal can be estimated by Equation 3.

$$x_s = 1 - \frac{1}{V_M \cdot N_A \cdot \rho_P} \sim 1 - \frac{1.23 \text{ Å}^3/\text{Da}}{V_M} \quad \text{Equation 3}$$

V_m = Matthew coefficient
 N_A = Avogadro constant
 ρ_P = protein density ~ 1.35 g/cm³

3.4.3 Phase determination

A structure factor F_{hkl} can be represented as complex vector according to Equation 4 (Drenth, 1999; Rhodes, 2000).

$$F_{hkl} = A_{hkl} + iB_{hkl} \quad \text{Equation 4}$$

where A_{hkl} is a vector of length $|A_{hkl}|$ on the real-number line, and B_{hkl} is a vector of length $|B_{hkl}|$ on the imaginary-number line. F_{hkl} can be decomposed into its amplitude $|F_{hkl}|$ and its phase angle α_{hkl} which is the angle, the vector makes with the real number line (Equation 5).

$$F_{hkl} = |F_{hkl}| \cdot (\cos \alpha_{hkl} + i \sin \alpha_{hkl}) = |F_{hkl}| \cdot e^{i\alpha_{hkl}} = |F_{hkl}| \cdot e^{2\pi i \alpha'_{hkl}} \quad \text{Equation 5}$$

in which α is the phase angle in radians and α' the angle in cycles.

The electron density ρ at any point x, y, z can be calculated by Fourier synthesis according to equation 6 if the structure factors F_{hkl} of a crystal (Equation 5) are determined .

$$\rho(x,y,z) = \frac{1}{V} \sum_h \sum_k \sum_l |F_{hkl}| \cdot e^{-2\pi i(hx + ky + lz - \alpha'_{hkl})} \quad \text{Equation 6}$$

in which V is the volume of the unit cell and h,k,l are the indices of independent reflections.

The amplitude $|F_{hkl}|$ of every structure factor is proportional to the square root of the measured intensity, $(I_{hkl})^{1/2}$. The phase angle α' of every structure factor can principally be determined by four different techniques: Isomorphous replacement, single or multiple wavelength anomalous diffraction, molecular replacement or direct methods. In this work, isomorphous replacement and single wavelength anomalous diffraction have been used.

The isomorphous replacement method requires the attachment of heavy atoms to the protein molecules in the crystal. The heavy atom must not disturb crystal packing or the conformation of the protein. Furthermore, there must be measurable changes in at least a moderate number of reflection intensities between a native and derivative dataset. These intensity differences are then exclusively due to the attached heavy atoms.

By analysis of a difference Patterson function, the heavy atoms can be located in the asymmetric unit (Drenth, 1999; Rhodes, 2000). When these sites of the heavy atoms are known, one can calculate the structure factors of the heavy atoms alone according to Equation 7.

$$F_{hkl} = \sum_{j=1}^n f_j \cdot e^{2\pi i \cdot (hx_j + ky_j + lz_j)} \quad \text{Equation 7}$$

where n is the number of heavy atoms located by the difference Patterson function.

A single structure factor of the derivative dataset F_{HP} can be expressed by the corresponding structure factor of the native dataset F_P and the structure factor F_H derived from the heavy atoms according to Equation 8.

$$F_{HP} = F_H + F_P \quad \text{Equation 8}$$

$|F_P|$ and $|F_{HP}|$ can be derived from the measured intensity of the reflection. The structure factor F_H including phase angle can be calculated according to Equation 7. The phase angle of structure factor F_P can then be determined geometrically or numerically (Rhodes, 2000).

An alternative means of obtaining phases from heavy-atom derivatives takes advantage of the heavy atom's capacity to absorb X-rays of specified wavelength. The pairs of structure factors F_{hkl} and F_{-h-k-l} are called Friedel pairs, and it can be shown that $|F_{hkl}| = |F_{-h-k-l}|$ and $\alpha_{hkl} = -\alpha_{-h-k-l}$ (Friedel's law, Friedel, 1913). However, as a result of X-ray absorption by heavy atoms, Friedel pairs are not equal in intensity and do not have the same absolute value of α . This phenomenon is called anomalous scattering or anomalous dispersion.

$F_{hkl}^{HP\lambda 1}$ represents a structure factor for the heavy atom derivative which is measured at a wavelength $\lambda 1$ where anomalous scattering does not occur. It can be expressed by $F_{hkl}^{HP\lambda 2}$ which represents the equivalent structure factor at a wavelength $\lambda 2$ where anomalous scattering does occur according to Equation 9.

$$F_{hkl}^{HP\lambda 2} = F_{hkl}^{HP\lambda 1} + \Delta F_r + \Delta F_i \quad \text{Equation 9}$$

where the vectors representing anomalous scattering contributions are ΔF_r (real) and ΔF_i (imaginary).

The magnitude of anomalous scattering contributions ΔF_r and ΔF_i for a given element at a given wavelength is constant and can be found in crystallographic tables. The phases of ΔF_r and ΔF_i can be computed when the locations of the anomalous scatterers are determined by Patterson methods (Drenth, 1999). The phase angle of structure factor F_{HP} can then be determined from the difference in F_{hkl} and F_{-h-k-l} by geometrical or numerical means (Rhodes, 2000).

SHELXD (Schneider and Sheldrick, 2002) was used to find selenium sites of selenomethionine substituted crystals by using the anomalous signal of the selenium atoms and the isomorphous signal between native and selenomethionine substituted crystals (SIRAS phasing). Selenium sites were refined and initial phases calculated using the program Sharp (Buster Development Group). Solvent flattening was carried out using the program SOLOMON. An initial model was built using the program XFit from the XtalView program package (McRee, 1999).

3.4.4 Refinement

Refinement is an iterative process required to improve the initial phases and to correct the geometry of the model. An initial model is improved by minimizing the

energy of a geometrical and a crystallographic energy term. The geometrical term of a model contains bond length, bond angles, torsion angles, non-bonded interactions, hydrogen bonds, van-der-Waals interaction, planar restraints and chiral centre restraints of the input model. The crystallographic term appreciates the amplitudes of the measured reflections $|F_{obs}|$. With the refined model, new structure factors (F_{calc}) are calculated. A measure of the quality of a model can be derived from R_{cryst} which compares measured and calculated structure factors according to Equation 10.

$$R_{cryst} = \frac{\sum ||F_{obs}| - |F_{calc}||}{\sum |F_{obs}|} \quad \text{Equation 10}$$

Using the calculated phases and the measured reflection intensities, an improved electron density map can be calculated. Since the calculated phases are biased towards the potentially wrong model, a test set of reflections is excluded from the refinement (typically 5–10% of the reflections). These reflections are used to calculate R_{free} similar to Equation 10 (Brunger, 1992; Brunger, 1997). R_{free} is a rather non-biased measure of the quality of the protein model.

The program Refmac5 was used for refinement here (Murshudov et al., 1997). Typically, it refines the temperature factors of every atom and then the position. 5% of the reflections were used as test set. A typical refinement cycle started with 10 cycles of TLS (translation, libration, screw-rotation displacement) refinement using 10 independent protein bodies (Winn et al., 2003) followed by 5 cycles of positional refinement using a high weight for the geometrical energy term in comparison to the crystallographic term.

The model was validated by the programs Procheck (Laskowski et al., 1993) and Whatcheck (Hoofst et al., 1996). Contacting amino acids in the Rap1GAP dimer interface were identified using the CCP4 program Contact (Bailey, 1994). The plot of contacting amino acids in the dimer interface was generated using the program Ligplot (Wallace et al., 1995). The area of buried surface between two monomers was determined using the CNS program suite (Brunger et al., 1998). The structure alignment between the catalytic domain of Rap1GAP and Ras was performed using the program structalign (Shindyalov and Bourne, 1998).

3.4.5 Figure preparation

Ribbon plots and ball-and-stick models were prepared using the program Molscript (Kraulis, 1991). All surface plots were prepared using the program GRASP (Nicholls et al., 1993). Electron density plots were prepared using the program Bobscript (Kraulis, 1991). The stereo image was generated using the program gl_render and rendered with Povray (www.povray.org). All other plots were rendered with Raser3D (Merritt and Bacon, 1997). The final figures were prepared with Adobe Photoshop and CorelDraw10 (Corel Corporation).

4 Results

4.1 Initial characterisation of Rap1GAP

4.1.1 Expression

It has previously been shown by deletion analysis that residues 75–415 of Rap1GAP are sufficient for full Rap1GAP activity (Rubinfeld et al., 1991). To characterise Rap1GAP mediated catalysis, the catalytic domain of Rap1GAP (amino acids 75–415, from here Rap1GAP) was expressed as GST fusion and purified by affinity chromatography according to Brinkmann (2000) (see 3.3.5). To remove bacterial GroEL, which was bound to Rap1GAP, the column had to be washed extensively with buffer containing potassium ions and ATP. GST was finally cleaved with thrombin to obtain catalytically active Rap1GAP. A typical protein purification yielding at least 80% pure protein is documented in Figure 16.

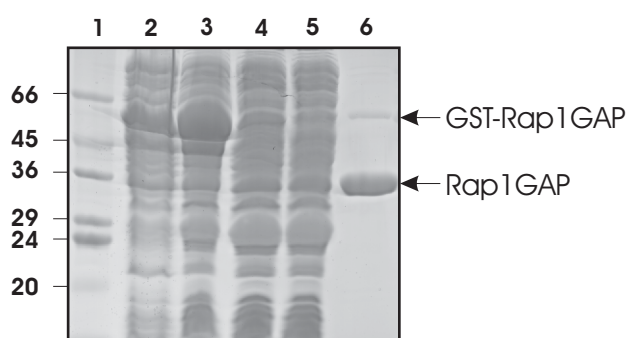


Figure 16. Human Rap1GAP was expressed in bacteria as GST fusion and purified using affinity chromatography. 1) Marker. 2) Non-induced culture. 3) Induced culture. 4,5) Soluble extract before (4) and after (5) application on a GSH column. 6) Purified protein after thrombin cleavage.

4.1.2 Biochemical characterisation of Rap1GAP

The enzymatic activity of Rap1GAP was characterised in cooperation with T. Brinkmann (Brinkmann et al., 2002). To obtain Michaelis-Menten parameters for the Rap1GAP stimulated GTPase reaction, Rap1GAP was used in constant concentration (100 nM) as enzyme and Rap1•GTP in varying concentrations as substrate. Initial rates of GAP stimulated GTP hydrolysis were determined by a radioactive charcoal assay (3.3.15). The reaction showed a typical Michaelis-Menten behaviour (Figure 17).

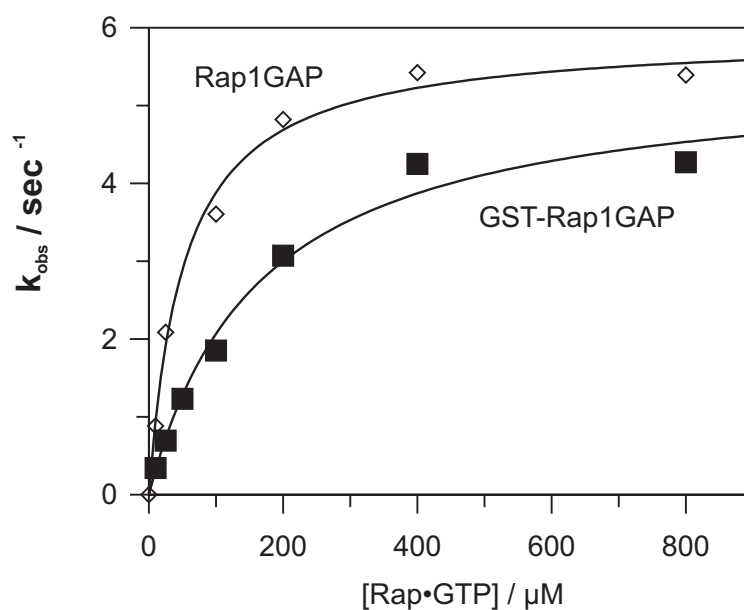


Figure 17. Michaelis-Menten kinetic of the Rap1GAP-stimulated reaction. 100 nM Rap1GAP or GST-Rap1GAP were used as enzyme and increasing concentrations of Rap1•[γ - ^{32}P]GTP as substrate, in standard buffer at 25 °C . GTP hydrolysis was monitored by measuring P_i release. Observed rate constants were fitted to Michaelis-Menten equation for determination of k_{cat} and K_m . These data were provided by T. Brinkmann (Brinkmann et al., 2002).

By non-linear regression fitting of the observed rates, a k_{cat} of 6 sec^{-1} and a K_m of $50 \mu\text{M}$ were obtained. The k_{cat} is in a similar range to that of GAP stimulated reactions of Ras (Ahmadian et al., 1997a), Rho (Graham et al., 1999), Ran (Klebe et al., 1995) and Rab (Albert et al., 1999) which are all in the range of 5 to 20 sec^{-1} . When comparing the k_{cat} (6 sec^{-1}) to the non-stimulated reaction ($2 \cdot 10^{-5} \text{ sec}^{-1}$) under these conditions, a more than 10^5 -fold acceleration of GTP hydrolysis in Rap1 is observed. These results clearly indicate that the purification protocol yields a highly active, folded Rap1GAP protein.

GST often stabilises proteins which are expressed as GST fusions. Since the following experiments required many Rap1GAP mutants and it was speculated that the mutants might be less stable than wild-type, GST-Rap1GAP was also tested for activity using Michaelis-Menten kinetics (Figure 17). Indeed, similar rates for k_{cat} (6 sec^{-1}) and an only somewhat higher K_m ($160 \mu\text{M}$) were observed. Thus, the GST fusion proteins could be used for the subsequent experiments.

4.1.3 Arginine mutants

With the exception of RanGAP and possibly ArfGAP, GAPs for small GNBPs contain a catalytic arginine which is inserted into the catalytic site of the GNPB to complement the incomplete catalytic machinery. It was asked whether Rap1GAP also employs a catalytic arginine which should then be conserved among different Rap1GAPs.

To identify the conserved arginines in Rap1GAP, sequences from human Rap1GAP, Spa1, E6TP1, *Drosophila melanogaster* Rap1GAP and *Caenorhabditis elegans* Rap1GAP and Spa1 were aligned (Table 3).

Seven conserved arginines were identified (R91, R128, R132, R284, R286, R388 and R390). To test whether they are involved in catalysis, they were individually mutated to alanine and the mutant proteins were purified according to standard procedures. For one of the mutants, R132A, only little amount of soluble protein could be obtained which was only partially cleavable by thrombin indicating that the mutation destabilised the protein. The activity of the mutants was checked at a Rap1•GTP concentration of 200 μ M using the charcoal assay (Figure 18).

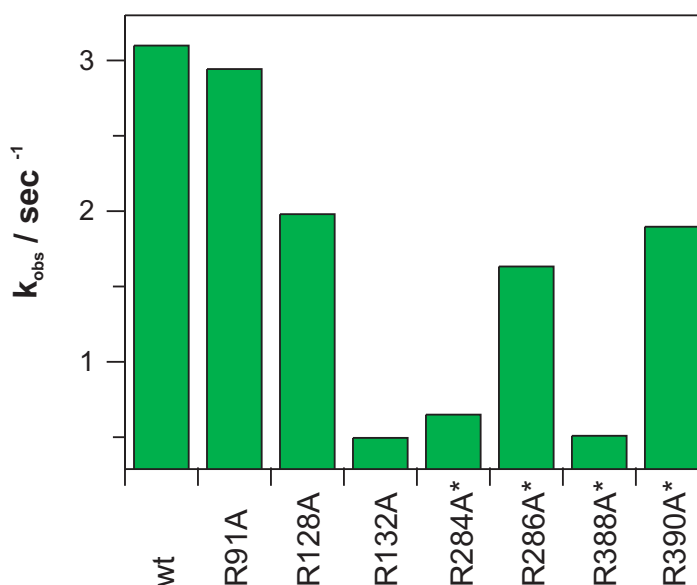


Figure 18. Probing the GAP mechanism by arginine mutations. Invariant arginine residues were mutated to alanine. The mutants were purified and the GAP activity was measured under the standard condition, which is 100 nM Rap1GAP, 200 μ M Rap1•[γ - 32 P]GTP in standard buffer at 25 °C. Initial rates were determined by measuring several time points and plotted in a bar diagram. Mutants indicated with * were examined by T. Brinkmann (Brinkmann, 2000).

Under these conditions, the R91A, R128A, R286A, and R390A mutants retained more than 50% of wild-type activity whereas the mutants R284A and R388A exhibited a 3- to 4-fold decrease in GAP activity. The mutant R132A showed between 10% and 20% of the wild-type activity depending on the preparation, which might be explained by the instability of this protein. None of the mutants had a dramatically decreased Rap1GAP activity as expected for a catalytic arginine which in the case of RasGAP reduces activity more than 1000-fold when mutated to alanine. It can be concluded that Rap1GAP does not possess a catalytic arginine indicating a novel mechanism of GAP mediated GTP hydrolysis.

4.1.4 Lysine and glutamine mutants

Since none of the arginines appeared to contribute to catalysis, other conserved residues were analysed which might replace the missing arginine residue. Since lysine, similar to arginine, could in principle be used for stabilisation of the GTP hydrolysis transition state as found for the nitrogenase complex in the $\text{ADP}\cdot\text{AlF}_4^-$ bound state (Schindelin et al., 1997), all three invariant lysine residues of Rap1GAP were mutated to alanine and the activity of the mutants measured using the charcoal assay. While lysine K368 does not appear to be important for catalysis, a large drop in catalytic activity was found for the mutants K194A and K285A. Using a GAP concentration of 2 μM and 5 μM , respectively, it was estimated that K194A and K285A are at least 25- and 100-fold less active than the wild-type at a concentration of 200 μM Rap1•GTP (Figure 19A).

To find out whether the mutants K194A and K285A have a lower affinity to Rap1 or a reduced catalytic activity, they were analysed using Michaelis-Menten kinetics (Figure 19B). It was not possible to saturate these mutants by using up to 800 μM Rap1•GTP. This clearly shows that the mutants have a reduced affinity for Rap1•GTP. However, it can not be excluded that they might also have reduced catalytic activity.

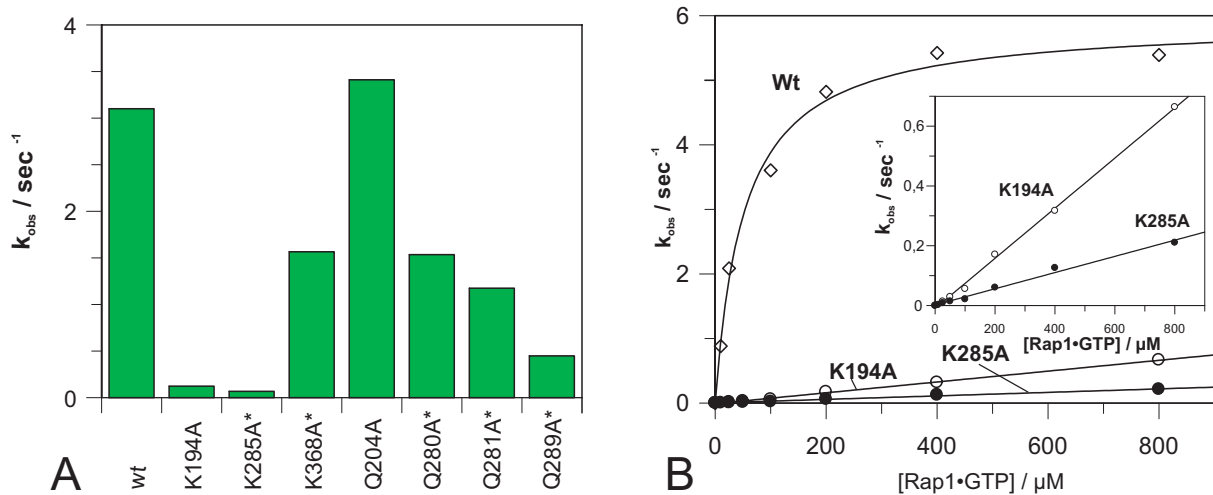


Figure 19. Mutational analysis of conserved lysine and glutamine residues. **A)** Conserved lysines and glutamines of Rap1GAP were mutated to alanine and the GAP activity analysed under standard conditions. Mutants indicated with * were analysed by T. Brinkmann. For the mutants K194A and K285A, an enzyme concentration of 2 μM and 5 μM was used. **B)** For further analysis, Michaelis-Menten kinetics of mutants K194A and K285A (*) were measured under standard conditions, shown in comparison to wild-type. The inset has a different scale.

Members of the Rap family do not use a catalytic glutamine, nevertheless are able to hydrolyse GTP. Since glutamine is of crucial importance for the GTP-hydrolysis reaction of most other small GNBPs, it was examined whether Rap1GAP might provide a catalytic glutamine in trans to stimulate GTP hydrolysis in Rap1. All four invariant glutamine residues (glutamines Q204, Q280, Q281 and Q298) were mutated to alanine and the activity of the mutants was analysed. As shown in Figure 19A, the Q204A mutation had no effect on catalysis. The Q280A and Q281A mutants had a 2-fold and the Q298A mutant a 6-fold reduced activity at a concentration of 200 μM Rap1•GTP. This is, however, much less than what would be expected for a residue replacing glutamine Q61 whose mutation in Ras or Ran reduces GAP activity by more than five orders of magnitude.

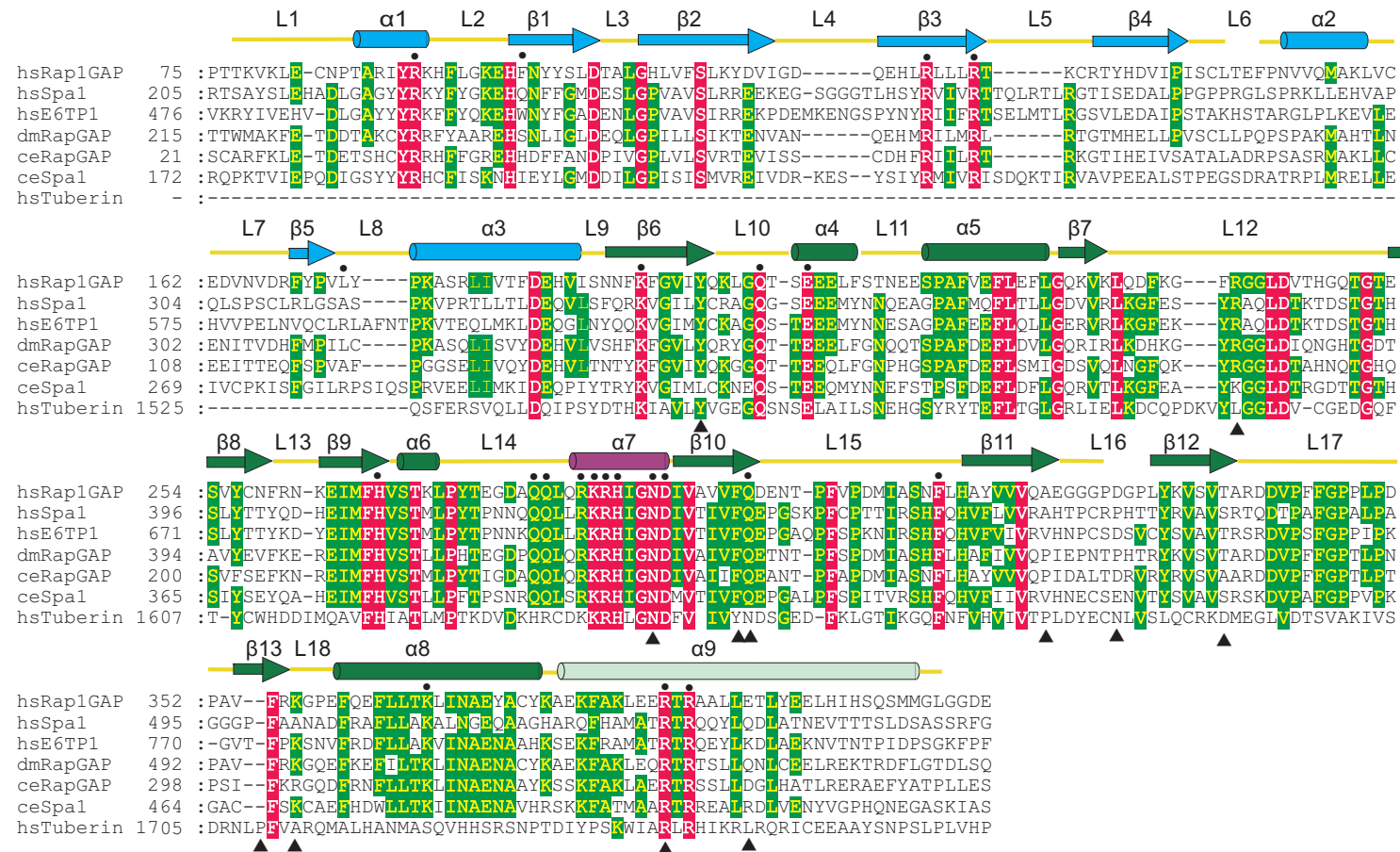


Table 3 Sequence alignment of various Rap1GAPs and Tuberin. The sequences are *Homo sapiens* Rap1GAP (Swiss-Prot accession number (SW) P47736), *Homo sapiens* Spa1 (SW O60618), *Homo sapiens* E6TP1 (SW Q9UNU4), *Drosophila melanogaster* RapGAP (SW O44090), *Caenorhabditis elegans* RapGAP (SW P91315), *Caenorhabditis elegans* Spa1 (SW Q20016) and *Homo sapiens* Tuberin (SW P49815). Completely conserved residues are boxed in red, highly conserved residues (>50 %) in green. Secondary structure elements as derived from the Rap1GAP structure are depicted on top (Figure 24A). The interaction helix with the catalytic asparagine is coloured in purple. Mutations in Tuberin found in tuberous sclerosis patients are indicated with ▲.

4.2 The Rap1GAP structure

From the results in chapter 4.1 it was concluded that Rap1GAP uses a completely novel mechanism to stimulate GTP hydrolysis in Rap1. No arginine is provided for catalysis and no catalytic glutamine is involved in this reaction. However, two lysine residues, lysine K194 and lysine K285, were identified whose mutation drastically reduced the Rap1GAP activity. To clarify the role of these two lysines and to get insights into the mechanism of GTPase stimulation, the structure of Rap1GAP was determined by X-ray crystallography.

4.2.1 Purification

Since the initially described purification procedure yielded protein which still contained GroEL contaminations, Rap1GAP was further purified using size exclusion chromatography. HEPES was chosen as a buffer, since PBS in which the protein was initially purified is not suited for crystallisation and since it was observed that diluting the protein in TRIS buffer led to protein precipitation. In HEPES buffer, the protein could be concentrated up to 100 mg/ml without any precipitation. Surprisingly, Rap1GAP did not elute as a monomer but as a protein with an apparent mass of 100 kD from gel filtration.

4.2.2 Degradation and partial digest

Rap1GAP was more than 95% pure after size exclusion chromatography as judged by SDS-PAGE analysis (Figure 20). However, after several days at 8 °C, Rap1GAP degradation was observed (Figure 20, lane 2 and 4). This implies that Rap1GAP has flexible loops which are accessible for contaminating proteases. Degradation poses a problem for crystallisation for which stable fragments are required.

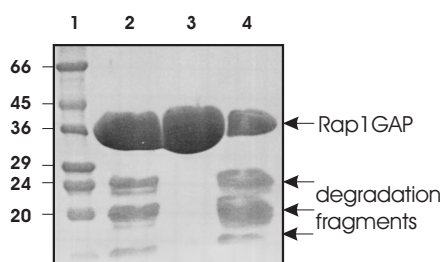


Figure 20. Degradation of Rap1GAP. 1) Marker 2) Rap1GAP after 8 days at 8 °C. 3) Rap1GAP after purification. 4) Rap1GAP after 14 days at 8 °C.

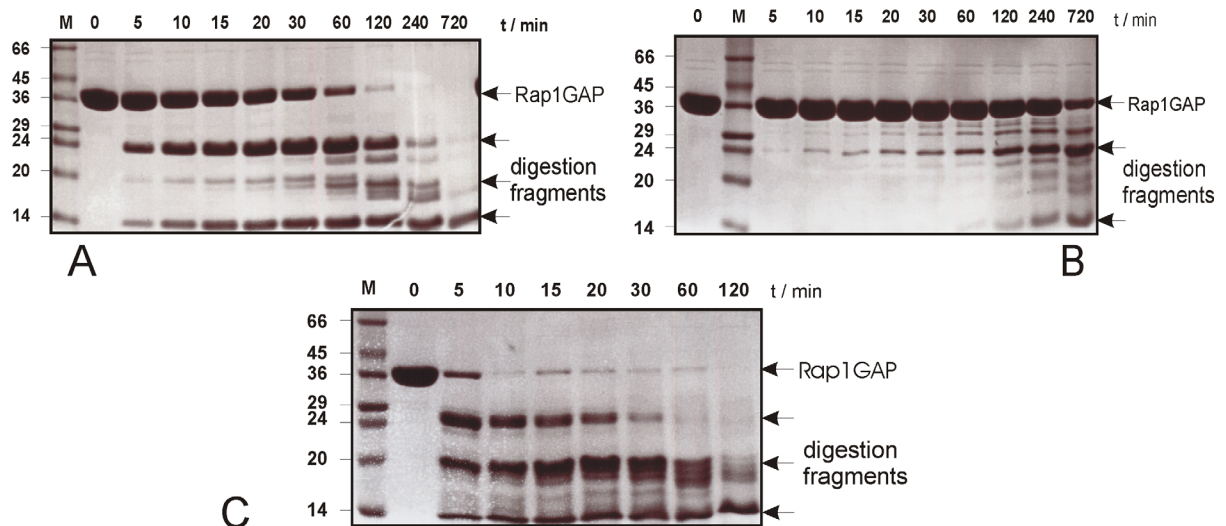


Figure 21. Partial digests of Rap1GAP (3.3.10) with trypsin (A), elastase (B) and papain (C). Digests were started by addition of protease. After the indicated time points, aliquots were taken and analysed by SDS-PAGE using 15% polyacrylamide gels.

To obtain a stable Rap1GAP fragment, various proteases were tested in a partial-digest experiment (see 3.3.10). Trypsin, elastase and papain led to specific degradation bands (Figure 21).

A peptide fragment which appeared in degradation experiments and partial digests run as a 24 kD band in SDS-PAGE. Its exact mass was determined by MALDI to be 24,4 kD. By further MALDI analysis, it was shown to be a C-terminal Rap1GAP fragment (see 3.3.9) corresponding to amino acids 178-415 of Rap1GAP. This fragment was expressed as a GST fusion in *E.coli* but appeared only in the insoluble fraction.

4.2.3 High throughput cloning

To obtain a soluble stable Rap1GAP fragment for crystallisation, various Rap1GAP homologues were tested for expression. Since human Rap1GAP could be expressed as a soluble GST fusion in bacteria and Rap1GAPs show an extensive homology it was reasoned that this expression system is also appropriate for the other Rap1GAP homologues.

Based on the Rap1GAP construct, two constructs of human E6TP1, two of human Spa1, seven of *Drosophila melanogaster* Rap1GAP, one of *Dictyostelium* Rap1GAP and five of human Tuberin were prepared (see 3.2.11). However, the expressed proteins were either insoluble, degraded or precipitated upon removal of GST. None of them could be used for crystallisation trials.

Consequently, shortened human Rap1GAP constructs were prepared since flexible N- or C-termini might interfere with crystallisation. An N-terminal truncated GST-Rap1GAP construct comprising amino acids 85-405 could be prepared and showed Rap1GAP activity. However, it was not possible to remove the GST by thrombin cleavage. Probably, the thrombin cleavage site was not accessible. However, Rap1GAP⁷⁵⁻⁴⁰⁵ truncated by ten amino acids at the C-terminus could be purified in large amounts and showed Rap1GAP activity comparable to the original construct (data not shown).

4.2.4 Crystallisation

Rap1GAP and Rap1GAP⁷⁵⁻⁴⁰⁵ were used for crystallisation trials using the hanging drop method. As an initial condition, the standard solutions from Hampton Research screens were used in a 1:3 dilution. To reduce degradation problems, all crystallisation trials were carried out at 4 °C or 12 °C.

Initial tiny protein needles from Rap1GAP could be obtained using ammonium sulfate as a precipitant at 4 °C (Table 4A, details in 3.4.1). The size of the crystals could be improved by adjusting these conditions (Table 4B). However, this crystal form did not diffract X-rays.

For Rap1GAP⁷⁵⁻⁴⁰⁵, spherulites (microcrystals) were found using PEG as a precipitant (Table 4C). Optimisation of the condition led to tiny needles (Table 4D). Using the same condition but switching back to Rap1GAP, small needles were obtained (Table 4E) which could be optimised to yield small three-dimensional crystals (Table 4F). The size of these crystals could be increased by using the Rap1GAP^{Q204A} mutant (Table 4G). This mutant has similar activity as the wild-type (4.1.4) but could be purified in 3-fold higher amounts. The optimised conditions yielded protein crystals with dimension 200x100x100 μm^3 (Table 4H).

These crystals were tested for diffraction. However, even after extensive adjustment of the cryo freezing conditions, their maximal diffraction was only 3,5 Å at a synchrotron beamline. Furthermore, the crystals exhibited a large orthorhombic unit cell size (300 x 140 x 100 Å³) with predicted 8-12 monomers in the asymmetric unit which made de novo phase determination difficult to achieve.

To find another crystal form with smaller unit cell, new crystal screens were performed. By modifying the pH and testing 50 new salt conditions, a new crystal form with smaller unit cell size was discovered (Table 5). These crystals could be

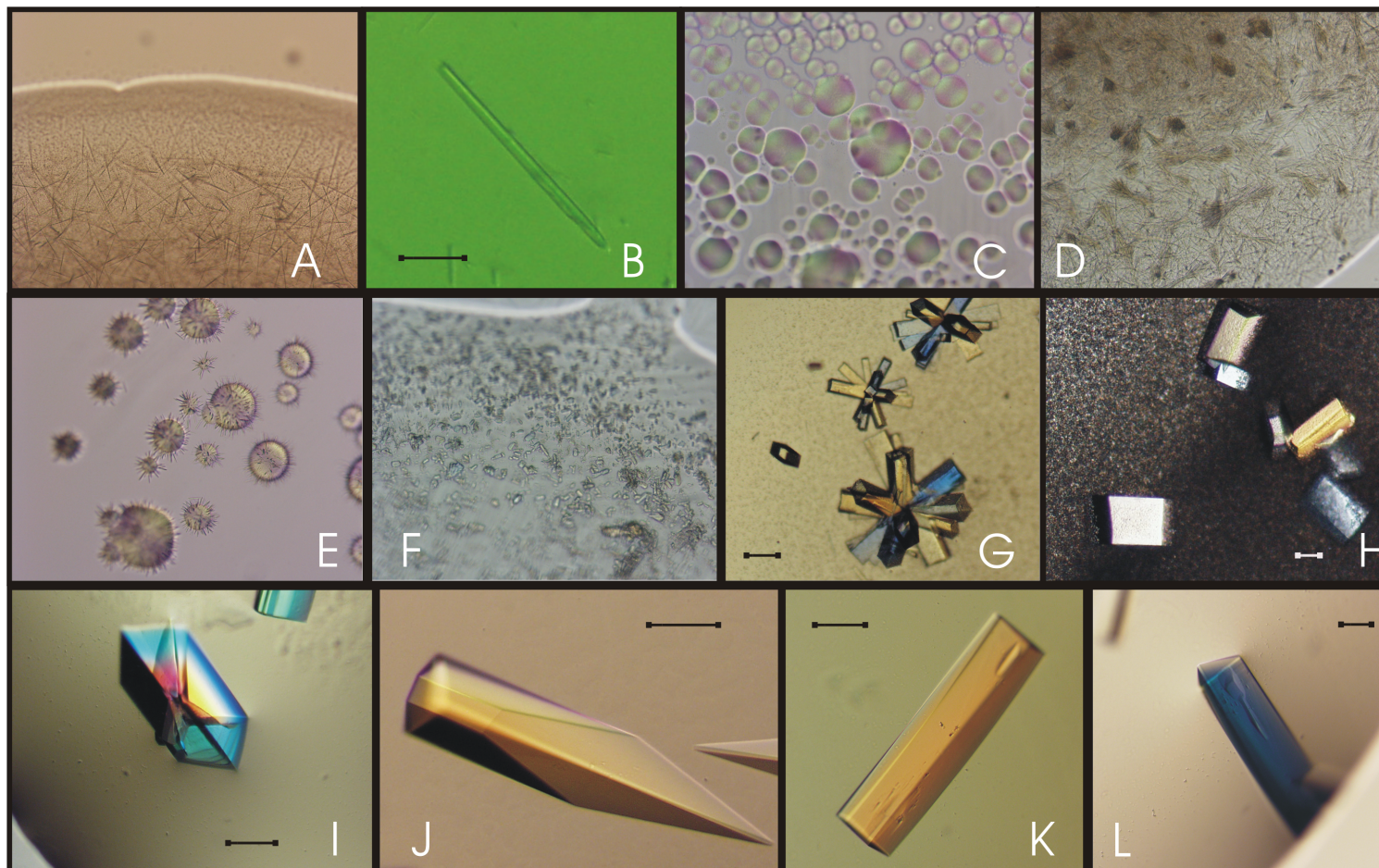


Table 4 Photos of several Rap1GAP crystals. A) Initial needles of Rap1GAP using ammonium sulfate as a precipitant. B) Fine-tuned condition of A. C) Rap1GAP⁷⁵⁻⁴⁰⁵ spherulites using PEG as a precipitant. D) Fine-tuned condition of C. E) Reservoir solution similar than in D but Rap1GAP used instead of Rap1GAP⁷⁵⁻⁴⁰⁵. F) Condition similar to E but Rap1GAP^{Q204A} used instead of Rap1GAP. G,H) Optimised condition from F. I, J, K,L) Final Rap1GAP^{Q204A} crystals. The bar indicates 100 μm.

improved to a final size of 300x100x100 μm^3 (Table 4 I, J, K). They were flash cooled in a cryo-solution and diffracted to 3,2 Å on a copper rotating anode. Selenomethionine substituted protein was prepared and crystallised by using the same conditions as for the wild-type protein.

4.2.5 Structure determination

Datasets of native and selenomethionine substituted Rap1GAP crystals were collected at the European Synchrotron Radiation Facility (ESRF), beamline ID14-EH1 in Grenoble. The native crystals diffracted to a maximal resolution of 2,9 Å and have an orthorhombic space group with unit cell dimensions 170x224x49 Å³. Assuming four molecules in the asymmetric unit, a Matthews coefficient of 3,1 Å³/Da was calculated, indicating approximately 60% solvent content in the crystal. The selenomethionine substituted crystals diffracted to 3,1 Å and have nearly identical unit cell dimensions. Data collection statistics of both native and selenomethionine substituted crystals are summarised in Table 5.

Table 5 Data statistics of native and selenomethionine substituted crystals.

Data collection	Native	SeMet ^a
Wavelength	0,934 Å (ID14-EH1)	0,934 Å (ID14-EH1)
Resolution	20 – 2,9 Å	20 – 3,1 Å
Space group	P2 ₁ 2 ₁ 2	P2 ₁ 2 ₁ 2
Unit cell	a = 170,7 Å, b = 224,4 Å, c = 48,7 Å, $\alpha = \beta = \gamma = 90^\circ$	a = 171,3 Å, b = 224,2 Å, c = 48,8 Å, $\alpha = \beta = \gamma = 90^\circ$
V _M (Å ³ /Da)	3,09	3,10
Completeness (%)	98,2	97,9
Reflections (unique)	208333 (42290)	356220 (65145)
R _{symm} ^{a,b}	4,9 (4,8)	5,5 (5,4)
I/σ(I)	17,3 (4,0)	13,3 (4,0)
Wilson-B (Å ²)	71	73

^aFor the SeMet data Friedel pairs were treated as separate observations

^bR_{symm} = $\sum |I(h)_i - \langle I(h) \rangle| / \sum I(h)_i$ where I(h)_i is the scaled observed intensity of the i-th symmetry-related observation of reflection h and $\langle I(h) \rangle$ is the mean value

Using the anomalous differences of the derivative data and the isomorphous differences between the native and selenomethionine data, initial protein phases could be calculated and improved by solvent flattening. The electron density indicated four molecules in the asymmetric unit, although only three were clearly defined in the electron density. The best defined molecule (in the following molecule A) was built. By using the non-crystallographic symmetry operators derived from the selenium sites, the model could be extended to the asymmetric unit. After few rounds of initial rigid body refinement, the model was improved by several rounds of B-factor and positional refinement and manually rebuilt. Apart from the protein molecules, 60 water, 2 sulfate ions and 2 MPD molecules were included in the final model. The model has an R_{cryst} of 23,3% and an R_{free} of 27,6% which is in the normal range of models at this resolution. The Ramachandran plot shows no residues in the disallowed region (Figure 22). This proves that the weighting of the geometry term during refinement was high enough. Phasing and refinement statistics are summarised in Table 6.

Table 6 Phasing and refinement statistics of the Rap1GAP model.

Phasing statistics	
Phasing power anomalous (highest resolution shell)	1,3 (0,8)
Phasing power isomorphous (highest resolution shell)	2,0 (2,1)
FOM (highest resolution shell)	46% (34%)
FOM after solvent flattening (highest resolution shell)	83% (64%)
Refinement statistics	
Resolution (Å)	15-2,9
Unique reflections (test set)	40001 (2103)
Number of amino acids (protein atoms)	1041 (8168)
Number of sulfate ions	2
Number of MPD molecules	2
H ₂ O	60
R_{cryst} (R_{free}) (%)	23,3 (27,6)
Resolution (Å)	15-2,9
Rms deviation from standard geometry	
Bond length (Å)	0,015
Angle (°)	1,7
Torsion angle (°)	7,6

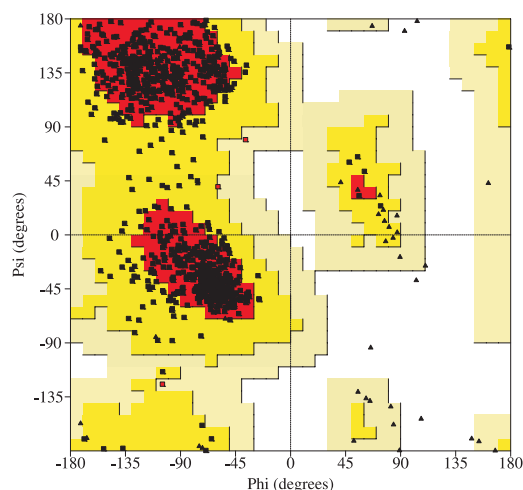


Figure 22. Ramachandran plot showing the torsion angles of all peptide bonds of the Rap1GAP model. Triangles represent glycine and proline residues, squares all other amino acids. 85% of all amino acids have torsion angles in the most favoured region (red background), 14,5% in the additional allowed region (yellow background) and 0,5% in the generously allowed region (red squares). None of the residues has a phi-psi combination in the disallowed region. The plot was generated using the program Procheck (Laskowski et al., 1993).

Two of the four molecules are well defined in the electron density (molecule A and molecule C), molecule B is less well defined and molecule D could be build only partially. Additionally, molecule D has the highest temperature factors (B-factors) and molecule B has higher temperature factors than molecule A and C (Figure 23). This indicates that molecule B and especially molecule D are not well ordered within the crystal. This assumption can be explained by the crystal packing since molecules B and D have only few crystallographic contacts. Especially molecule D has only contacts to symmetry-related D molecules. In contrast, molecule A interacts extensively with molecule C leading to stabilisation in the crystal. Since disordered atoms in a crystal do not contribute significantly to the diffraction pattern, this would explain why the R values from refinement are in a normal range despite more than 200 amino acids of molecule D are not included in the model. A disordered molecule D could also be the reason for the rather poor diffraction quality of the crystals.

The model of molecule A which is described in the following includes amino acids 78-147, 150-325 and 330-412. Amino acids 146, 147 and 411 are modelled as alanines due to missing electron density for the side chains. Molecule B includes amino acids 79-145, 150-232, 239-242, 250-275, 279-322, 332-411 and several residues were modelled as alanines. In molecule C, residues 77-144, 148-323, 330-409 could be modelled and amino acids 143, 144, 148, 215, 322 were modelled

as alanines. Finally, in molecule D, residues 90-103, 113-120, 126-131, 151-154, 168-186 and 395-409 are built and several residues were modelled as alanines.

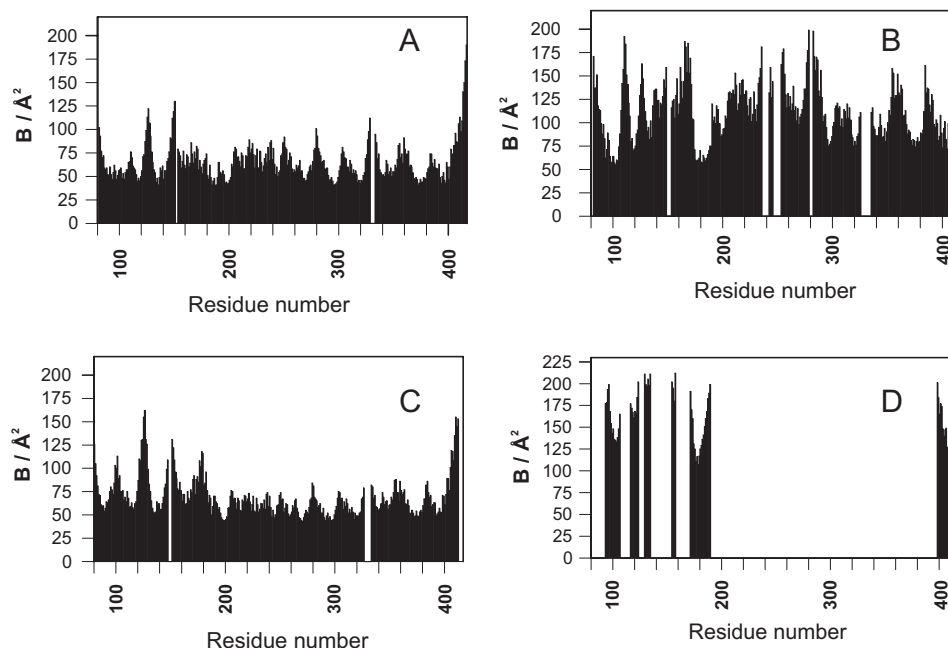


Figure 23. Temperature (B-) factors of molecules A–D. Molecule A and C have comparable temperature factors and nearly all residues could be built. Molecule B has higher temperature factors and some residues are missing whereas in chain D, only few amino acids could be built which have very high temperature factors indicating the high flexibility of molecule D within the crystal lattice.

4.2.6 Topology

Secondary structure elements were numbered according to their appearance ($\alpha 1$ - $\alpha 9$, $\beta 1$ - $\beta 13$, L1-L18), starting from the N-terminus (Table 3, Figure 24, Figure 25). Each Rap1GAP molecule consists of two domains, both containing a central β -sheet surrounded by α -helices. The smaller domain (residues 75-189) was termed the “dimerisation domain”, the larger domain (residues 190-379) which is homologous to Tuberin was called the “catalytic domain” (for explanation see below). The long C-terminal helix $\alpha 9$ (residues 380-409) folds back from the catalytic onto the dimerisation domain.

The N-terminal dimerisation domain contains a central 5-stranded anti-parallel β -sheet (Figure 24, Figure 25). Helix $\alpha 2$ on one side and helices $\alpha 1$, $\alpha 3$ and $\alpha 9$ on the other side are packed against the central β -sheet. Helix $\alpha 9$ (amino acids 382-412) has extensive hydrophobic contacts to helix $\alpha 3$ and strand $\beta 1$ of the dimerisation domain but nearly no contacts to the catalytic domain.

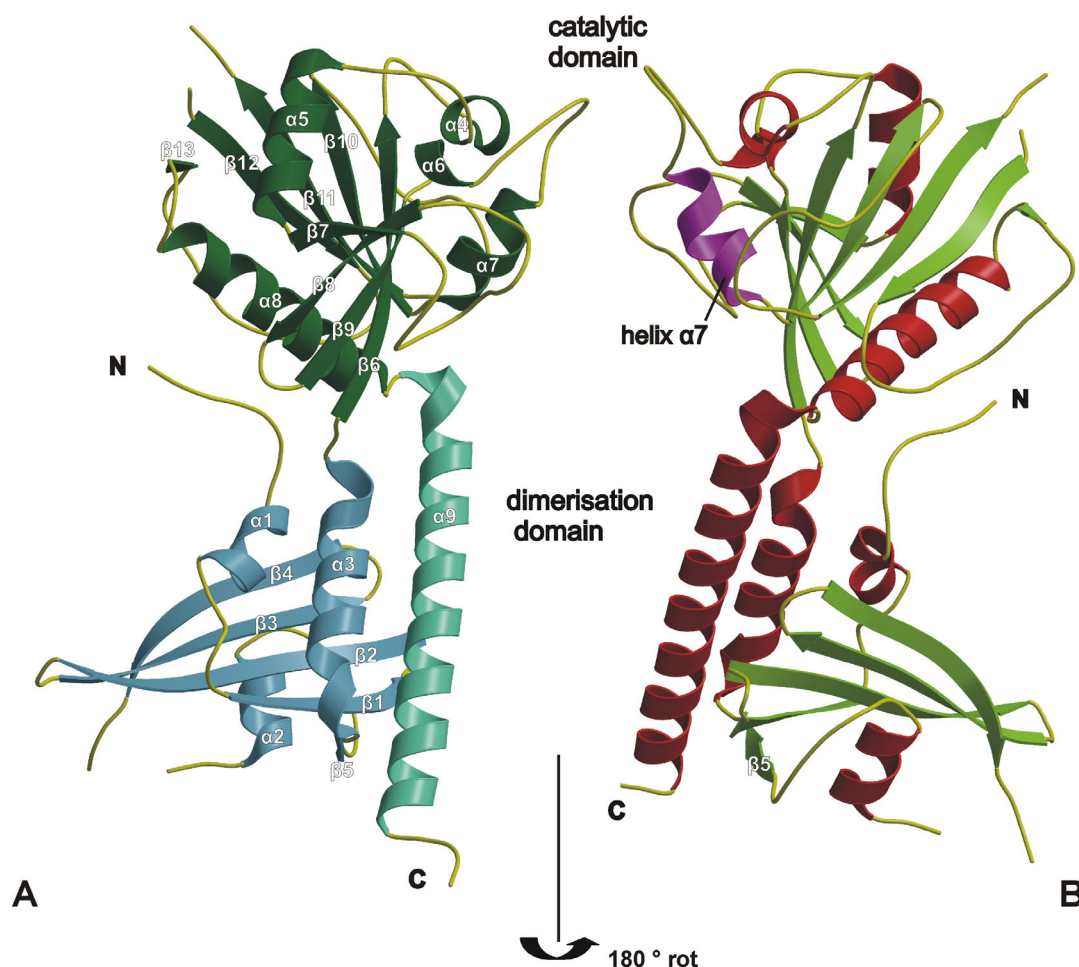


Figure 24. Ribbon type presentation of the Rap1GAP monomer with views from opposing sides. In A secondary structure elements are coloured according to the domain architecture. In B helices are coloured in red and strands in green. Helix $\alpha 7$ is shown in magenta.

The catalytic domain shows higher sequence conservation than the dimerisation domain within the Rap1GAP family. It is built of amino acids 190-379 and contains an 8-stranded mixed, curved β -sheet. Helices $\alpha 5$ and $\alpha 8$ from one side and helices $\alpha 4$, $\alpha 6$ and $\alpha 7$ from the other side are packed against the central β -sheet (Figure 24).

The catalytic and the dimerisation domain are connected only loosely and it was asked whether they might be connected by a flexible hinge. This could be reflected in different angles between catalytic and dimerisation domain in the different molecules of the asymmetric unit. To test this hypothesis, all visible molecules were overlaid and the angles between the domains analysed using the program dyndom (data not shown, Bailey (1994)).

Molecules A, B and C could be overlaid with low deviations of their C_{α} carbon atoms (0,5 Å rmsd for molecule A and B, 0,7 Å rmsd for molecule A and C). No hint for a hinge between the both domains was found. Thus in the crystal structure, the two

domains appear to be fixed relative to each other, although it cannot be excluded that they are more flexible in solution.

In comparison to GAPs of other GNBPs, the Rap1GAP fold is unique. To find out whether other proteins than GAPs possess structural similarity to Rap1GAP, a structural homology search was performed against all published protein structures using the DALI server (Holm and Sander, 1993). Surprisingly, the closest relative of Rap1GAP was found to be the superfamily of small GNBPs including Ras and Rap1 which have structural homology to the Rap1GAP catalytic domain.

Strands $\beta 1$ - $\beta 5$ and additionally helices $\alpha 1$, $\alpha 2$ and $\alpha 5$ can be superimposed to strands $\beta 6$ - $\beta 11$ and helices $\alpha 5$, $\alpha 7$, $\alpha 8$ of the Rap1GAP catalytic domain, respectively (Figure 25, Figure 26). At the P-loop position of Ras, Rap1GAP has a much longer insertion consisting of two loops and helix $\alpha 4$. Switch I of Ras is replaced by an insertion in Rap1GAP consisting of an additional strand $\beta 7$ and a large loop. An equivalent to strand $\beta 7$ in Rap1GAP can be found as strand $\beta 2E$ for example in the small GNBPs Ran (Scheffzek et al., 1995) and in the GDP bound forms of Arf (Greasley et al., 1995) and Arl (Hillig et al., 2000). Helix $\alpha 2$ of switch II in Ras superimposes with helix $\alpha 7$ of Rap1GAP. Finally, helix $\alpha 3$ of Ras is replaced by a long loop in Rap1GAP and helix $\alpha 4$ and strand $\beta 6$ of Ras are completely different from strands $\beta 12$ and $\beta 13$ in Rap1GAP.

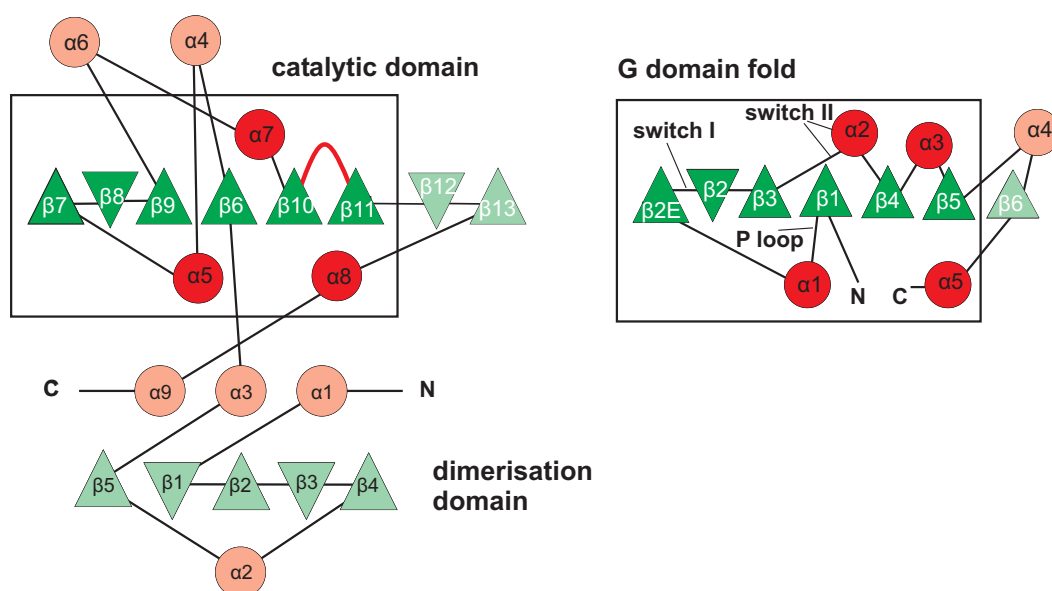


Figure 25. Topology of the Rap1GAP monomer (left) shown in comparison to the G domains which have an extra β -sheet ($\beta 2E$) (for example Ran, Arf, Arl right). Helices are depicted as red circles, strands as triangles with orientation according to their direction in the β -sheet. The secondary structure elements which can be overlaid in Rap1GAP and Ras are boxed.

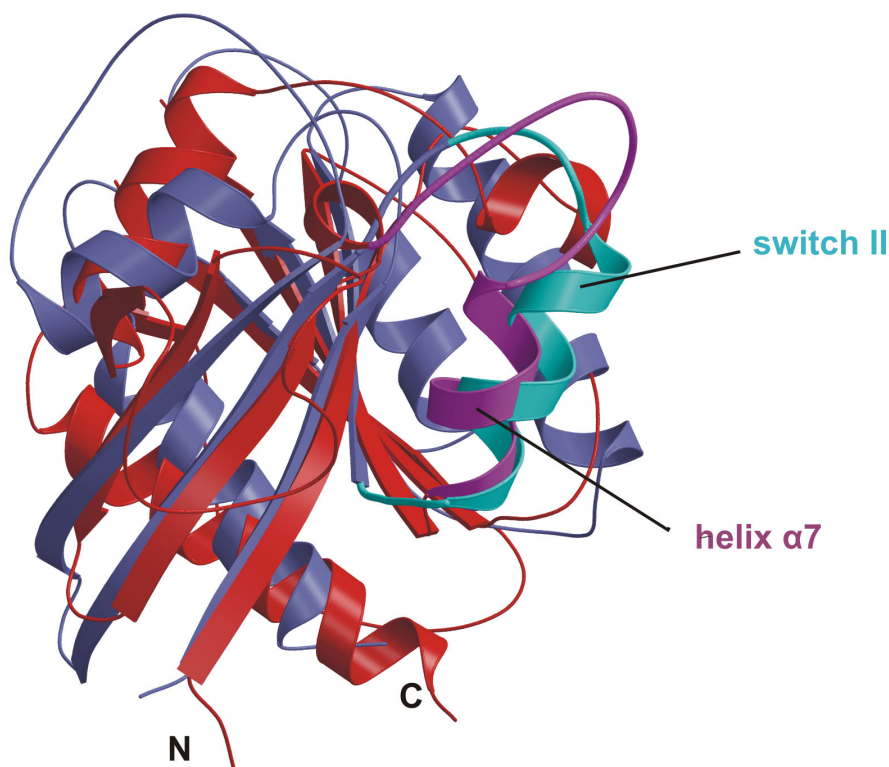


Figure 26. Ribbon plot showing the catalytic domain of Rap1GAP (in red) superimposed with the aligned Ras molecule in blue (pdb code 121P). Switch II of Ras is coloured in cyan, the corresponding helix $\alpha 7$ in Rap1GAP is shown in purple. Clearly, most of the secondary structure elements can be superimposed.

The structural similarity is hardly reflected on the sequence level, for which only 9% sequence identity was found. However, the structural similarity clearly suggests that Rap1GAP and the family of small GNBPs are derived from a common ancestor.

4.2.7 Description of the dimer

Rap1GAP (molecular mass of the monomer 39 kD) eluted as an apparent 100 kD species in size exclusion chromatography. Two elongated dimers (molecule A-B and molecule C-D) with approximate dimensions of $35 \times 35 \times 130 \text{ \AA}^3$ were observed in the asymmetric unit of the crystal (Figure 27A, B). The higher apparent molecular weight observed in size exclusion chromatography likely results from the extended shape of the dimer leading to a greater hydrodynamic radius than expected for a globular protein. The two-fold axis between the two monomers can easily be recognised in Figure 27B.

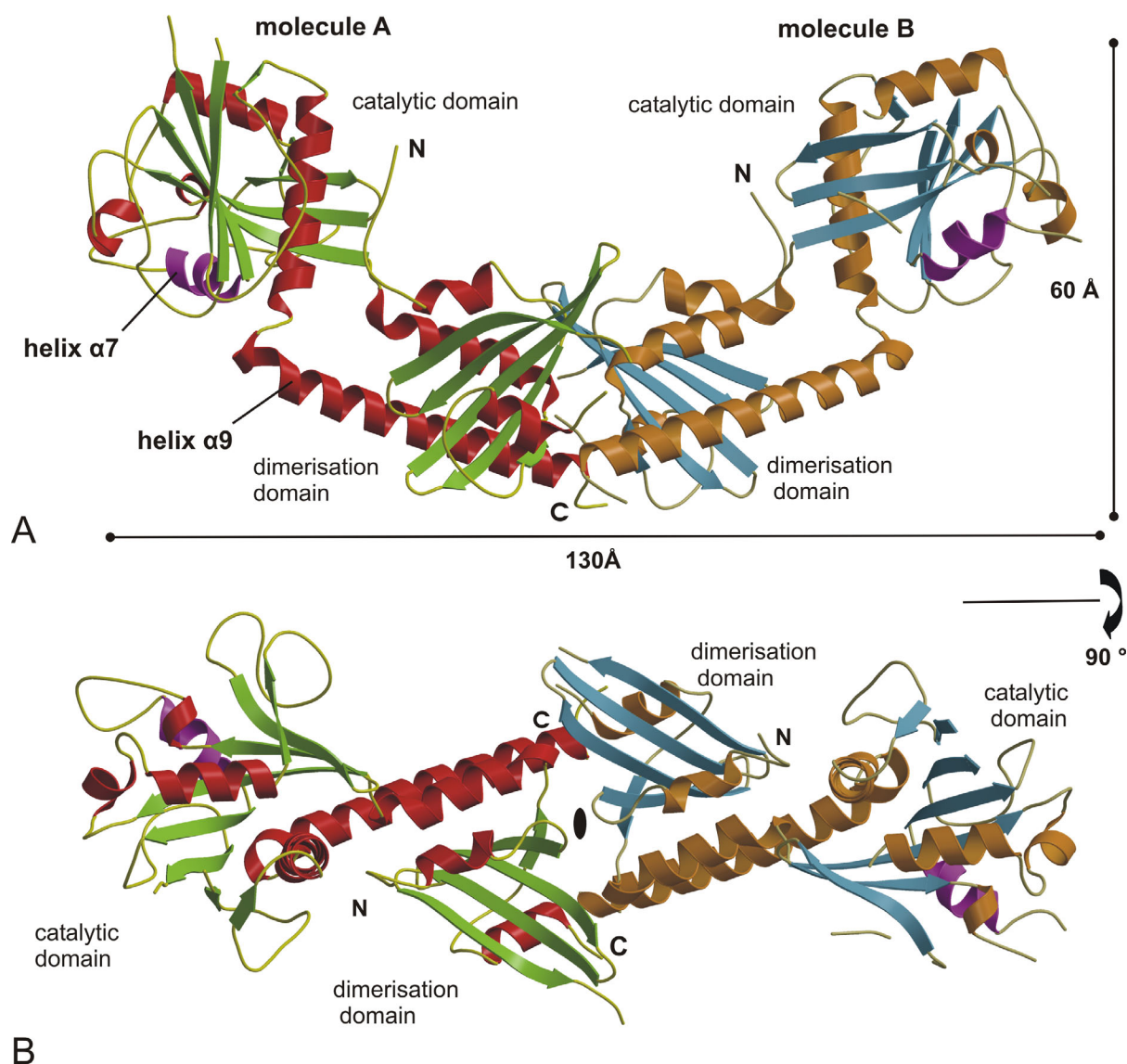


Figure 27. Two views of the elongated Rap1GAP dimer. Helix $\alpha 7$ is shown in magenta. The two-fold axis is indicated in B.

The size of the dimer interface (Figure 28) was determined to be approximately 2400 \AA^2 (see 3.4.5), which is in a typical range for physiological relevant protein interfaces (Jones et al., 2000). It is built symmetrically of amino acids from molecule A and B (Figure 28). Strand $\beta 1$, $\beta 2$ and $\beta 5$, helix $\alpha 2$ and $\alpha 3$, and the loops L2, L6 and L8 are involved in the contacts (Figure 28B). The interface is mainly built of hydrophobic residues with polar amino acids involved only in the periphery. The hydrophobic nature of the interface also explains why it was not possible to separate the two monomers even by high salt concentrations (up to 1M NaCl) (data not shown).

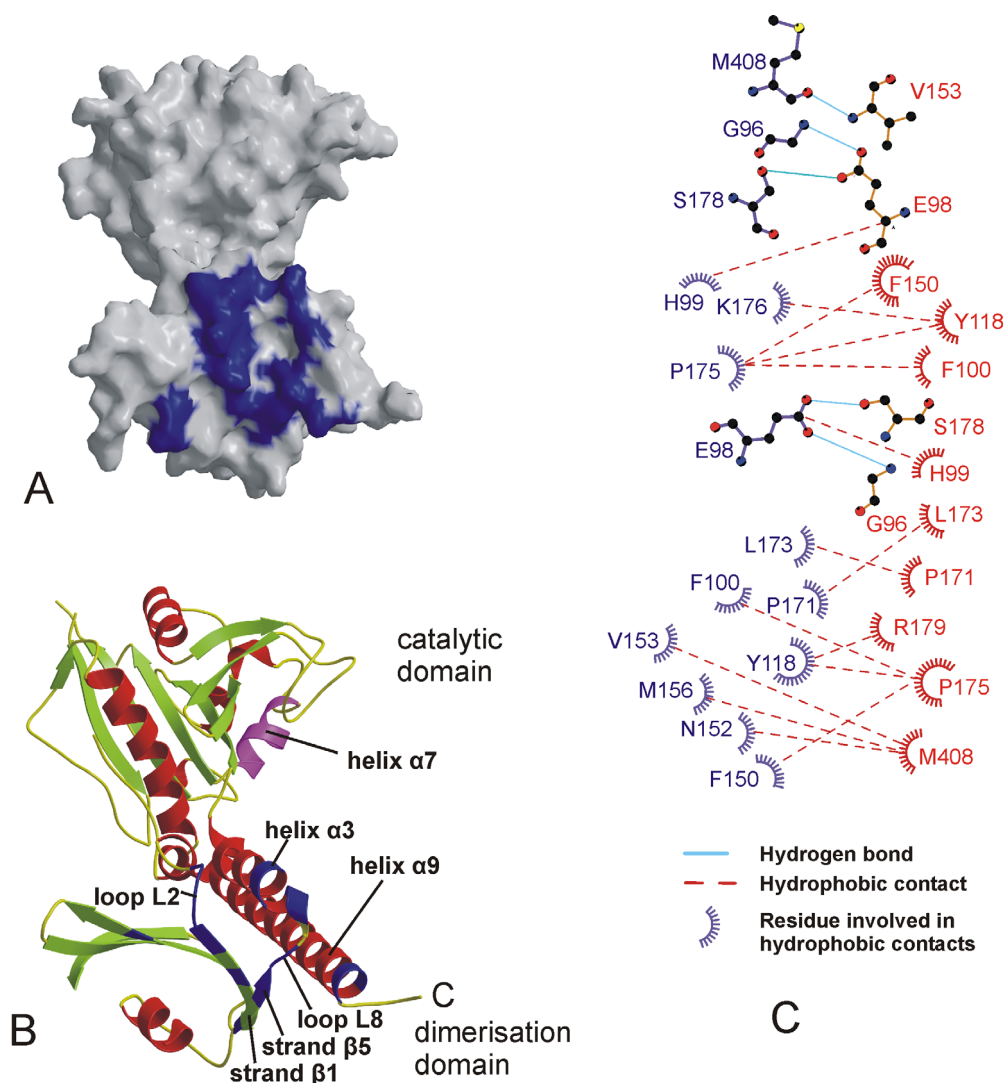


Figure 28. The Rap1GAP dimer interface. **A)** Surface representation. All surface exposed residues of molecule A which are involved in the interface are shown in blue. **B)** Ribbon type presentation in the same orientation as in A showing in blue the secondary structure elements involved in the formation of the interface. **C)** Schematical representation of the amino acids contacts of molecule A (blue letters) and molecule B (red letters). Amino acids involved in polar interactions are shown as ball-and-stick representation.

4.2.8 The catalytic centre

Since different members of the Rap1GAP family are expected to interact with Rap1 in a similar way, it was reasoned that amino acids which contact Rap1 should be at least partially conserved. To identify the Rap1 binding interface, the distribution of conserved amino acids in the Rap1GAP structure was analysed. Tuberin was excluded from this alignment since it is a GAP for the small GNPB RheB and thus residues involved in binding are not necessarily conserved. A Rap1GAP surface presentation illustrating the distribution of conserved residues is shown in Figure 29.

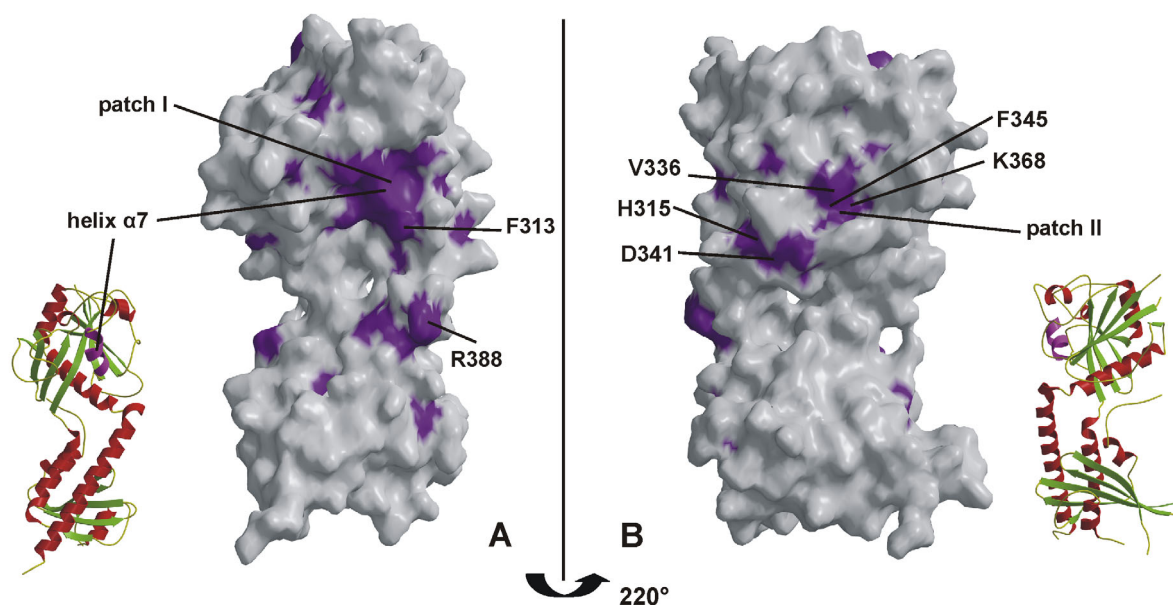


Figure 29. Surface representation of Rap1GAP with front and back view showing in magenta all residues which are conserved among the Rap1GAP family. The position of several conserved amino acids is indicated. Ribbon plots indicate the orientation of the molecule. In A the conserved patch I is shown, in B the conserved patch II.

The conserved residues cluster in two patches on the Rap1GAP surface. Patch I is larger and is located around helix $\alpha 7$ in the catalytic domain (Figure 29A). Also the conserved arginine R388 of helix $\alpha 9$ is in vicinity of this cluster. The second patch found on the opposite side of patch I consists of two hydrophobic residues (phenylalanine F345 and valine V336) and lysine K368.

Since mutation of lysine K368 to alanine reduced the Rap1GAP activity only 2-fold (Figure 19), this residue was not expected to be involved in catalysis. Also phenylalanine F345 and valine V336 are no putative catalytic residues because they lack polar side-chains. Thus, it was concluded that patch II is probably not involved in Rap1 binding but might have a different function (see Discussion). It was hypothesised that Rap1 binds in the area of the conserved patch I around helix $\alpha 7$ and $\alpha 9$. Residues important for catalysis have then to be located on this side of the Rap1GAP molecule.

To further characterise the putative interaction site, an electrostatic surface was calculated (Figure 30). Rap1GAP has a calculated isoelectric point of 5,6, indicating a negative net charge at a physiological pH. However, no strong charges could be identified near patch I, the putative interaction side. A negatively charged surface spot was found in the catalytic domain and a positively charged surface spot in the dimerisation domain (Figure 30). These surface spots did not superimpose with the conserved residues in patch I or patch II, and their significance is unclear yet.

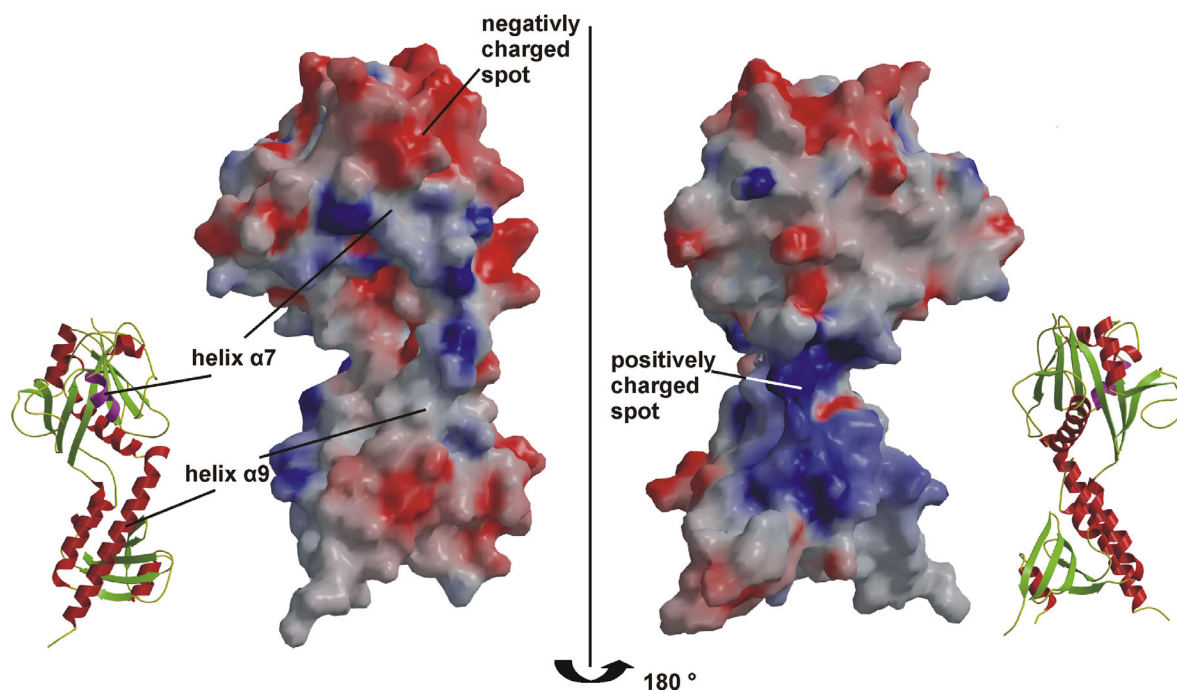


Figure 30. Electrostatic surface of Rap1GAP. Red colour indicates negative charge, blue colour positive charge at neutral pH. The surface was calculated using the program Grasp (Nicholls et al., 1993).

It was rationalised that the catalytic centre of Rap1GAP and the site of Rap1 interaction is close to those amino acids whose mutations reduce Rap1GAP activity dramatically. Therefore, lysine K194 and lysine K285 (see 4.1.4) were analysed in more detail. Strikingly, both lysines are part of the conserved surface patch I (Figure 29) and form contacts to other highly conserved residues (Figure 31).

Lysine K194 is a residue of strand $\beta 6$. In molecule A and C, it forms a salt bridge to aspartate D291 of helix $\alpha 7$ and a hydrogen bond to the carbonyl oxygen of asparagine N290 (Figure 31). Aspartate D291 in turn forms a hydrogen bond to histidine H267 in strand $\beta 9$. Lysine K194, histidine H267 and aspartate D291 are completely conserved among Rap1GAPs and Tuberin (Table 3). These three amino acids seem to be important for the relative orientation of strand $\beta 6$, $\beta 9$ and helix $\alpha 7$.

Lysine K285 is part of helix $\alpha 7$, like asparagine N290 and aspartate D291. Its ammonium group is involved in a salt bridge with glutamate E207 of helix $\alpha 4$ and in a hydrogen bond to the carbonyl oxygen of alanine A310 in loop L15 (Figure 31). Thus, lysine K285 appears to orient helix $\alpha 7$ relative to helix $\alpha 4$ and loop L15. Destroying this interaction by mutating lysine to alanine leads to a dramatic decrease in Rap1GAP activity. Since the ammonium group of lysine K285 is involved in a network of polar contacts, it is rather unlikely that it contributes to catalysis.

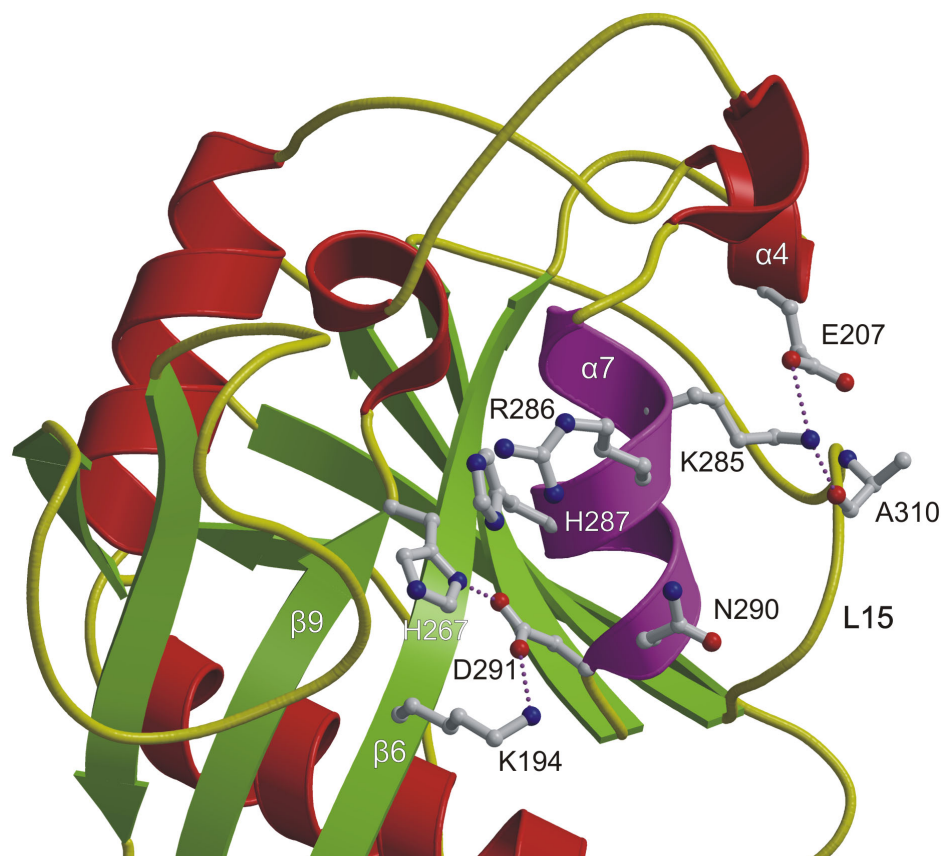


Figure 31. Ribbon type presentation of the Rap1GAP catalytic domain showing the involvement of lysine K194 and lysine K285 in a network of polar interactions. Hydrogen bonds and ionic interactions are represented by dashed lines. Additionally, surface exposed residues of helix $\alpha 7$ (coloured in purple) are depicted.

The analysis of conserved residues in the Rap1GAP family and the examination of lysines K194 and K285 indicated that the catalytic centre of Rap1GAP and the site of Rap1 interaction is likely to be around helix $\alpha 7$. This helix is from hereon referred to as Rap1 interaction helix.

Surprisingly, both lysines are solvent exposed in molecule B and do not make the contacts described above. This might reflect a certain flexibility of helix $\alpha 7$. It should also be mentioned that molecule A and C have a crystallographic contact close to helix $\alpha 7$ which is not present in molecule B.

4.3 The hydrolysis mechanism of Rap1GAP

Based on the Rap1GAP structure, new constructs and point mutants were designed to elucidate details of the GAP mechanism.

4.3.1 Dimerisation and Rap1GAP function

Rap1GAP eluted as a dimer from gel filtration and two dimers were observed in the asymmetric unit of the crystal. It was asked whether dimerisation is a prerequisite for GAP function. Thus, it was intended to disrupt the dimer interface by targeted mutagenesis. Since the interface is built of mainly hydrophobic residues, it was reasoned that the introduction of charged residues might disrupt dimerisation. Thus, two central amino acids of the Rap1GAP interface, phenylalanine F100 and leucine L173 were exchanged to glutamate generating four negatively charged residues in the interface (Figure 32).

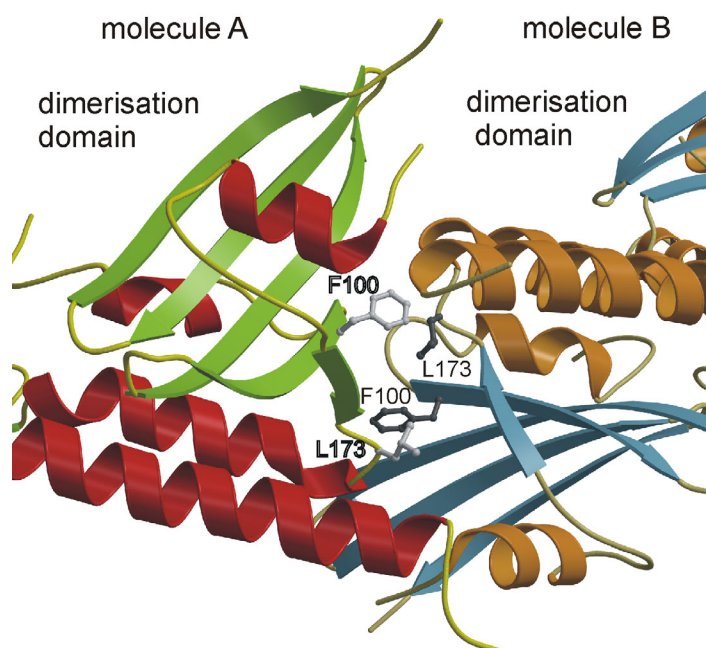


Figure 32. Ribbon type presentation of the Rap1GAP dimer interface. Phenylalanine F100 and leucine L173 (white in molecule A, black in molecule B) were substituted with a glutamate to disrupt dimerisation.

The Rap1GAP^{F100E,L173E} double mutant eluted primarily as a monomer in size exclusion chromatography showing that dimerisation was indeed inhibited by the mutations. It did however not elute as a clear single peak but appeared also in fractions of smaller molecular weight (data not shown) indicating that the amino acid

substitutions partially destabilised or unfolded the protein. However, in a multiple-turnover GAP assay using 100 μM Rap1•GTP as substrate, this mutant showed only a marginally reduced activity compared to Rap1GAP wild-type (Figure 33). It can be concluded that dimerisation is not important for the GAP reaction.

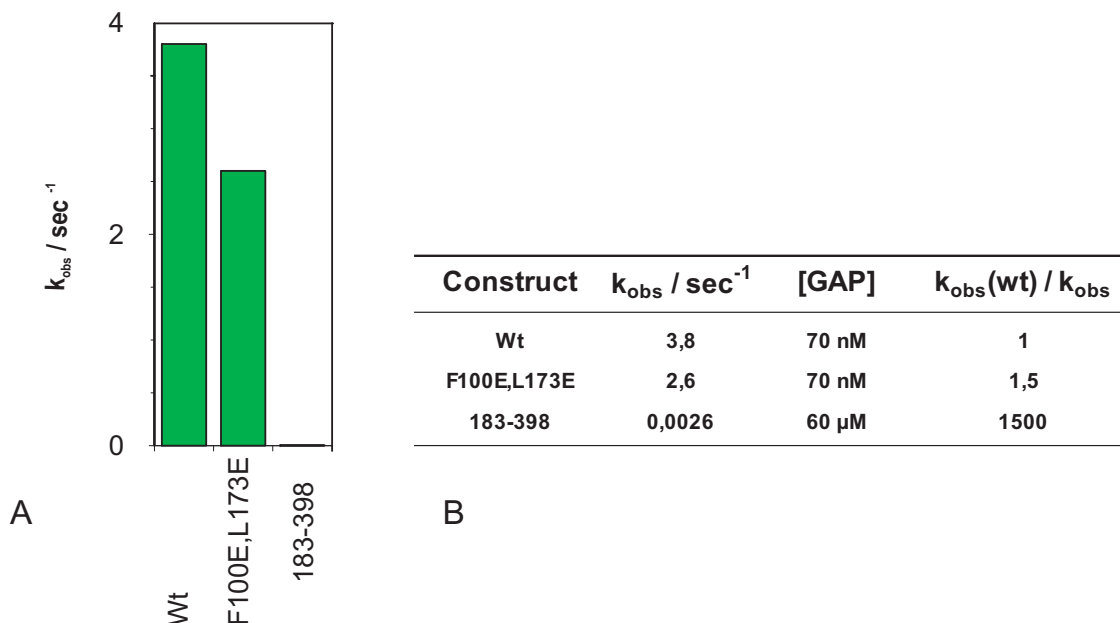


Figure 33. Mutational analysis of the Rap1GAP interface mutant and of the Rap1GAP catalytic domain. Initial rates of Rap1GAP stimulated GTP hydrolysis in Rap1•GTP were measured at 20 °C using a Rap1•GTP concentration of 100 μM and HPLC analysis and plotted in a bar diagram. The explicit k_{obs} values at the respective GAP concentration are indicated in B.

4.3.2 Involvement of both domains in the GAP mechanism

The catalytic domain is much higher conserved than the dimerisation domain in the Rap1GAPs family. Furthermore, lysines K194 and K285 which most dramatically affected Rap1GAP activity when mutated to alanine are both located in the catalytic domain, and Tuberin has homology only to the catalytic domain. This implies that primarily the catalytic domain is involved in Rap1GAP activity. However, the R388A mutation reduces the affinity for Rap1 (Brinkmann, 2000) and arginine R388 is a surface exposed residue of the C-terminal helix α_9 (Figure 34). This helix has many contacts to the dimerisation domain. This suggests that also residues outside the catalytic domain might be involved in Rap1GAP function.

To test whether the catalytic domain in combination with arginine R388 preserves Rap1GAP activity, a construct was prepared containing the complete catalytic domain and parts of the C-terminal helix ending with arginine R388 (Rap1GAP¹⁸⁸⁻³⁸⁸).

This protein could be prepared as GST fusion but showed no Rap1GAP activity. Upon removal of GST, the protein precipitated indicating that it might not be properly folded. Thus, no conclusion could be drawn from this construct.

It was postulated that the interaction between helices $\alpha 3$ and $\alpha 9$ which are N-terminal and C-terminal of the catalytic domain, respectively, might stabilise the catalytic domain. Therefore, a new construct (Rap1GAP¹⁸³⁻³⁹⁸) containing parts of both helices was prepared (Figure 34). This construct was highly soluble, did not precipitate upon removal of GST and eluted as a monomer in size exclusion chromatography.

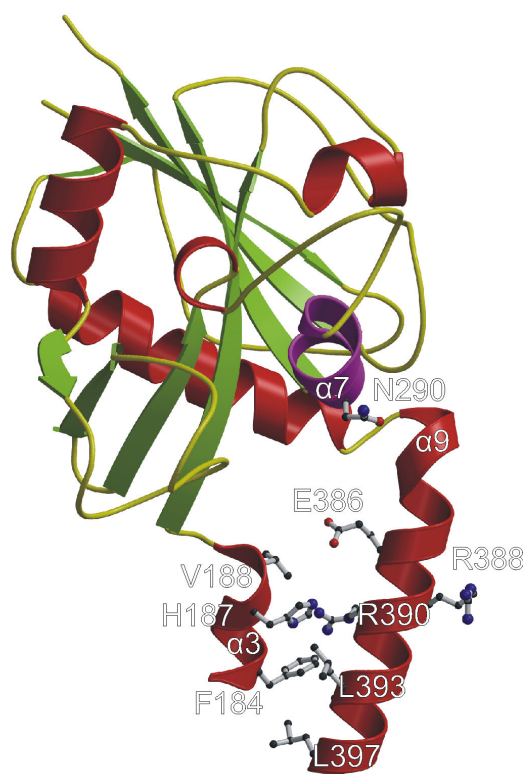
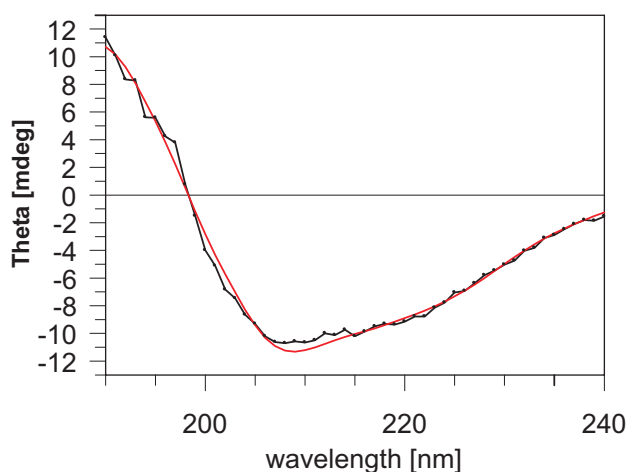


Figure 34. The Rap1GAP¹⁸³⁻³⁹⁸ construct including the catalytic centre around helix $\alpha 7$. Arginine R388 on helix $\alpha 9$ is expected to bind to Rap1. The position of helix $\alpha 9$ is stabilised by hydrophobic interactions with helix $\alpha 3$.

Rap1GAP¹⁸³⁻³⁹⁸ was tested in the standard Rap1•GTP hydrolysis assay (Figure 33) and showed a residual Rap1GAP activity. However, at least a 1000-fold concentration of GAP was required in comparison to wild-type to stimulate GTP hydrolysis to a similar extent (Figure 33B).

To find out whether Rap1GAP¹⁸³⁻³⁹⁸ is folded, a CD spectrum (Figure 35) was recorded. The analysis of the CD spectrum predicted that the protein contained 28% β -strands, in good agreement to what is calculated from the structure. The helix proportion of Rap1GAP¹⁸³⁻³⁹⁸ predicted from CD analysis to be 18% is somewhat less than what is expected from the structure (32%).



	helix	strand	turns/unordered
predicted (spectrum)	18%	28%	54%
calculated (structure)	32%	27%	41%

Figure 35. CD spectrum of Rap1GAP183-398 and data evaluation (3.3.17). The measured curve is shown in black, the fitted curve in red.

These results indicate that the central β -sheet of the catalytic domain and thus the core is folded. Some helical elements, likely the peripheral helices, may not be correctly folded.

Therefore, it is concluded that the catalytic domain alone is not sufficient for full Rap1GAP activity and that the dimerisation domain is required either for correct folding or correct positioning of the peripheral helices, especially helix α 9 (see also Discussion).

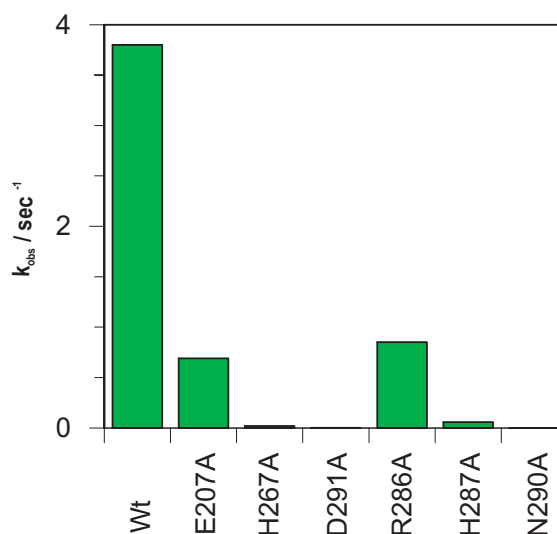
4.3.3 Role of helix stabilisation for Rap1GAP function

The structure revealed that lysine K194 and K285 in molecule A and C are both involved in stabilising helix α 7, the putative interaction helix (Figure 31). To confirm that stabilisation of this helix is important for Rap1GAP activity, the interaction partners of lysine K194 and lysine K285 were mutated to alanine, and the GAP activity of the mutants determined in a Rap1•GTP standard hydrolysis assay.

Lysine K285 is involved in an ionic interaction with glutamate E207 and a hydrogen bond with the main chain oxygen of alanine A310. The E207A mutant shows a relatively mild reduction in activity compared to the K285A mutant (Figure 36), which can be attributed to the fact that lysine K285 is still stabilised by the main chain contact to alanine A310 (Figure 31).

Lysine K194 forms a salt bridge to aspartate D291. The activity of the D291A mutant was analysed in the standard GAP assay, and nearly no stimulation of GTPase

activity was detected. Aspartate D291 interacts additionally with histidine H267. The H267A mutation also leads to a dramatically reduced GAP activity (Figure 36).



Construct	$k_{\text{obs}} / \text{sec}^{-1}$	[GAP]	$k_{\text{obs}}(\text{wt}) / k_{\text{obs}}$
Wt	3,8	70 nM	1,0
E207A	0,69	300 nM	5,5
H267A	0,019	8000 nM	200
D291A	0,0017	30000 nM	2200
R286A	0,85	70 nM	4,5
H287A	0,057	4000 nM	67
N290A	no activity	30000 nM	-

Figure 36. Mutational analysis of residues in and around helix $\alpha 7$. GAP activity was measured as described in the legend of Figure 33. The concentration of GAP used in the experiments is indicated.

4.3.4 The catalytic residue

Since stabilisation of the interaction helix is crucial for Rap1GAP activity, it was asked whether this helix might contain the catalytic residue of Rap1GAP. Therefore, all surface exposed conserved residues in the interaction helix were mutated to alanine (arginine R286, histidine H287, asparagine N290), and the activity of the mutants was analysed in the standard hydrolysis assay (Figure 36).

The R286A mutant has a 4-fold reduced activity using 100 μM Rap1•GTP, similarly as described in 4.1.3. Histidine H287 is rather buried, and the H287A mutant has a dramatically reduced activity. Finally, the surface exposed asparagine N290 did not show any stimulation of GTPase activity in Rap1•GTP when mutated to alanine.

To follow a single reaction cycle of GTP hydrolysis, a previously established fluorescence assay was applied (Kraemer et al., 2002). This assay monitors the association of Rap1GAP to fluorescently labelled Rap1•GTP leading to an increase

in fluorescence, and, after GTP hydrolysis, the concomitant dissociation of the complex resulting in a decrease of the fluorescence back to the basis level.

The previously described reaction course for Rap1GAP wild-type (Kraemer et al., 2002) could be confirmed (Figure 37). For the R286A mutant, the hydrolysis reaction was three-fold slower than for the wild-type, similar to what was observed in the multiple-turnover assay (Figure 36). This confirms that arginine R286 is not a residue of central importance in catalysis, in contrast to the arginine fingers of RasGAP, RhoGAP and RabGAP (Vetter and Wittinghofer, 2001). No association with Rap1•GTP was seen for the H287A mutant. However, surprisingly, association but no dissociation was observed for the N290A mutant (Figure 37).

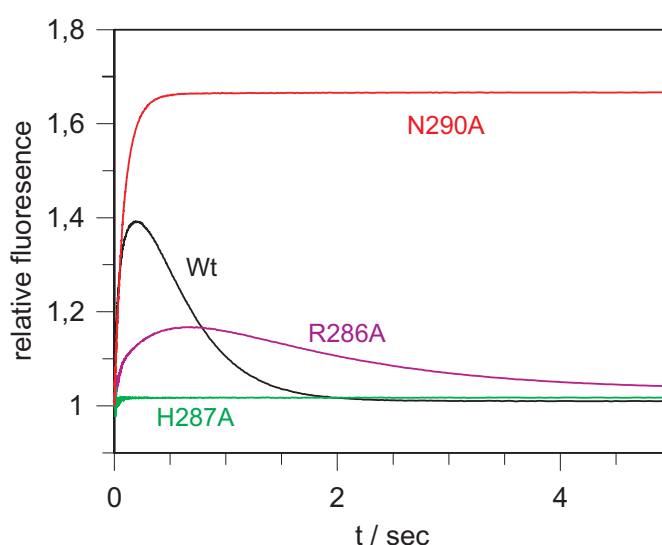


Figure 37. Fluorescence based GAP assay with Rap1GAP and single point mutants of residues in the interaction helix. The reaction of 1 μM Rap1-Aedans•GTP with 25 μM Rap1GAP or the indicated Rap1GAP mutants was followed in the fluorescence stopped-flow assay as described in 3.3.16.1.

The affinity of Rap1GAP wild-type to Rap1-Aedans•GTP under similar reaction conditions was previously found to be 14 μM (Kraemer et al., 2002). To examine whether the N290A mutation led to a decreased affinity for Rap1, the fluorescence assay was employed using varying concentrations of Rap1GAP^{N290A} (Figure 38A). Observed rate constants were determined and plotted against the concentration of Rap1GAP^{N290A} (Figure 38B), and the slope of the straight line corresponding to k_{on} was fitted to be 0,32 $\text{sec}^{-1}\cdot\mu\text{M}^{-1}$ (see Appendix). The k_{off} rate was determined to be 1,1 sec^{-1} by preparing a fluorescent Rap1-Aedans•GTP•Rap1GAP^{N290A} complex and following the displacement of fluorescently labelled Rap1•GTP upon addition of an excess non-labelled Rap1•GTP (Figure 38C). Using $K_{\text{D}} = k_{\text{off}}/k_{\text{on}}$, a K_{D} of 3 μM was calculated (see also 7.2.1).

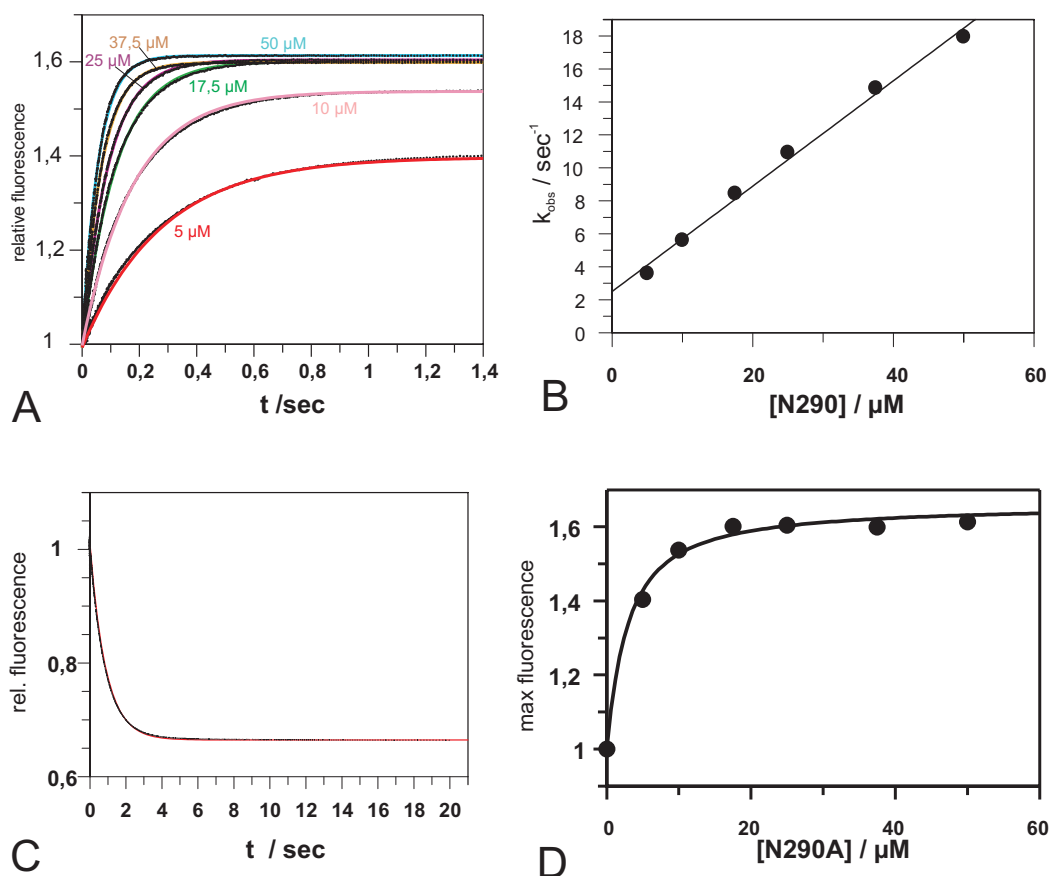


Figure 38. A) Determination of N290A affinity to Rap1•GTP. The binding reaction of 1 μM Rap1-Aedans•GTP with increasing concentrations of Rap1GAP^{N290A} was monitored using stopped-flow. B) Plotting the observed rate constants and fitting them to a linear equation results in a slope of $0,32 \text{ sec}^{-1}\cdot\mu\text{M}^{-1}$ which corresponds to the k_{on} . C) Determination of k_{off} . 2 μM Rap1-Aedans•GTP and 20 μM Rap1GAP^{N290A} were mixed with 200 μM non-labelled Rap1•GTP. The determined rate constant corresponds to k_{off} and is $1,1 \text{ sec}^{-1}$. With a k_{on} of $0,32 \text{ sec}^{-1}\cdot\mu\text{M}^{-1}$, a K_{D} of $3,4 \mu\text{M}$ is derived. D) Determination of K_{D} by equilibrium titration. Plotting the maximal amplitudes in A and fitting them to a quadratic equation results in a K_{D} of $2,4 \mu\text{M}$.

Since there is no complex dissociation, an alternative approach to determine K_{D} could be applied by using an equilibrium titration equation (see Appendix). The amplitudes of the fluorescent transients (Figure 38A) were plotted against the N290A concentration and fitted to a quadratic binding equation (Figure 38D, see 7.2.2). Using this method a K_{D} of $2,4 \mu\text{M}$ was obtained.

In summary, the affinity of the Rap1GAP^{N290A} mutant for Rap1•GTP is around $3 \mu\text{M}$ which is even higher than the wild-type affinity. This clearly implies that asparagine N290 is not involved in the binding to Rap1 but is directly involved in catalysis. Therefore, Rap1GAP constitutes the first example of a GAP which provides a catalytic asparagine to stimulate GTP hydrolysis in a GNBPs.

4.3.5 Binding to a transition state analogue of GTP hydrolysis

AlF_x along with GDP (or ADP) is a known mimic of the transition state for many phosphoryl transfer enzymes such as myosin and $\text{G}\alpha$ subunits of heterotrimeric G proteins (Chabre, 1990). It has been shown that aluminium fluoride binds to Ras-like proteins only in the presence of their respective GAPs (Ahmadian et al., 1997b; Mittal et al., 1996; Graham et al., 1999), thus demonstrating that the active site of Ras-like proteins needs to be complemented by residues from GAP.

To prove that asparagine N290 is directly involved in catalysis, the association of Rap1GAP with fluorescently labelled Rap1•GDP• AlF_3 was followed by stopped-flow measurements. As shown in Figure 39, wild-type Rap1GAP indeed associates with Rap1•GDP• AlF_3 leading to an increase in the fluorescence signal. The association is slow, similar to what is seen for Ras and Rho proteins (A. Wittinghofer, unpublished). While the R286A mutant also associates but shows a smaller fluorescence amplitude on complex formation, no association is seen for the N290A mutant (Figure 39). This shows unambiguously that asparagine N290 is directly involved in the catalytic process by stabilising the transition state of GTP hydrolysis.

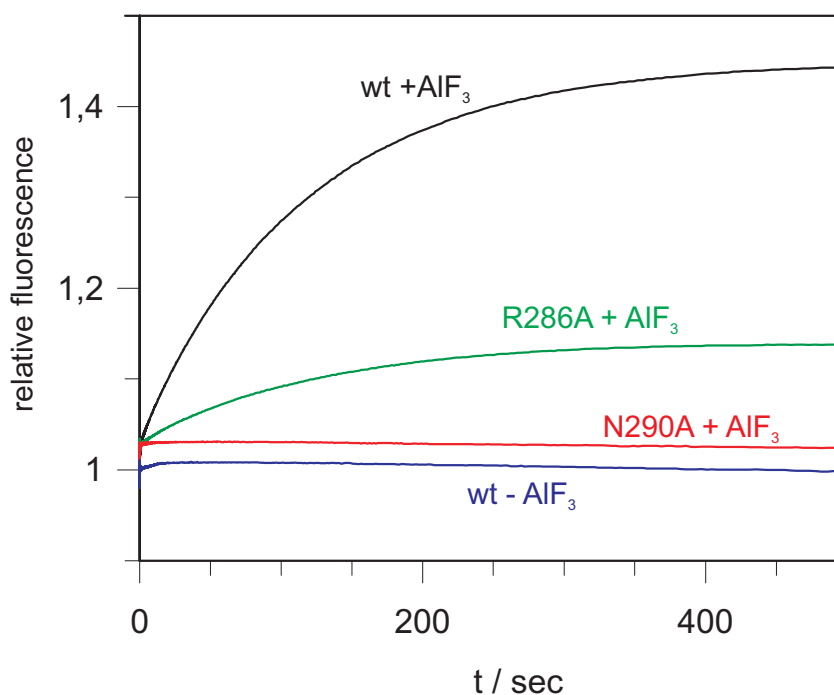


Figure 39. Stabilisation of the transition state of GTP hydrolysis. Complex formation between Rap1•GDP and Rap1GAP is measured as a time-dependent increase of fluorescence, and is dependent on the presence of aluminium fluoride. While the R286A mutant shows complex formation with a decreased amplitude, no complex formation is observed for the N290A mutant.

4.3.6 Other important residues in Rap1GAP

The region around asparagine N290 was more closely examined to find other important residues involved in catalysis in Rap1GAP (Figure 40).

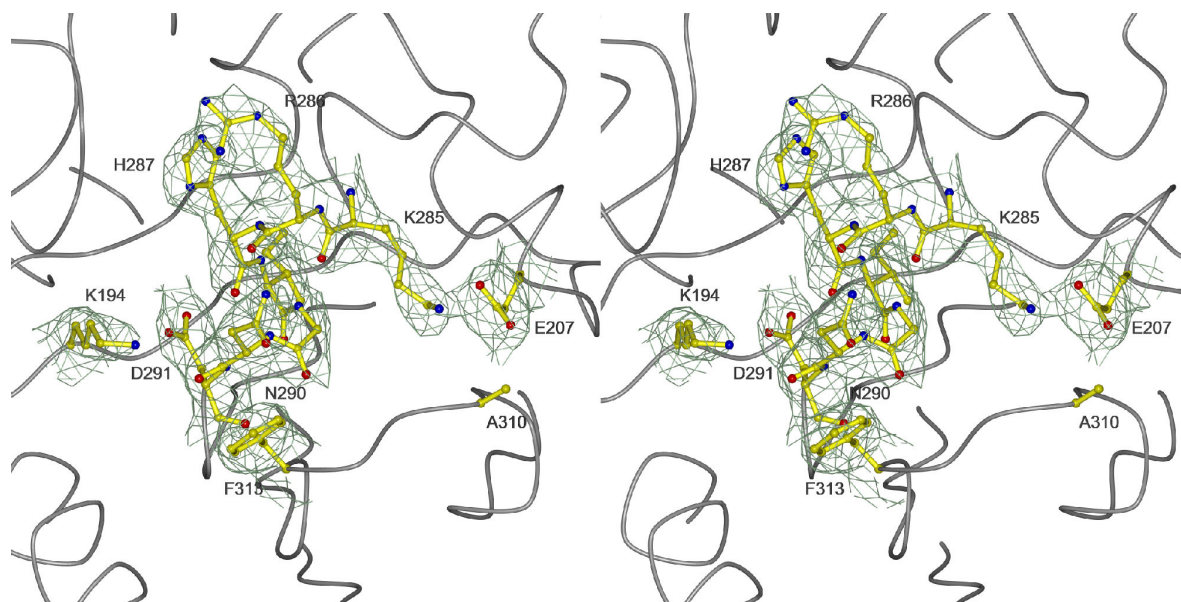


Figure 40. Stereo view of the electron density around asparagine N290. In direct vicinity of asparagine N290, the completely invariant phenylalanine F313 is located.

Indeed, close to asparagine N290, a completely conserved phenylalanine (phenylalanine F313) was found. This phenylalanine is linked to the helix $\alpha 7$ through the interaction of lysine K285 and the carbonyl oxygen of alanine A310 (Figure 31). Phenylalanine F313 was mutated to alanine. The activity of the mutant was followed in the multiple-turnover assay and the fluorescence assay (Figure 41). In the multiple-turnover assay, an 8-fold reduced activity was found at a Rap1•GTP concentration of 100 μ M (Figure 41A). Also in the fluorescence assay, a clearly reduced activity could be observed (Figure 41B). Since phenylalanine does not possess a putative catalytic function, it can be assumed that it is either involved in binding to Rap1, in positioning asparagine N290 for catalysis or in influencing the properties of the catalytic asparagine.

The R388A mutation in Rap1GAP was previously found to reduce the affinity for Rap1 (Brinkmann et al., 2002). This mutant was also tested in both hydrolysis assays (Figure 41). In agreement with previous data (4.1.3), the mutant has a 4-fold reduced activity at a Rap1•GTP concentration of 100 μ M. Surprisingly, nearly no signal was observed for the R388A mutant in the fluorescence GAP assay (Figure 41). This suggests that the fluorescence change depends on an interaction between

arginine R388 and a residue close to cysteine C86 in Rap1 where the fluorophore is attached or the fluorophore itself (see Discussion).

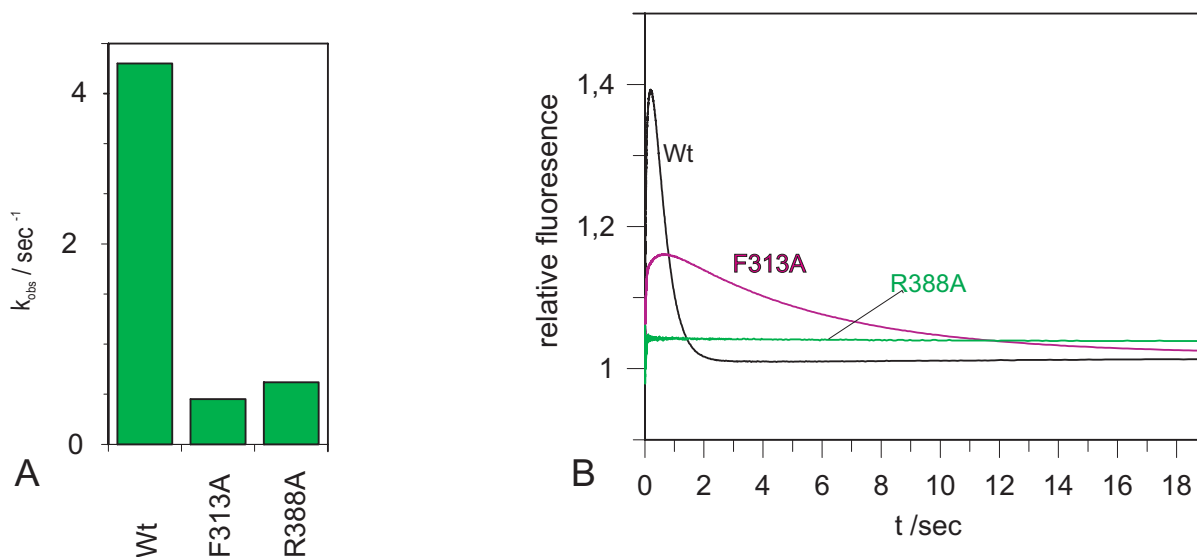


Figure 41. A) Multiple turnover analysis of Rap1GAP^{F313A} and Rap1GAP^{R388A} mutants as described in the legend of Figure 33. B) Fluorescence GAP assay with Rap1GAP^{F313A} and Rap1GAP^{R388A}, shown in comparison to wild-type as described in the legend of Figure 37.

4.3.7 Role of the carboxamide for GAP activity

Rap1GAP is the only known GAP which provides a catalytic asparagine to the GNPB, and Rap1 does not have a catalytic glutamine. It was asked whether the missing carboxamide in the N290A mutant can principally be substituted by a glutamine on position 61 of Rap1. Therefore, this reaction was set up by using the Aedans labelled Rap1^{T61Q} mutant together with the Rap1GAP^{N290A} mutant and measuring the fluorescence in a long-term stopped-flow experiment ($t = 500$ sec). Surprisingly, $25 \mu\text{M}$ Rap1GAP^{N290A} could stimulate GTP hydrolysis in $1 \mu\text{M}$ Rap1^{T61Q}•GTP with an observed rate of $0,16 \text{ min}^{-1}$ (Figure 42). The rate of non-stimulated GTP hydrolysis of the Rap1^{T61Q} mutant at $10 \text{ }^\circ\text{C}$ was determined to be $5,2 \cdot 10^{-4} \text{ min}^{-1}$ by standard HPLC measurements (data not shown). Thus, the stimulated reaction is 300-fold faster than the non-stimulated reaction, while for wild-type Rap1 no acceleration of GTP hydrolysis was observed in this time-frame.

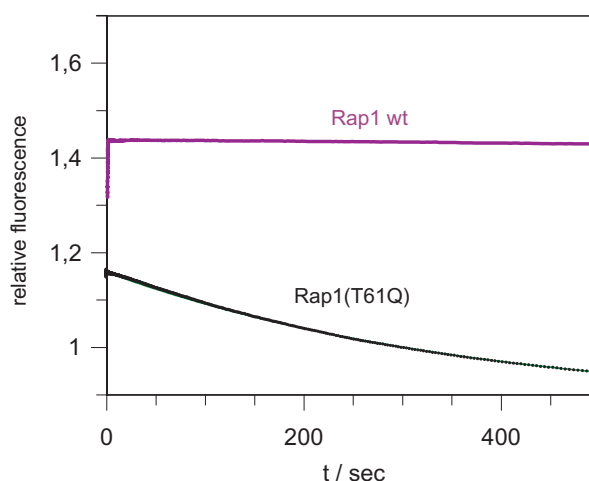


Figure 42. Fluorescence GAP assays. The reaction of 1 μM Rap1^{T61Q}-Aedans-GTP or Rap1 wild-type with 25 μM Rap1GAP^{N290A} was monitored using stopped-flow as described in 3.3.16. Since the reaction was followed over 500 sec in this setup, not enough data point could be gathered in the first milliseconds to visualise the fluorescence increase upon mixing.

To determine the affinity of Rap1GAP^{N290A} to Rap1^{T61Q}, the same approach as for Rap1 wild-type was employed. Maximal amplitudes for equilibrium titration experiment were obtained by measuring the fluorescence in a time range of 1 sec upon mixing, where no GTP hydrolysis is expected (Figure 43A,C). Since the Rap1^{T61Q}•GTP•Rap1GAP^{N290A} complex dissociates over time due to GTP hydrolysis, k_{off} could not be obtained by a displacement reaction. Thus, k_{off} was determined by plotting the observed rates against the concentration of Rap1GAP^{N290A} and determining the intercept with the y-axis (Figure 43B, for deduction of the formula see Appendix).

The results are summarised in Figure 43D. k_{on} was determined to be $0,65 \text{ sec}^{-1} \cdot \mu\text{M}^{-1}$, and k_{off} to be 16 sec^{-1} , resulting in a K_{D} of 25 μM . In comparison to Rap1 wild-type, the k_{on} rate is in a similar range ($0,32 \text{ sec}^{-1} \cdot \mu\text{M}^{-1}$). However, k_{off} is explicitly higher ($1,1 \text{ sec}^{-1}$ for wild-type). By fluorescence titration, the K_{D} was determined to be 15 μM which is slightly lower than what is derived from the association kinetics.

Assuming a K_{D} of 20 μM , the reaction shown in Figure 42 is only to 60% saturated. This indicates that the observed rate is lower than the maximal rate. It can be concluded that Rap1GAP^{N290A} accelerates the intrinsic reaction of Rap1^{T61Q} more than 300-fold.

This result shows that a carboxamide in Rap1 in position 61 can indeed substitute partially for the catalytic asparagine N290. However, it seems that glutamine Q61 can not be positioned accurately since the GTPase stimulation is still at least 500-fold reduced in comparison to the wild-type system.

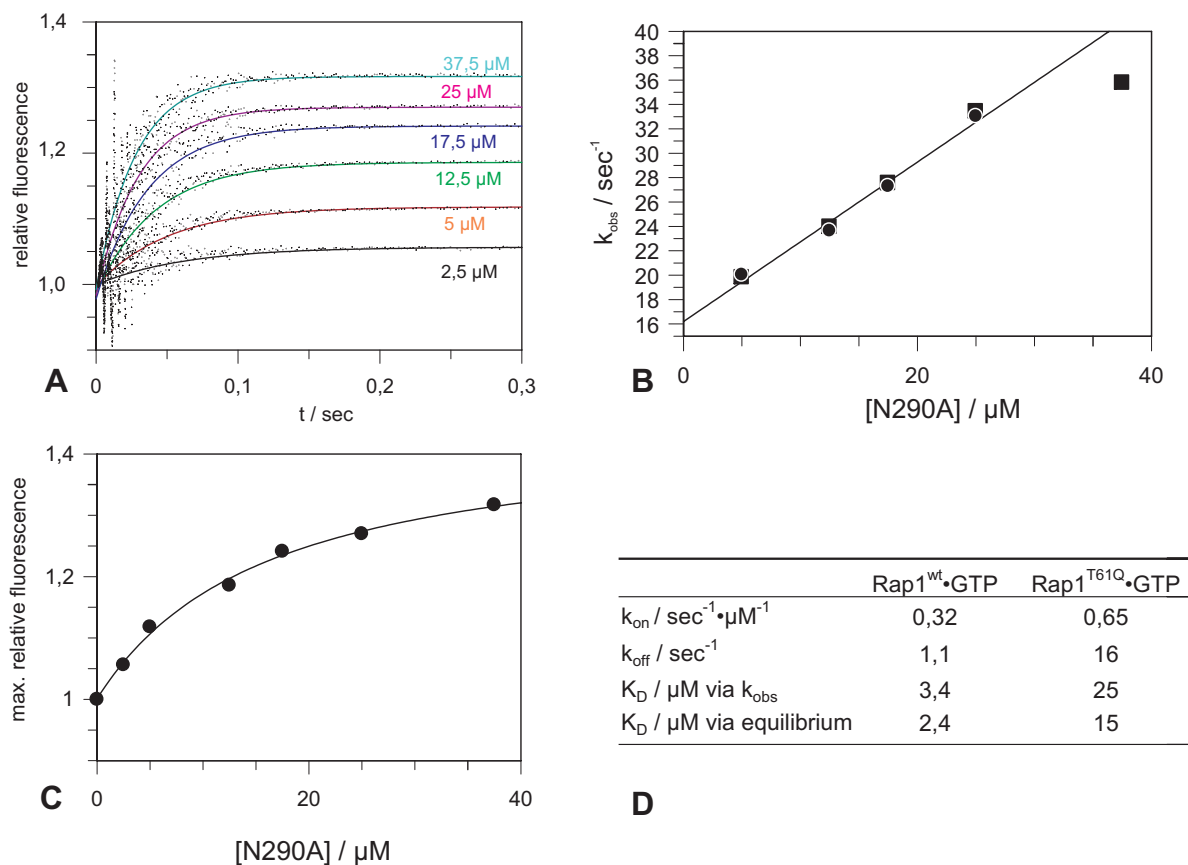


Figure 43. Determination of Rap1GAP^{N290A} affinity to Rap1^{T61Q}•GTP. **A)** 2 μM Rap1^{T61Q}•Aedans•GTP was 1:1 mixed with various concentrations of Rap1GAP^{N290A}. The fluorescence was monitored using stopped-flow as described in 3.3.16. **B)** Plotting the observed rate constants and fitting them to a linear equation results in a slope of $0,65 \text{ sec}^{-1} \cdot \mu\text{M}^{-1}$ corresponding to k_{on} and an intercept with the y-axis of 16 sec^{-1} corresponding to k_{off} . **C)** Determination of K_D by equilibrium titration. Plotting the maximal amplitudes in Figure 43A and fitting them to a quadratic equation results in a K_D of $15 \mu\text{M}$. **D)** Comparison of k_{on} and k_{off} rates and the K_D for Rap1GAP^{N290A} with Rap1 wildtype and Rap1^{T61Q}.

4.3.8 Implications for Tuberous sclerosis

Tuberin is a GAP for the small GNPB RheB. Loss of function mutations in the *Tsc2* gene lead to Tuberous sclerosis, a disease characterised by benign tumours. Single point mutations have been found in the GAP domain of Tuberin in Tuberous sclerosis patients (Maheshwar et al., 1997; Au et al., 1998; Jones et al., 1999; Dabora et al., 2001) (Table 3). The sites of these mutations, indicated in the Rap1GAP catalytic domain, are shown in Figure 44.

Most of the mutations described cluster in the core of the catalytic domain and most likely destabilise the protein. Mutations Y1549C in strand $\beta 6$ (Rap1GAP numbering),

Y1650C and N1651S in strand β 10, P1675L in strand β 11, D1690Y in strand β 12 and P1709L in strand β 13 belong to this kind of mutations.

Mutation N1681K is located in loop L16 which is not completely defined in the Rap1GAP structure. Also mutation A1712D is located in a loop (L18 in Rap1GAP). Since these mutations are rather far away from the putative RheB binding interface, it is difficult to predict their effect on Tuberin function.

Mutation L1594M is located in the long loop L12. It is in vicinity of the catalytic centre and one might speculate that it is involved in RheB binding (see also Discussion).

R1576 of Tuberin corresponds most likely to the surface exposed highly conserved arginine R388 in Rap1GAP (Table 3). As already discussed (see 4.3.6), it is located in helix α 9 and its mutation in Rap1GAP leads to a reduced affinity for Rap1 (Brinkmann et al., 2002). R1576 was found to be mutated to proline or glutamine in tuberous sclerosis patients. The R388P mutant of Rap1GAP has an even more reduced activity than the R388A mutant (Figure 44). Since arginine R388 is not in direct vicinity but on the same face as the catalytic asparagine, it is reasonable to assume that it constitutes to the binding interface with RheB (see Discussion). Thus, mutations in arginine R388 in Rap1GAP and most likely the R1576P/Q mutations in Tuberin interfere with binding to the small GNPB.

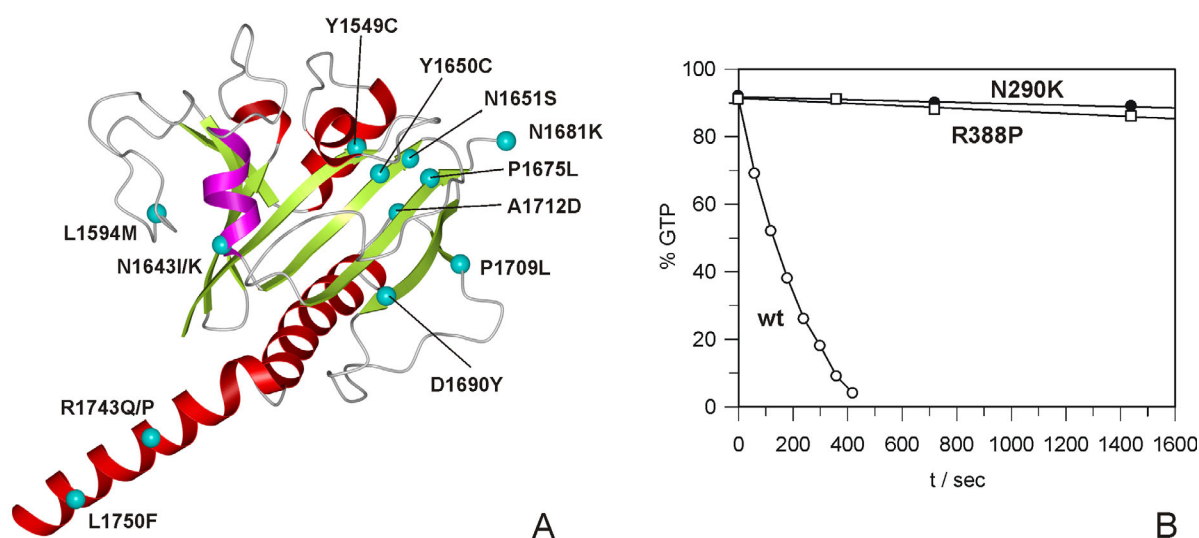


Figure 44. A) Ribbon type presentation of Tuberin mutation sites which are found in tuberous sclerosis patients (see Table 3), based on the Rap1GAP structure. B) Standard HPLC measurement using standard conditions as described in the legend of Figure 33. 70 nM of Rap1GAP wild-type and of the Rap1GAP^{R388P} mutant were used and 60 μ M for Rap1GAP^{N290K}.

Tuberin mutations N1643K (Maheshwar et al., 1997; Jones et al., 1999) and N1643I (Au et al., 1998) can be most easily explained by analogy to Rap1GAP. Asparagine N1643 in Tuberin is homologous to the catalytic asparagine N290 in Rap1GAP and the equivalent mutations in Rap1GAP render the protein either completely inactive (N290K) (Figure 44) or insoluble (N290I) (data not shown). The loss of the catalytic asparagine in Tuberin clearly implies that patients bearing this mutation can not down-regulate RheB.

5 Discussion

Members of the Rap family do not possess a catalytic glutamine which is essential for GAP mediated GTP hydrolysis in nearly all other GNBPs examined so far. In this work, the reaction mechanism and the structure of Rap1GAP were examined.

By mutational analysis it was shown that Rap1GAP does not use an arginine finger. However, two lysine residues were identified, whose mutations dramatically reduced Rap1GAP activity. The X-ray structure of the Q204A Rap1GAP mutant was solved and showed two Rap1GAP dimers in the asymmetric unit. Each monomer consists of two domains, one involved in dimerisation of Rap1GAP, which was named the dimerisation domain, and one in which the previously identified lysines were located, which was named the catalytic domain. Rap1GAP has a completely novel GAP fold, but the catalytic domain shows structural similarity to the G domain of small GNBPs. Both lysines described above are involved in polar interactions around the putative Rap1 interaction helix whose primary sequence is highly conserved in the Rap1GAP family. When the interaction partners of these lysines were mutated, Rap1GAP activity is also strongly reduced. Asparagine N290 in the interaction helix was demonstrated to be the crucial catalytic residue, since mutating it to alanine completely eliminated Rap1GAP activity without interfering with the binding to Rap1. Furthermore, in contrast to wild-type, the N290A mutant cannot bind to a transition state analogue of GTP hydrolysis. The importance of a carboxamide in GAP mediated GTP hydrolysis was demonstrated since the N290A mutant of Rap1GAP could at least partially stimulate the activity of a Rap1 mutant in which a catalytic glutamine was introduced by a site-directed mutation.

5.1 Dimerisation and role of two domains in Rap1GAP

Rap1GAP eluted as dimer from gel filtration and two dimers were observed in the asymmetric unit (Figure 27). Since Rap1GAP is the first dimeric GAP described to date it was therefore of interest to analyse dimerisation in more detail.

A monomeric Rap1GAP retained *in vitro* Rap1GAP activity comparable to wild-type (Figure 33). This result was in agreement with the identification of the catalytic asparagine and thus the catalytic centre of Rap1GAP in the catalytic domain which is more than 40 Å away from the dimerisation interface (Figure 27). Therefore, it is not

expected that Rap1 has contacts with the second Rap1GAP molecule during catalysis. It was therefore asked whether the observed dimer might be an artefact of the crystallisation condition or the construct chosen.

Several arguments speak in favour of Rap1GAP existing as a dimer in the cell. (1) At physiological salt concentrations, the Rap1GAP catalytic domain elutes as a dimer in size-exclusion chromatography. It elutes as a single peak indicating that the dimer is rather stable. (2) In a yeast-two-hybrid screen, full-length Rap1GAP was found to interact with itself (H. Bos, personal communication). This shows that dimerisation is not an artefact of the chosen construct. (3) The dimer interface contains many hydrophobic residues (Figure 28). Since protein aggregation via the hydrophobic interface might be expected, this observation suggests that in the cell an interaction partner is needed. In fact, aggregation was already a problem for bacterial expressed protein since a major fraction of the expressed protein turned out to be insoluble and still a portion of the soluble protein was associated with the bacterial chaperone GroEL (Brinkmann, 2000). However, this association was not observed when the dimerisation mutant with two charged residues in the hydrophobic interface was expressed. This indicates that the hydrophobic Rap1GAP interface is likely associated with chaperone binding, aggregation and misfolding of the protein.

It can only be speculated about the role of dimerisation in the cell. The Rap1GAP dimer might provide a functional scaffold for a complete module of signal transduction components which was already described for other signal-transduction systems (Pawson and Saxton, 1999). This would be in agreement with the original Rap1GAP purification protocol in which a Rap1GAP activity was purified from bovine brain cytosol as a 250-400 kD complex (Kikuchi et al., 1989). Alternatively, the dimer might supply two binding sites for an interaction partner for example at the membrane to increase the local concentration and thus the avidity for this putative partner. A similar phenomenon was described for the tetrameric lac repressor which needs two independent binding sites at the DNA to bind with high avidity to the target sequence (Oehler et al., 1994) and for many other DNA binding proteins.

Both Rap1GAP domains are necessary for GAP activity (Figure 33). The catalytic domain contains the catalytic asparagine and a network of interactions stabilising the interaction helix (Figure 31). However, the role of the dimerisation domain is not so evident.

As shown in this and in previous work (Figure 41 and Brinkmann et al., 2002), arginine R388 of helix $\alpha 9$ is likely to be involved in Rap1 binding. It is completely

surface-exposed and the R388A mutation reduces the affinity to Rap1 (Brinkmann et al., 2002). Furthermore, the R388P mutant which presumably interferes completely with the arrangement of helix $\alpha 9$ has nearly no GAP activity (Figure 44). Thus, residues of helix $\alpha 9$ seem to be involved in Rap1 binding. In contrast, residues of the dimerisation domain are not located close to the catalytic asparagine or even on the same side (Figure 27). Thus, no direct contact between Rap1 and the dimerisation domain is expected during catalysis. However, helix $\alpha 3$ and strand $\beta 1$ of the dimerisation domain have many hydrophobic contacts with helix $\alpha 9$ which likely influence the position of helix $\alpha 9$. Thus, the role of the dimerisation domain might be the correct positioning of helix $\alpha 9$.

Tuberin has sequence homology only to the catalytic domain including parts of the C-terminal helix $\alpha 9$ although no extensive homology is seen in the latter part (Table 3). Since experiments in our laboratory indicate that the isolated GAP domain of Tuberin has no GAP activity towards RheB under standard conditions (P. Chakrabarti, unpublished), it might be speculated that other parts of Tuberin or Hamartin might have a similar role as the Rap1GAP dimerisation domain in positioning the equivalent of the C-terminal helix $\alpha 9$.

5.2 Interacting partners of Rap1GAP

$G\alpha$ proteins of heterotrimeric G proteins were described as interaction partners of Rap1GAP (Meng et al., 1999; Jordan et al., 1999; Mochizuki et al., 1999). In full-length Rap1GAP, a sequence stretch comprising 74 amino acids precedes the N-terminus of the construct crystallised. This stretch was shown to interact with the $G\alpha$ subunits of $G_{\alpha z}$ (Meng et al., 1999). In RapGAPII, it contains the GoLoco motif (Mochizuki et al., 1999) which binds in the nucleotide binding pocket of $G_{\alpha i}$ and makes direct contacts with the GDP α - and β -phosphate (Kimple et al., 2002). The interaction with $G_{\alpha i}$ relocalises RapGAPII from the cytosol to the membrane concomitant with a reduction of cellular Rap1•GTP. Thus, it is expected that a Rap1GAP dimer can interact simultaneously with one or two $G\alpha$ proteins and Rap1•GTP. Since Rap1 and $G\alpha$ proteins are both membrane-bound one would expect that the long axis of the Rap1GAP dimer will be in parallel to the membrane in this complex, since it would prove difficult otherwise to contact $G\alpha$ and Rap1 to the same time. Clearly, only the structure of a Rap1GAP construct including the first

75 amino acids and the catalytic domain, ideally in complex with a G α -protein, will clarify the exact mode of interaction.

In a yeast-two-hybrid screen, the multi-domain protein AF-6 was found as putative interaction partner of Spa-1 and later shown to bind also to Rap1GAP (Su et al., 2003). AF-6 contains a Ras-binding domain which interacts with Rap1 (Linnemann et al., 1999). Furthermore, genetic interaction experiments in *Drosophila* suggest that the AF-6 homologue Canoe and Rap1 act in the same molecular pathway (Boettner et al., 2000). It was proposed that AF-6 controls integrin-mediated cell adhesion by simultaneously recruiting Rap1 and Rap1GAP (Su et al., 2003).

The binding sites for Rap1GAP and AF-6 were mapped (Su et al., 2003). It was proposed that the PDZ domain of human AF-6 binds to an internal peptide sequence in the catalytic domain comprised of amino acids ₄₃₂IVF in Spa1 and ₂₉₅VVF in Rap1GAP (Su et al., 2003). PDZ domains which belong to the most abundant protein domains in multi-cellular organisms most often interact with a short stretch (< 10 amino acids) at the C-terminus of target proteins (reviewed in Zhang and Wang, 2003). However, it was demonstrated that they can also interact with internal peptide sequences that adopt a β -hairpin structure (Hillier et al., 1999; Tochio et al., 1999; Tochio et al., 2000).

The identified peptide sequence in Rap1GAP is not in agreement with the solved structure since the proposed interaction motif is located five residues C-terminal of the catalytic asparagine in the interior of the Rap1GAP catalytic domain. It is without contact to the Rap1GAP surface and thus, no interaction with any partner protein can be expected. The in-vitro interaction observed is likely an artefact of the construct chosen by Su et al. which was generated by an in-vitro transcription and translation system. This construct starts in the middle of the dimerisation domain and ends in the middle of the catalytic domain and is therefore unlikely to fold. In line with this explanation, no interaction was observed between the bacterially expressed PDZ domain of AF-6 and the Rap1GAP construct described here (H. Rehmann, personal communication). Since it was reported that also full-length Spa-1 was co-immunoprecipitated with AF-6 and vice versa (Su et al., 2003), it still might be speculated that other domains of AF-6 and/or of Spa-1 are involved in this interaction.

To locate binding sites for putative common interaction partner in the Rap1GAP family, the distribution of conserved amino acids on the surface can be analysed (Figure 29). A cluster of residues which are conserved in sequence among Rap1GAP

family members but not in Tuberin could be located opposite of the catalytic centre in the catalytic domain (Figure 29B). In the vicinity of this cluster in the dimerisation domain, a positively charged surface spot is located (Figure 30). This face of Rap1GAP family members might thus represent a putative interaction site with a negatively charged protein.

A second putative interaction site might be located in loop L10 which contains glutamine Q204 in wild-type. This glutamine is completely conserved among Rap1GAPs. However, mutating it to alanine did not interfere with GAP function, and the Q204A mutant could be prepared in larger amounts, seemed to be more stable and crystallised better than the wild-type. The methyl group of alanine A204 points towards the interior of loop 10, an orientation which is certainly not possible for the long glutamine side-chain in wild-type (Figure 45). It is therefore expected that loop L10 is oriented differently in wild-type and the Q204A mutant. Since glutamine 204 is completely invariant and probably surface-exposed in wild-type and is neither required for catalytic activity nor structural integrity, one might expect another function, e.g. binding of a partner protein.

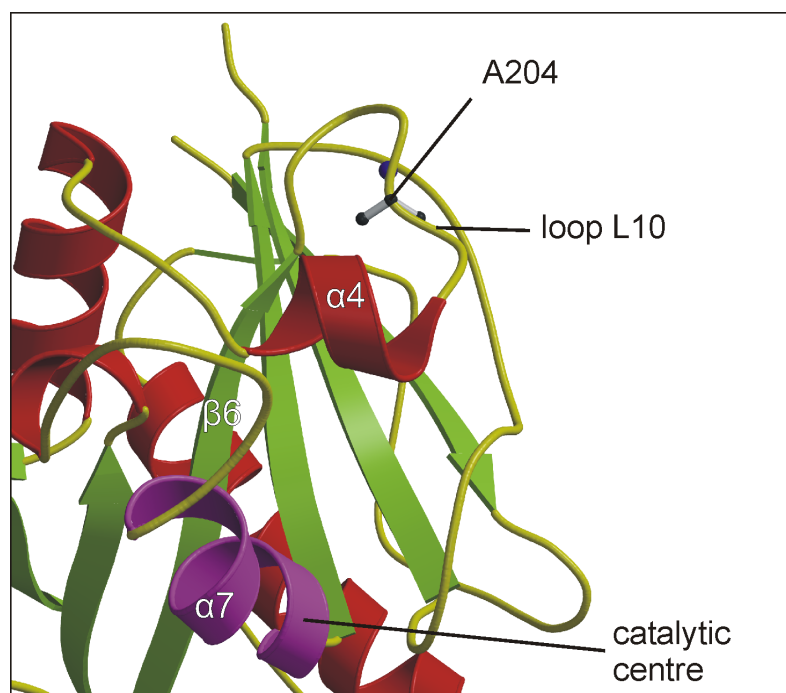


Figure 45. Ribbon type presentation of the catalytic domain of Rap1GAP showing in ball-and-stick alanine A204 in loop L10. The methyl side-chain of alanine A204 points to the interior of the loop, a position likely not compatible with a glutamine side-chain of the wild-type.

5.3 The novel GAP mechanism

The mechanism of GAP-stimulated GTPase reactions on most Ras-like proteins involves two main residues. A glutamine is located on the GNPB, while the GAP apart from stabilising the catalytic machinery, very often supplies a so-called arginine finger (Scheffzek et al., 1998). Mutation of the glutamine in Ras, Rho and Ran almost completely eliminates the GTPase reaction (Der et al., 1986; Xu et al., 1997; Seewald et al., 2002). However, the importance of the arginine finger varies in the different systems. It is most important for Ras (Ahmadian et al., 1997c) and Rab (Albert et al., 1999), somewhat lower for Rho (Rittinger et al., 1997b; Rittinger et al., 1997a), while Ran does not employ an arginine finger (Seewald et al., 2002), and its importance for ArfGAP is still debated (Goldberg, 1999; Mandiyan et al., 1999, see Introduction).

In this work, the mechanism of Rap1GAP was explored which does not use an arginine finger but provides an asparagine for catalysis. In contrast to most other small GNBP, Rap1 does not have a catalytic glutamine but a threonine residue at the equivalent position. This substitution reduces the intrinsic GTP hydrolysis rate (Frech et al., 1990). Threonine T61 is also not required for GAP stimulated GTP hydrolysis in Rap1 (Maruta et al., 1991 and P. Chakrabarti, unpublished). The small GNPB RheB whose GTPase reaction is accelerated by the Rap1GAP homologue Tuberin, has a glutamine at the equivalent position of glutamine Q61 in Ras, which is however not required for Tuberin stimulated GTP hydrolysis (Li et al., 2004). What might be the role of the catalytic asparagine in Rap1GAP ?

Since asparagine is neutral at physiological pH – in contrast to the arginine finger - it can not provide positive charge to stabilise the transition state of GTP hydrolysis. This suggests that it has a different role, e.g. the positioning of the attacking water molecule.

This assumption is supported by the analysis of the Rap1^{G12V} mutant. In most examined GNBP, mutations at the third position in the P loop, equivalent to glycine G12 of Ras, can not be down-regulated by GAPs, since any side-chain at this position interferes with the arrangement of the catalytic glutamine and the arginine finger in the transition state of GTP hydrolysis (Scheffzek et al., 1997; Rittinger et al., 1997b). However, Rap1GAP can downregulate the Rap1^{G12V} mutant (Brinkmann et al., 2002). Furthermore, RheB has an arginine residue at the equivalent position of glycine G12 in Ras and still can be activated by Tuberin. This indicates that the

catalytic asparagine will occupy a different position than the arginine finger in the RasGAP-Ras or RhoGAP-Rho system where no interference with a side-chain at the third position in the P loop will occur.

Since the catalytic asparagine is necessary for binding to a transition state mimic of GTP hydrolysis (Figure 39), it is reasonable to assume that it will bind – directly or indirectly – to the aluminium fluoride and hence to the γ -phosphate during the real transition state. Direct binding could be mediated by a hydrogen bond from the side-chain carboxamide to the terminal γ -phosphate oxygens. This would however place the asparagine in a similar position than the arginine finger which is unlikely to happen (see argumentation of the G12V mutant above). Indirect binding could be mediated by a hydrogen bond to the attacking water molecule which in turn is complexed by aluminium fluoride. In this case, the position of the asparagine would be in hydrogen bond distance to the attacking water molecule but rather in an extension of an axis built from the γ -phosphate and the attacking water molecule. At this position, no interference with a mutation in glycine G12 would be expected. Thus, it is proposed here, that the catalytic asparagine takes over the role of the catalytic glutamine in other GNBPs to position the attacking water molecule.

What is the common theme of GAP catalysis ? Three components are essential for catalysis in all GNP-GAP systems described to date. (1) A divalent metal ion has to be present for GTP binding and hydrolysis. Mg^{2+} and Mn^{2+} are both suitable and they are similarly octahedrally coordinated in the active site (Schweins et al., 1997). They counterbalance the negative charge of the nucleotide and arrange residues in the active site (Sprang, 1997).

(2) The P loop is present in all system described. It is required for nucleotide and magnesium binding but has also a role in catalysis. The third and second-last residue of the P loop corresponding to glycine G13 and lysine K16 in Ras, respectively, form strong hydrogen bonds to the β -phosphate (Redfield and Papastavros, 1990). The main chain amid group of glycine G13 in Ras was proposed to promote catalysis by binding to the β - γ phosphate bridging oxygen (Maegley et al., 1996). Lysine K16 from the GKS motif of the P loop was proposed to stabilise the transition state of GTP hydrolysis by binding to the non-bridging β -phosphate oxygen (Allin et al., 2001).

(3) All GAPs assist in positioning the attacking water molecule relative to the γ -phosphate. In $G\alpha$ proteins and the small GNBPs with the exception of Rap1 and Sar1, this task is mediated by a catalytic glutamine present in the GNP which is correctly positioned by the interaction with the arginine finger (Scheffzek et al., 1998).

In the complex of signal recognition particle with its receptor, the attacking water molecules are positioned by aspartate residues (Focia et al., 2004; Egea et al., 2004, see Introduction). A histidine is responsible for water positioning in Sar1 and most likely in EF-Tu (Cool and Parmeggiani, 1991; Berchtold et al., 1993; Zeidler et al., 1995; Vogeley et al., 2001; Mohr et al., 2002). Finally it is proposed in this work, that in the case of Rap1 and RheB, an asparagine provided from the GAP positions the water. When a glutamine is reintroduced in Rap1 at position 61, the resulting Rap1^{T61Q} mutant can be at least partially stimulated by the Rap1GAP^{N290A} mutant which misses the catalytic asparagine (Figure 42). Thus, placing the attacking water at a position close to the γ -phosphate is a principle likely applied by all GNBPs.

In most GNBPs but not in Ran and Rap1, a catalytic arginine is additionally supplied for catalysis. This arginine is thought to stabilise an associative or dissociative transition state (Scheffzek et al., 1997; Allin et al., 2001) or to assist in positioning the attacking water molecule by binding to the catalytic glutamine (Scheffzek et al., 1997; Rittinger et al., 1997b). As shown by Seewald et al. (2002) and in this work, however the arginine finger is not universally applied in all GAP systems.

5.4 Proposed model of the Rap1GAP-Rap1 complex

The interaction site with Rap1 was extensively mapped in this thesis by mutational analysis. It was shown that mutations in and around helix $\alpha 7$ whose sequence is highly conserved in the Rap1GAP family and Tuberin reduce the affinity or catalytic activity towards Rap1. The identified amino acids resulting in loss of activity when mutated to alanine could be classified in the following categories. (1) Amino acids which are involved in interactions stabilising helix $\alpha 7$. Glutamate E207, lysine K285, lysine K194, aspartate D291 and histidine H267 can be included here. (2) Surface-exposed amino acids in helix $\alpha 7$, probably involved in Rap1 binding. Arginine R286 and histidine H287 can be included here. (3) The catalytic residue, asparagine N290. (4) Residues likely to be involved in Rap1 binding which are not members of helix $\alpha 7$. Phenylalanine F313 and arginine R388 belong in this category.

Residues of category 2, 3 and 4 can be used to predict the putative Rap1 interface since they are expected to directly contact Rap1.

Several arguments should be considered before setting up an interaction model. In contrast to the arginine fingers of Ras and Rho, the catalytic asparagine of Rap1GAP

is not located in a flexible loop but at the end of helix $\alpha 7$ (Scheffzek et al., 1997; Rittinger et al., 1997b). The position of this helix is fixed by hydrogen bonds and ionic interactions although a certain flexibility of the helix could be deduced from molecule B in which the stabilising interactions are not observed. Nonetheless, it is not expected that major conformational changes will take place around helix $\alpha 7$, in contrast to the arginine finger loops of other GAPs (Scheffzek et al., 1997; Rittinger et al., 1997b).

Arginine R388 is located in the C-terminal helix $\alpha 9$ which is proposed to be positioned by the dimerisation domain (see Discussion above and Figure 34). Since only few interactions are observed between the catalytic and dimerisation domain it can be argued that the relative position of the domains and thus of arginine R388 to the catalytic domain changes during Rap1 binding.

The Rap1 structure, on the other side, was solved in the GppNHp bound state only in a complex containing RafRBD (Nassar et al., 1995). Alternatively, the structure of Rap2 which shows ~60% sequence identity to Rap1 was solved in the GTP and GDP bound state (Cherfils et al., 1997). Since the switch regions of small GNBPs are known to make contacts to GAPs and undergo major conformational changes upon GAP or effector binding (e.g. Scheffzek et al., 1998; Nassar et al., 1995) it is difficult to predict their exact conformation in the Rap1-Rap1GAP complex. Some predictions, however, can be made which Rap1 in the predicted complex should fulfil. Phenylalanine F64 of Rap1 should be involved in the interface since a mutation to alanine renders the resulting mutant completely insensitive to Rap1GAP (Brinkmann et al., 2002). Alanine A86 should be close to the interaction face since the fluorescent reporter group was attached at position 86 and is unquenched upon Rap1GAP binding (Kraemer et al., 2002). Furthermore, residue 86 of Rap1 is expected to be close to arginine R388 of Rap1GAP since the R388A mutant has an approximately 4-fold reduced activity but does not show any fluorescence change in the fluorescent reporter assay (Figure 41). This argues that arginine R388 might be in direct vicinity of the fluorescent reporter group. Finally, the γ -phosphate should be freely accessible for asparagine N290, and asparagine should be able to position the attacking water molecule. Having defined these prerequisites, it was possible to find an arrangement in which all parameters described above are fulfilled (Figure 46).

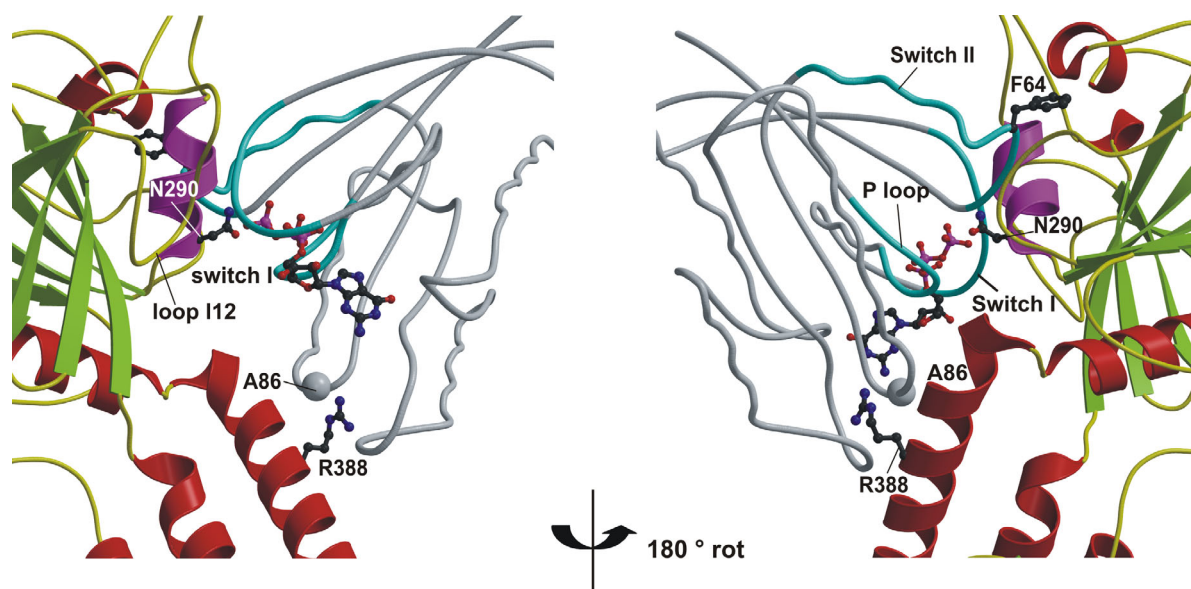


Figure 46. Two opposing views of a model of the Rap1GAP·Rap1·GTP complex (pdb coordinates for Rap1 from the Rap1·GppNHp·RafRBD complex (PDB code 1C1Y). Rap1GAP is shown as ribbon type presentation in standard colours. Rap1·GTP is shown as a grey $C\alpha$ worm in which the switches and the P loop are coloured in cyan. Selected residues are shown as ball-and-stick. The site of fluorophore attachment in Rap1 is shown as blue ball.

In this model, asparagine N290 approaches the γ -phosphate from a similar position than the catalytic glutamine in Ras and could allow the positioning of the attacking water molecule. Switch I of Rap1 is in close vicinity to the interaction helix $\alpha 7$ of Rap1GAP and glutamate E37 of Rap1 contacts histidine H287 from the interaction helix which is known to dramatically reduce GAP activity when mutated to alanine (Figure 36, Figure 37). Switch I interacts also with loop L12 of Rap1GAP. In the equivalent loop of Tuberin, mutations were found in tuberous sclerosis patients (Figure 44).

Phenylalanine F64 in switch II of Rap1 clashes with glutamate E207 of helix $\alpha 4$ and loop L15 containing alanine A310 in Rap1GAP. Mutations in this region of Rap1GAP in which also lysine K285 is located strongly reduce Rap1GAP activity (Figure 36). It could be speculated that this interaction will rearrange switch II and allows asparagine N290 to access into the active site.

Phenylalanine F313 which is completely conserved in the Rap1GAP family and whose mutation interferes with Rap1GAP activity (Figure 40, Figure 41) is in van-der-Waals contact to the P-loop of Rap1.

Arginine R388 of Rap1GAP contacts the loop between strand $\beta 4$ and helix $\alpha 3$ of Rap1 in which residue 86 and thus the site of fluorophore attachment is located. Mutations in arginine R388 to alanine could interfere locally with Rap1 binding which

would explain why no fluorescent signal can be observed for the R388A mutant (Figure 41).

In summary, the model of the Rap1GAP-Rap1 complex presented here agrees well with all data gained from mutagenesis, kinetic and structural studies. Certainly, conformational changes will occur in Rap1 and Rap1GAP upon binding, especially in switch I and II of Rap1 which are not predicted in this model. Thus, the structure of Rap1GAP in complex with Rap1•GDP•AlF₃ or a non-hydrolysable GTP analogue is ultimately needed. However, as long as no complex structure is available, the model described here might serve as a guideline for the development of further experiments.

5.5 Implications for Tuberous Sclerosis and cancer

Tuberous sclerosis is an autosomal dominant syndrome which is caused by mutations in the genes *Tsc1* encoding Hamartin or *Tsc2* encoding Tuberin (Kwiatkowski, 2003). The disease is characterised by the development of benign tumours, hamartomas, which are most often found in brain, skin, kidney and heart (Gomez et al., 1999). They are rarely malignant but cause neurological disorders and seizure due to their involvement in the brain.

The development of tuberous sclerosis seems to follow in most cases the classical Knudson paradigm for tumour suppressor genes (Knudson, Jr., 1971). Initially, one loss of function germline mutation is present in either the *Tsc1* or *Tsc2* gene (first hit). Loss of heterozygosity leading to loss of function in the second allele will cause hamartoma development (Kwiatkowski, 2003).

Tsc1 and *Tsc2* form a complex in vivo. Recent findings in *Drosophila* have established a link between the Tsc complex, insulin signalling and the mTOR pathway (Figure 47) (reviewed in Manning and Cantley (2003), Li et al. (2004)). In this pathway, the Tsc complex acts as GAP towards the small GNBPs RheB and suppresses mTOR signalling and cell growth. Upon signalling by growth factors, the Tsc complex becomes inactivated by phosphorylation and concomitantly RheB becomes activated. RheB promotes mTOR signalling and thus cell growth through a yet not identified mechanism. In the absence of a functional Tsc complex, mTOR signalling is switched on continuously, leading to uncontrolled cell growth.

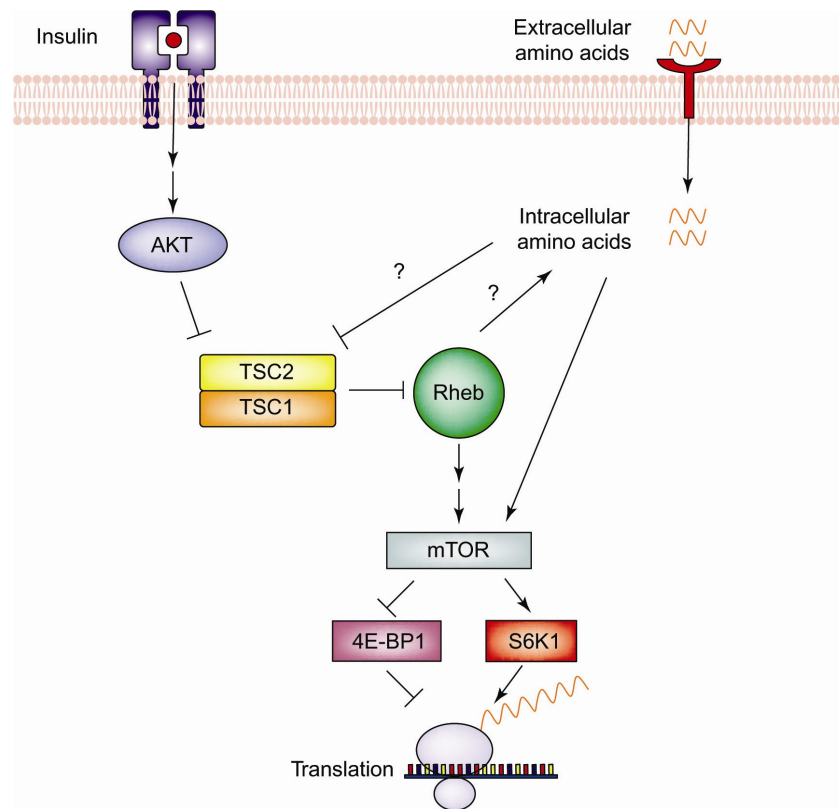


Figure 47. The Tsc signalling pathway (from Li et al., 2004). Activation of the Akt-kinase by growth factors such as insulin leads to phosphorylation and concomitant inactivation of the Hamartin-Tuberin complex. Since this complex acts as GAP towards the small GNBP RheB, GTP bound RheB can accumulate and activates through an unknown mechanism the kinase mTOR which is a central regulator of cell growth. mTOR in turn regulates protein expression by inhibiting the initiation factor 4E-BP1 and by activation of the protein kinase S6K1. mTOR can be regulated also by cellular nutrient level but the role of Tsc1/Tsc2 in this regulation is unclear.

Most of the mutations found in Tuberous sclerosis patients are deletions or non-sense mutations in the *Tsc2* gene (Dabora et al., 2001). However, also single point mutations were described in various parts of the *Tsc2* gene many of which are located in the region homologous to the catalytic domain of Rap1GAP (Figure 44). Many of the mutations seem to cluster in or close to the hydrophobic core of the structure, and thus most likely destabilise the protein. However, in the case of the N1643K and N1643I mutation, the catalytic residue necessary for GAP function is mutated (Figure 44). This implies that the mutation of a single residue crucial for catalysis can induce Tuberous sclerosis. A similar case was described for the disease neurofibromatosis, in which a point mutation of the catalytic arginine in the RasGAP NF1 can induce the formation of benign tumours (Klose et al., 1998). In the case of tuberous sclerosis, it confirms that it is the up-regulated RheB in the mTOR pathway that leads to un-regulated cell growth.

Two further mutations in Tuberous sclerosis patients can be explained by the interaction model presented above (Figure 46). R1576Q/P in Tuberin corresponds to the surface exposed highly conserved arginine R388 in Rap1GAP which is located in helix $\alpha 9$ of the catalytic domain. The corresponding R388P mutation in Rap1GAP dramatically reduces GAP activity. In the interaction model, arginine R388 is proposed to interact with a loop between strand $\beta 4$ and helix $\alpha 3$ of Rap1. Thus, the R1576Q/P mutation is likely to interfere with the binding of RheB to Tuberin.

The L1594M mutation is proposed to be in a loop equivalent to loop L12 in Rap1GAP which in the interaction model is involved in binding to switch I of Rap1. Although this mutation does not seem to be so dramatic, it might also interfere with Tuberin binding to RheB.

Recently, the *Rap1GAP* homologues *Spa1* (Ishida et al., 2003) and *E6TP1* (Gao et al., 2001a) have been described as tumour suppressor genes. It is expected that inactivating mutations in the Rap1GAP domain of *Spa1* or *E6TP1* will be identified in certain tumours. When these mutations are identified, the structure of Rap1GAP and the Rap1GAP-Rap1 model will help to explain the molecular details how these mutations might interfere with GAP function.

5.6 Evolution of the Rap1GAP system

Surprisingly, the catalytic domain of Rap1GAP showed structural similarity to the G domain, especially of small GNBPs as determined in a DALI homology search (Figure 25, Figure 26). The catalytic asparagine is positioned in a helix equivalent to the switch II helix $\alpha 2$ in Ras. This argues that Rap1 and the catalytic domain of Rap1GAP might have evolved from a common ancient GGBP. This GGBP might have stimulated its GTPase activity through transient dimerisation, similar to what is described for the signal recognition particle and its receptor (Focia et al., 2004; Egea et al., 2004) and what is proposed for the GNBPs GBP1 and IIGP (Prakash et al., 2000; Uthaiyah et al., 2003). The highly flexible switch II might have proven especially suitable to promote catalysis in the other GGBP. After gene duplication, one GGBP might have specialised as GAP and lost its ability to bind nucleotides accompanied by the loss of the P-loop and the rebuilding of switch I as seen in the case of Rap1GAP.

GAPs for Rap1 with the chain fold of the Rap1GAP catalytic domain are present from yeast to human. *Schizosaccharomyces pombe* but not *Saccharomyces cerevisiae* has a Tuberin homologue (Matsumoto et al., 2002) which is likely to activate the GTPase activity of the yeast RheB homologue Rhb1 responsible for regulation of cell growth (Mach et al., 2000). This might indicate that the first GAP of the Rap1GAP family was a Tuberin homologue since no protein in yeast exists with the combination of dimerisation and catalytic domain as described here for Rap1GAP. Alternatively, yeast might have lost its *Rap1GAP* homologue during evolution. Proteins with the typical Rap1GAP domain arrangement are described in *Dictyostelium* in which a Rap1GAP homologue was found (J. Faix, unpublished) and in the nematode *Caenorhabditis elegans* in which a *Rap1GAP* as well as *Spa1* homologue were identified.

However, also GAPs for Rap1 were described which do not have any sequence similarity to the Rap1GAP family. In *Saccharomyces cerevisiae*, the putative Rap1 homologue Bud1 is involved in selection of the new budding site (Chant and Herskowitz, 1991). In contrast to Ras and Rap1, it contains an isoleucine at position 61. Interestingly, the GAP for Bud1 which is called Bud2 has sequence homology to the RasGAP family and has also a putative arginine finger as judged from sequence comparison (Park et al., 1993). Likewise, the human GAP^{IP4BP} has sequence homology to the RasGAP family, but GAP activity towards Ras and Rap1 has been described (Cullen et al., 1995). Unexpectedly, results in our laboratory indicate that the GAP^{IP4BP} catalytic domain has appreciable GAP activity only towards Ras but not Rap1 (L.C. Polte and O. Daumke, unpublished). However, the full-length GAP^{IP4BP} activates Ras and Rap1 with comparable rates. Furthermore, the GAP activity towards Ras seems to be dependent on the arginine finger whereas the GAP activity towards Rap1 is not (P. Cullen, unpublished). These observations indicate that GAP^{IP4BP} uses a different mechanism to stimulate GTP hydrolysis in Ras and Rap1. It can be speculated that equivalent to the dimerisation domain of Rap1GAP, a second domain in GAP^{IP4BP} is needed for full GAP activity towards Rap1.

6 References

- Admiraal,S.J. and Herschlag,D. (1995). Mapping the transition state for ATP hydrolysis: implications for enzymatic catalysis. *Chem. Biol.* 2, 729-739.
- Ahmadian,M.R., Hoffmann,U., Goody,R.S., and Wittinghofer,A. (1997a). Individual rate constants for the interaction of Ras proteins with GTPase-activating proteins determined by fluorescence spectroscopy. *Biochemistry* 36, 4535-4541.
- Ahmadian,M.R., Mittal,R., Hall,A., and Wittinghofer,A. (1997b). Aluminum fluoride associates with the small guanine nucleotide binding proteins. *FEBS Lett.* 408, 315-318.
- Ahmadian,M.R., Stege,P., Scheffzek,K., and Wittinghofer,A. (1997c). Confirmation of the arginine-finger hypothesis for the GAP-stimulated GTP-hydrolysis reaction of Ras. *Nat Struct. Biol.* 4, 686-689.
- Albert,S., Will,E., and Gallwitz,D. (1999). Identification of the catalytic domains and their functionally critical arginine residues of two yeast GTPase-activating proteins specific for Ypt/Rab transport GTPases. *EMBO J* 18, 5216-5225.
- Allin,C., Ahmadian,M.R., Wittinghofer,A., and Gerwert,K. (2001). Monitoring the GAP catalyzed H-Ras GTPase reaction at atomic resolution in real time. *Proc. Natl. Acad. Sci U.S.A.* 98, 7754-7759.
- Allin,C. and Gerwert,K. (2001). Ras catalyzes GTP hydrolysis by shifting negative charges from gamma- to beta-phosphate as revealed by time-resolved FTIR difference spectroscopy. *Biochemistry* 2001, 40, 3037-3046.
- Almoguera,C., Shibata,D., Forrester,K., Martin,J., Arnheim,N., and Perucho,M. (1988). Most human carcinomas of the exocrine pancreas contain mutant c-K-ras genes. *Cell* 53, 549-554.
- Altschuler,D.L. and Ribeiro-Neto,F. (1998). Mitogenic and oncogenic properties of the small G protein Rap1b. *Proc. Natl. Acad. Sci. U. S. A* 95, 7475-7479.
- Asha,H., de Ruyter,N.D., Wang,M.G., and Hariharan,I.K. (1999). The Rap1 GTPase functions as a regulator of morphogenesis in vivo. *EMBO J* 18, 605-615.
- Au,K.S., Rodriguez,J.A., Finch,J.L., Volcik,K.A., Roach,E.S., Delgado,M.R., Rodriguez E Jr, and Northrup,H. (1998). Germ-line mutational analysis of the TSC2 gene in 90 tuberous-sclerosis patients. *Am. J Hum. Genet.* 62, 286-294.
- Bailey,S. (1994). The Ccp4 Suite - Programs for Protein Crystallography. *Acta Crystallographica Section D-Biological Crystallography* 50, 760-763.
- Barlowe,C., Orci,L., Yeung,T., Hosobuchi,M., Hamamoto,S., Salama,N., Rexach,M.F., Ravazzola,M., Amherdt,M., and Schekman,R. (1994). COPII: a membrane coat formed by Sec proteins that drive vesicle budding from the endoplasmic reticulum. *Cell* 77, 895-907.
- Barrett,T., Xiao,B., Dodson,E.J., Dodson,G., Ludbrook,S.B., Nurmahomed,K., Gamblin,S.J., Musacchio,A., Smerdon,S.J., and Eccleston,J.F. (1997). The structure of the GTPase-activating domain from p50rhoGAP. *Nature* 385, 458-461.
- Beranger,F., Goud,B., Tavitian,A., and de Gunzburg,J. (1991). Association of the Ras-antagonistic Rap1/Krev-1 proteins with the Golgi complex. *Proc. Natl. Acad. Sci. U. S. A* 88, 1606-1610.

- Berchtold,H., Reshetnikova,L., Reiser,C.O., Schirmer,N.K., Sprinzl,M., and Hilgenfeld,R. (1993). Crystal structure of active elongation factor Tu reveals major domain rearrangements. *Nature* 365, 126-132.
- Bi,X., Corpina,R.A., and Goldberg,J. (2002). Structure of the Sec23/24-Sar1 pre-budding complex of the COPII vesicle coat. *Nature* 419, 271-277.
- Bigay,J., Gounon,P., Robineau,S., and Antony,B. (2003). Lipid packing sensed by ArfGAP1 couples COPI coat disassembly to membrane bilayer curvature. *Nature* 426, 563-566.
- Boettner,B., Govek,E.E., Cross,J., and Van Aelst,L. (2000). The junctional multidomain protein AF-6 is a binding partner of the Rap1A GTPase and associates with the actin cytoskeletal regulator profilin. *Proc. Natl. Acad. Sci. U. S. A* 97, 9064-9069.
- Bos,J.L., de Rooij,J., and Reedquist,K.A. (2001). Rap1 signalling: adhering to new models. *Nat. Rev. Mol. Cell Biol.* 2, 369-377.
- Bourne,H.R., Sanders,D.A., and McCormick,F. (1990). The GTPase superfamily: a conserved switch for diverse cell functions. *Nature* 348, 125-132.
- Bourne,H.R., Sanders,D.A., and McCormick,F. (1991). The GTPase superfamily: conserved structure and molecular mechanism. *Nature* 349, 117-127.
- Bradford,M.M. (1976). A rapid and sensitive method for the quantitation of microgram quantities of protein utilizing the principle of protein-dye binding. *Anal. Biochem.* 72, 248-254.
- Brinkmann, T. (2000) Untersuchung der GAP katalysierten GTP-Hydrolyse-reaktion von Ras und Rap. Doctoral thesis, Giessen.
- Brinkmann,T., Daumke,O., Herbrand,U., Kuhlmann,D., Stege,P., Ahmadian,M.R., and Wittinghofer,A. (2002). Rap-specific GTPase activating protein follows an alternative mechanism. *J Biol. Chem.* 2002 277, 12525-12531.
- Brunger,A.T. (1992). Free R-Value - A Novel Statistical Quantity for Assessing the Accuracy of Crystal-Structures. *Nature* 355, 472-475.
- Brunger,A.T. (1997). Free R value: Cross-validation in crystallography. *Macromolecular Crystallography, Pt B* 277, 366-396.
- Brunger,A.T., Adams,P.D., Clore,G.M., Delano,W.L., Gros,P., Grosse-Kunstleve,R.W., Jiang,J.S., Kuszewski,J., Nilges,M., Pannu,N.S., Read,R.J., Rice,L.M., Simonson,T., and Warren,G.L. (1998). Crystallography & NMR system: A new software suite for macromolecular structure determination. *Acta Crystallographica Section D-Biological Crystallography* 54, 905-921.
- Castro,A.F., Rebhun,J.F., Clark,G.J., and Quilliam,L.A. (2003). Rheb Binds Tuberous Sclerosis Complex 2 (TSC2) and Promotes S6 Kinase Activation in a Rapamycin- and Farnesylation-dependent Manner. *J Biol. Chem* 278, 32493-32496.
- Cepus,V., Scheidig,A.J., Goody,R.S., and Gerwert,K. (1998). Time-resolved FTIR studies of the GTPase reaction of H-ras p21 reveal a key role for the beta-phosphate. *Biochemistry* 37, 10263-10271.
- Chabre,M. (1990). Aluminofluoride and beryllifluoride complexes: a new phosphate analogs in enzymology. *Trends Biochem. Sci.* 15, 6-10.
- Chant,J. and Herskowitz,I. (1991). Genetic control of bud site selection in yeast by a set of gene products that constitute a morphogenetic pathway. *Cell* 65, 1203-1212.

- Cherfils,J., Menetrey,J., Le Bras,G., Janoueix-Lerosey,I., de Gunzburg,J., Garel,J.R., and Auzat,I. (1997). Crystal structures of the small G protein Rap2A in complex with its substrate GTP, with GDP and with GTPgammaS. *EMBO J* 16, 5582-5591.
- Chung,C.T., Niemela,S.L., and Miller,R.H. (1989). One-step preparation of competent *Escherichia coli*: transformation and storage of bacterial cells in the same solution. *Proc. Natl. Acad. Sci. U. S. A* 86, 2172-2175.
- Coleman,D.E., Berghuis,A.M., Lee,E., Linder,M.E., Gilman,A.G., and Sprang,S.R. (1994). Structures of active conformations of Gi alpha 1 and the mechanism of GTP hydrolysis. *Science* 265, 1405-1412.
- Cool,R.H. and Parmeggiani,A. (1991). Substitution of histidine-84 and the GTPase mechanism of elongation factor Tu. *Biochemistry* 30, 362-366.
- Cukierman,E., Huber,I., Rotman,M., and Cassel,D. (1995). The ARF1 GTPase-activating protein: zinc finger motif and Golgi complex localization. *Science* 270, 1999-2002.
- Cullen,P.J., Hsuan,J.J., Truong,O., Letcher,A.J., Jackson,T.R., Dawson,A.P., and Irvine,R.F. (1995). Identification of a specific Ins(1,3,4,5)P4-binding protein as a member of the GAP1 family. *Nature* 376, 527-530.
- Dabora,S.L., Jozwiak,S., Franz,D.N., Roberts,P.S., Nieto,A., Chung,J., Choy,Y.S., Reeve,M.P., Thiele,E., Egelhoff,J.C., Kasprzyk-Obara,J., Domanska-Pakiela,D., and Kwiatkowski,D.J. (2001). Mutational analysis in a cohort of 224 tuberous sclerosis patients indicates increased severity of TSC2, compared with TSC1, disease in multiple organs. *Am. J Hum. Genet.* 68, 64-80.
- de Bruyn,K.M., Rangarajan,S., Reedquist,K.A., Figdor,C.G., and Bos,J.L. (2002). The small GTPase Rap1 is required for Mn(2+)- and antibody-induced LFA-1- and VLA-4-mediated cell adhesion. *J Biol. Chem.* 277, 29468-29476.
- de Rooij,J., Boenink,N.M., van Triest,M., Cool,R.H., Wittinghofer,A., and Bos,J.L. (1999). PDZ-GEF1, a guanine nucleotide exchange factor specific for Rap1 and Rap2. *J Biol. Chem.* 274, 38125-38130.
- de Rooij,J., Zwartkuis,F.J., Verheijen,M.H., Cool,R.H., Nijman,S.M., Wittinghofer,A., and Bos,J.L. (1998). Epac is a Rap1 guanine-nucleotide-exchange factor directly activated by cyclic AMP. *Nature* 396, 474-477.
- Der,C.J., Finkel,T., and Cooper,G.M. (1986). Biological and biochemical properties of human rasH genes mutated at codon 61. *Cell* 44, 167-176.
- Downward,J. (1998). Ras signalling and apoptosis. *Curr. Opin. Genet. Dev.* 8, 49-54.
- Drenth,J. (1999). *Principles of Protein X-Ray Crystallography*. Springer Verlag, Berlin.
- Druey,K.M., Blumer,K.J., Kang,V.H., and Kehrl,J.H. (1996). Inhibition of G-protein-mediated MAP kinase activation by a new mammalian gene family. *Nature* 379, 742-746.
- Egea,P.F., Shan,S.O., Napetschnig,J., Savage,D.F., Walter,P., and Stroud,R.M. (2004). Substrate twinning activates the signal recognition particle and its receptor. *Nature* 427, 215-221.
- Focia,P.J., Shepotinovskaya,I.V., Seidler,J.A., and Freymann,D.M. (2004). Heterodimeric GTPase core of the SRP targeting complex. *Science* 303, 373-377.

- Franke, B., Akkerman, J.W., and Bos, J.L. (1997). Rapid Ca²⁺-mediated activation of Rap1 in human platelets. *EMBO J* 16, 252-259.
- Frech, M., John, J., Pizon, V., Chardin, P., Tavitian, A., Clark, R., McCormick, F., and Wittinghofer, A. (1990). Inhibition of GTPase activating protein stimulation of Ras-p21 GTPase by the Krev-1 gene product. *Science* 249, 169-171.
- Freymann, D.M., Keenan, R.J., Stroud, R.M., and Walter, P. (1997). Structure of the conserved GTPase domain of the signal recognition particle. *Nature* 385, 361-364.
- Friedel, G. (1913). *Comptes Rendus* 157, 1533.
- Fu, Y. and Galan, J.E. (1999). A salmonella protein antagonizes Rac-1 and Cdc42 to mediate host-cell recovery after bacterial invasion. *Nature* 401, 293-297.
- Gao, Q., Singh, L., Kumar, A., Srinivasan, S., Wazer, D.E., and Band, V. (2001a). Human papillomavirus type 16 E6-induced degradation of E6TP1 correlates with its ability to immortalize human mammary epithelial cells. *J Virol.* 75, 4459-4466.
- Gao, Q., Srinivasan, S., Boyer, S.N., Wazer, D.E., and Band, V. (1999). The E6 oncoproteins of high-risk papillomaviruses bind to a novel putative GAP protein, E6TP1, and target it for degradation. *Mol Cell Biol.* 19, 733-744.
- Gao, X., Satoh, T., Liao, Y., Song, C., Hu, C.D., Kariya, K.K., and Kataoka, T. (2001b). Identification and characterization of RA-GEF-2, a Rap guanine nucleotide exchange factor that serves as a downstream target of M-Ras. *J Biol. Chem.* 276, 42219-42225.
- Garami, A., Zwartkruis, F.J., Nobukuni, T., Joaquin, M., Rocco, M., Stocker, H., Kozma, S.C., Hafen, E., Bos, J.L., and Thomas, G. (2003). Insulin activation of Rheb, a mediator of mTOR/S6K/4E-BP signaling, is inhibited by TSC1 and 2. *Mol Cell* 11, 1457-1466.
- Garcia-Ranea, J.A. and Valencia, A. (1998). Distribution and functional diversification of the ras superfamily in *Saccharomyces cerevisiae*. *FEBS Lett.* 434, 219-225.
- Glennon, T.M., Villa, J., and Warshel, A. (2000). How does GAP catalyze the GTPase reaction of Ras? A computer simulation study. *Biochemistry* 39, 9641-9651.
- Goehring, U.M., Schmidt, G., Pederson, K.J., Aktories, K., and Barbieri, J.T. (1999). The N-terminal domain of *Pseudomonas aeruginosa* exoenzyme S is a GTPase-activating protein for Rho GTPases. *J Biol. Chem.* 274, 36369-36372.
- Goldberg, J. (1999). Structural and functional analysis of the ARF1-ARFGAP complex reveals a role for coatamer in GTP hydrolysis. *Cell* 96, 893-902.
- Gomez, M., Sampson, J., and Whittemore V. (1999). *The tuberous sclerosis complex*. Oxford University Press, England.
- Gotoh, T., Hattori, S., Nakamura, S., Kitayama, H., Noda, M., Takai, Y., Kaibuchi, K., Matsui, H., Hatase, O., and Takahashi, H. (1995). Identification of Rap1 as a target for the Crk SH3 domain-binding guanine nucleotide-releasing factor C3G. *Mol Cell Biol.* 15, 6746-6753.
- Graham, D.L., Eccleston, J.F., Chung, C.W., and Lowe, P.N. (1999). Magnesium fluoride-dependent binding of small G proteins to their GTPase-activating proteins. *Biochemistry* 38, 14981-14987.
- Greasley, S.E., Jhoti, H., Teahan, C., Solari, R., Fensome, A., Thomas, G.M., Cockcroft, S., and Bax, B. (1995). The structure of rat ADP-ribosylation factor-1 (ARF-1) complexed to GDP determined from two different crystal forms. *Nat Struct. Biol.* 2, 797-806.

- Hattori,M., Tsukamoto,N., Nur-e-Kamal MS, Rubinfeld,B., Iwai,K., Kubota,H., Maruta,H., and Minato,N. (1995). Molecular cloning of a novel mitogen-inducible nuclear protein with a Ran GTPase-activating domain that affects cell cycle progression. *Mol Cell Biol.* 15, 552-560.
- Hillier,B.J., Christopherson,K.S., Prehoda,K.E., Brecht,D.S., and Lim,W.A. (1999). Unexpected modes of PDZ domain scaffolding revealed by structure of nNOS-syntrophin complex. *Science* 284, 812-815.
- Hillig,R.C., Hanzal-Bayer,M., Linari,M., Becker,J., Wittinghofer,A., and Renault,L. (2000). Structural and biochemical properties show ARL3-GDP as a distinct GTP binding protein. *Structure. Fold.* 8, 1239-1245.
- Hillig,R.C., Renault,L., Vetter,I.R., Drell,T., Wittinghofer,A., and Becker,J. (1999). The crystal structure of rna1p: a new fold for a GTPase-activating protein. *Mol Cell* 3, 781-791.
- Holm,L. and Sander,C. (1993). Protein structure comparison by alignment of distance matrices. *J Mol Biol.* 233, 123-138.
- Hoofstede,R.W.W., Vriend,G., Sander,C., and Abola,E.E. (1996). Errors in protein structures. *Nature* 381, 272.
- Hope,H. (1988). Cryocrystallography of biological macromolecules: a generally applicable method. *Acta Crystallogr. B* 44, 22-26.
- Huang,L., Hofer,F., Martin,G.S., and Kim,S.H. (1998). Structural basis for the interaction of Ras with RalGDS. *Nat Struct. Biol.* 5, 422-426.
- Ishida,D., Kometani,K., Yang,H., Kakugawa,K., Masuda,K., Iwai,K., Suzuki,M., Itohara,S., Nakahata,T., Hiai,H., Kawamoto,H., Hattori,M., and Minato,N. (2003). Myeloproliferative stem cell disorders by deregulated Rap1 activation in SPA-1-deficient mice. *Cancer Cell* 4, 55-65.
- Janoueix-Lerosey,I., Polakis,P., Tavittian,A., and de Gunzburg,J. (1992). Regulation of the GTPase activity of the ras-related rap2 protein. *Biochem. Biophys. Res. Commun.* 189, 455-464.
- John,J., Frech,M., and Wittinghofer,A. (1988). Biochemical properties of Ha-ras encoded p21 mutants and mechanism of the autophosphorylation reaction. *J Biol. Chem.* 263, 11792-11799.
- Jones,A.C., Shyamsundar,M.M., Thomas,M.W., Maynard,J., Idziaszczyk,S., Tomkins,S., Sampson,J.R., and Cheadle,J.P. (1999). Comprehensive mutation analysis of TSC1 and TSC2-and phenotypic correlations in 150 families with tuberous sclerosis. *Am. J Hum. Genet.* 64, 1305-1315.
- Jones,S., Marin,A., and Thornton,J.M. (2000). Protein domain interfaces: characterization and comparison with oligomeric protein interfaces. *Protein Eng* 13, 77-82.
- Joneson,T., White,M.A., Wigler,M.H., and Bar-Sagi,D. (1996). Stimulation of membrane ruffling and MAP kinase activation by distinct effectors of RAS. *Science* 271, 810-812.
- Jordan,J.D., Carey,K.D., Stork,P.J., and Iyengar,R. (1999). Modulation of rap activity by direct interaction of G α (o) with Rap1 GTPase-activating protein. *J Biol. Chem.* 274, 21507-21510.
- Kabsch,W. (1993). Automatic Processing of Rotation Diffraction Data from Crystals of Initially Unknown Symmetry and Cell Constants. *J. Appl. Crystallogr.* 26, 795-800.

- Kao,S., Jaiswal,R.K., Kolch,W., and Landreth,G.E. (2001). Identification of the mechanisms regulating the differential activation of the mapk cascade by epidermal growth factor and nerve growth factor in PC12 cells. *J Biol. Chem.* 276, 18169-18177.
- Katagiri,K., Hattori,M., Minato,N., Irie,S., Takatsu,K., and Kinashi,T. (2000). Rap1 is a potent activation signal for leukocyte function-associated antigen 1 distinct from protein kinase C and phosphatidylinositol-3-OH kinase. *Mol Cell Biol.* 20, 1956-1969.
- Katagiri,K., Hattori,M., Minato,N., and Kinashi,T. (2002). Rap1 functions as a key regulator of T-cell and antigen-presenting cell interactions and modulates T-cell responses. *Mol Cell Biol.* 22, 1001-1015.
- Kawasaki,H., Springett,G.M., Mochizuki,N., Toki,S., Nakaya,M., Matsuda,M., Housman,D.E., and Graybiel,A.M. (1998a). A family of cAMP-binding proteins that directly activate Rap1. *Science* 282, 2275-2279.
- Kawasaki,H., Springett,G.M., Toki,S., Canales,J.J., Harlan,P., Blumenstiel,J.P., Chen,E.J., Bany,I.A., Mochizuki,N., Ashbacher,A., Matsuda,M., Housman,D.E., and Graybiel,A.M. (1998b). A Rap guanine nucleotide exchange factor enriched highly in the basal ganglia. *Proc. Natl. Acad. Sci. U. S. A* 95, 13278-13283.
- Keenan,R.J., Freymann,D.M., Stroud,R.M., and Walter,P. (2001). The signal recognition particle. *Annu. Rev. Biochem.* 70, 755-775.
- Kikuchi,A., Sasaki,T., Araki,S., Hata,Y., and Takai,Y. (1989). Purification and characterization from bovine brain cytosol of two GTPase-activating proteins specific for smg p21, a GTP-binding protein having the same effector domain as c-ras p21s. *J Biol. Chem.* 264, 9133-9136.
- Kimple,R.J., Kimple,M.E., Betts,L., Sondek,J., and Siderovski,D.P. (2002). Structural determinants for GoLoco-induced inhibition of nucleotide release by Galpha subunits. *Nature* 416, 878-881.
- Kitayama,H., Sugimoto,Y., Matsuzaki,T., Ikawa,Y., and Noda,M. (1989). A ras-related gene with transformation suppressor activity. *Cell* 56, 77-84.
- Klebe,C., Bischoff,F.R., Ponstingl,H., and Wittinghofer,A. (1995). Interaction of the nuclear GTP-binding protein Ran with its regulatory proteins RCC1 and RanGAP1. *Biochemistry* 34, 639-647.
- Klose,A., Ahmadian,M.R., Schuelke,M., Scheffzek,K., Hoffmeyer,S., Gewies,A., Schmitz,F., Kaufmann,D., Peters,H., Wittinghofer,A., and Nurnberg,P. (1998). Selective disactivation of neurofibromin GAP activity in neurofibromatosis type 1. *Hum. Mol Genet.* 7, 1261-1268.
- Knox,A.L. and Brown,N.H. (2002). Rap1 GTPase regulation of adherens junction positioning and cell adhesion. *Science* 295, 1285-1288.
- Knudson,A.G., Jr. (1971). Mutation and cancer: statistical study of retinoblastoma. *Proc. Natl. Acad. Sci. U. S. A* 68, 820-823.
- Kobe,B. and Deisenhofer,J. (1995). Proteins with leucine-rich repeats. *Curr. Opin. Struct. Biol.* 5, 409-416.
- Koonin,E.V., Wolf,Y.I., and Aravind,L. (2000). Protein fold recognition using sequence profiles and its application in structural genomics. *Adv. Protein Chem.* 54, 245-275.

- Kraemer,A., Brinkmann,T., Plettner,I., Goody,R., and Wittinghofer,A. (2002). Fluorescently labelled guanine nucleotide binding proteins to analyse elementary steps of GAP-catalysed reactions. *J Mol Biol.* 324, 763-774.
- Kraulis,P.J. (1991). Molscript - A Program to Produce Both Detailed and Schematic Plots of Protein Structures. *J. Appl. Crystallogr.* 24, 946-950.
- Krengel,U., Schlichting,L., Scherer,A., Schumann,R., Frech,M., John,J., Kabsch,W., Pai,E.F., and Wittinghofer,A. (1990). Three-dimensional structures of H-ras p21 mutants: molecular basis for their inability to function as signal switch molecules. *Cell* 62, 539-548.
- Kurachi,H., Wada,Y., Tsukamoto,N., Maeda,M., Kubota,H., Hattori,M., Iwai,K., and Minato,N. (1997). Human SPA-1 gene product selectively expressed in lymphoid tissues is a specific GTPase-activating protein for Rap1 and Rap2. Segregate expression profiles from a rap1GAP gene product. *J Biol. Chem.* 272, 28081-28088.
- Kwiatkowski,D.J. (2003). Tuberous sclerosis: from tubers to mTOR. *Ann. Hum. Genet.* 67, 87-96.
- Laemmli,U.K. (1970). Cleavage of structural proteins during the assembly of the head of bacteriophage T4. *Nature* 227, 680-685.
- Laskowski,R.A., Macarthur,M.W., Moss,D.S., and Thornton,J.M. (1993). Procheck - A Program to Check the Stereochemical Quality of Protein Structures. *J. Appl. Crystallogr.* 26, 283-291.
- Leipe,D.D., Wolf,Y.I., Koonin,E.V., and Aravind,L. (2002). Classification and evolution of P-loop GTPases and related ATPases. *J Mol Biol.* 317, 41-72.
- Lenzen,C., Cool,R.H., and Wittinghofer,A. (1995). Analysis of intrinsic and CDC25-stimulated guanine nucleotide exchange of p21ras-nucleotide complexes by fluorescence measurements. *Methods Enzymol.* 255, 95-109.
- Leupold,C.M., Goody,R.S., and Wittinghofer,A. (1983). Stereochemistry of the elongation factor Tu X GTP complex. *Eur. J Biochem.* 135, 237-241.
- Li,Y., Corradetti,M.N., Inoki,K., and Guan,K.L. (2004). TSC2: filling the GAP in the mTOR signaling pathway. *Trends Biochem. Sci.* 29, 32-38.
- Linnemann,T., Geyer,M., Jaitner,B.K., Block,C., Kalbitzer,H.R., Wittinghofer,A., and Herrmann,C. (1999). Thermodynamic and kinetic characterization of the interaction between the Ras binding domain of AF6 and members of the Ras subfamily. *J Biol. Chem.* 274, 13556-13562.
- Lobley,A., Whitmore,L., and Wallace,B.A. (2002). DICHROWEB: an interactive website for the analysis of protein secondary structure from circular dichroism spectra. *Bioinformatics.* 18, 211-212.
- M'Rabet,L., Coffey,P., Zwartkuis,F., Franke,B., Segal,A.W., Koenderman,L., and Bos,J.L. (1998). Activation of the small GTPase rap1 in human neutrophils. *Blood* 92, 2133-2140.
- Mach,K.E., Furge,K.A., and Albright,C.F. (2000). Loss of Rbh1, a Rheb-related GTPase in fission yeast, causes growth arrest with a terminal phenotype similar to that caused by nitrogen starvation. *Genetics* 155, 611-622.
- Maegley,K.A., Admiraal,S.J., and Herschlag,D. (1996). Ras-catalyzed hydrolysis of GTP: a new perspective from model studies. *Proc. Natl. Acad. Sci. U. S. A* 93, 8160-8166.

- Maheshwar,M.M., Cheadle,J.P., Jones,A.C., Myring,J., Fryer,A.E., Harris,P.C., and Sampson,J.R. (1997). The GAP-related domain of tuberlin, the product of the TSC2 gene, is a target for missense mutations in tuberous sclerosis. *Hum. Mol Genet.* 6, 1991-1996.
- Mandiyani,V., Andreev,J., Schlessinger,J., and Hubbard,S.R. (1999). Crystal structure of the ARF-GAP domain and ankyrin repeats of PYK2-associated protein beta. *EMBO J* 18, 6890-6898.
- Manning,B.D. and Cantley,L.C. (2003). Rheb fills a GAP between TSC and TOR. *Trends Biochem. Sci.* 28, 573-576.
- Maruta,H., Holden,J., Sizeland,A., and D'Abaco,G. (1991). The residues of Ras and Rap proteins that determine their GAP specificities. *J Biol. Chem.*, 266, 11661-11668.
- Matsumoto,S., Bandyopadhyay,A., Kwiatkowski,D.J., Maitra,U., and Matsumoto,T. (2002). Role of the Tsc1-Tsc2 complex in signaling and transport across the cell membrane in the fission yeast *Schizosaccharomyces pombe*. *Genetics* 161, 1053-1063.
- Matthews,B.W. (1968). Solvent Content of Protein Crystals. *J. Mol. Biol.* 33, 491-&.
- McLeod,S.J., Ingham,R.J., Bos,J.L., Kurosaki,T., and Gold,M.R. (1998). Activation of the Rap1 GTPase by the B cell antigen receptor. *J Biol. Chem.* 273, 29218-29223.
- McRee,D.E. (1999). XtalView Xfit - A versatile program for manipulating atomic coordinates and electron density. *J. Struct. Biol.* 125, 156-165.
- Meng,J. and Casey,P.J. (2002). Activation of Gz attenuates Rap1-mediated differentiation of PC12 cells. *J Biol. Chem.* 277, 43417-43424.
- Meng,J., Glick,J.L., Polakis,P., and Casey,P.J. (1999). Functional interaction between Galpha(z) and Rap1GAP suggests a novel form of cellular cross-talk. *J Biol. Chem.* 274, 36663-36669.
- Merritt,E.A. and Bacon,D.J. (1997). Raster3D: Photorealistic molecular graphics., *Methods in Enzymology* pp. 505-524.
- Meyer,G. and Brose,N. (2003). Neuroscience. SPARring with spines. *Science* 302, 1341-1344.
- Mitra,R.S., Zhang,Z., Henson,B.S., Kurnit,D.M., Carey,T.E., and D'Silva,N.J. (2003). Rap1A and rap1B ras-family proteins are prominently expressed in the nucleus of squamous carcinomas: nuclear translocation of GTP-bound active form. *Oncogene* 2003 22, 6243-6256.
- Mittal,R., Ahmadian,M.R., Goody,R.S., and Wittinghofer,A. (1996). Formation of a transition-state analog of the Ras GTPase reaction by Ras-GDP, tetrafluoroaluminate, and GTPase-activating proteins. *Science* 273, 115-117.
- Mochizuki,N., Ohba,Y., Kiyokawa,E., Kurata,T., Murakami,T., Ozaki,T., Kitabatake,A., Nagashima,K., and Matsuda,M. (1999). Activation of the ERK/MAPK pathway by an isoform of rap1GAP associated with G alpha(i). *Nature* 400, 891-894.
- Mochizuki,N., Yamashita,S., Kurokawa,K., Ohba,Y., Nagai,T., Miyawaki,A., and Matsuda,M. (2001). Spatio-temporal images of growth-factor-induced activation of Ras and Rap1. *Nature* 411, 1065-1068.
- Mohr,D., Wintermeyer,W., and Rodnina,M.V. (2002). GTPase activation of elongation factors Tu and G on the ribosome. *Biochemistry* 41, 12520-12528.

- Morozov,A., Muzzio,I.A., Bourtchouladze,R., Van Strien,N., Lapidus,K., Yin,D., Winder,D.G., Adams,J.P., Sweatt,J.D., and Kandel,E.R. (2003). Rap1 couples cAMP signaling to a distinct pool of p42/44MAPK regulating excitability, synaptic plasticity, learning, and memory. *Neuron* 39, 309-325.
- Murshudov,G.N., Vagin,A.A., and Dodson,J. (1997). Refinement of macromolecular structures by the maximum-likelihood method. *Acta Crystallographica Section D-Biological Crystallography* 53, 240-255.
- Nassar,N., Hoffman,G.R., Manor,D., Clardy,J.C., and Cerione,R.A. (1998). Structures of Cdc42 bound to the active and catalytically compromised forms of Cdc42GAP. *Nat Struct. Biol.* 5, 1047-1052.
- Nassar,N., Horn,G., Herrmann,C., Block,C., Janknecht,R., and Wittinghofer,A. (1996). Ras/Rap effector specificity determined by charge reversal. *Nat Struct. Biol.* 3, 723-729.
- Nassar,N., Horn,G., Herrmann,C., Scherer,A., McCormick,F., and Wittinghofer,A. (1995). The 2.2 Å crystal structure of the Ras-binding domain of the serine/threonine kinase c-Raf1 in complex with Rap1A and a GTP analogue. *Nature* 375, 554-560.
- Nicholas,K.B., Nicholas H.B.Jr, and Deerfield,D.W.I. (1997). GeneDoc: Analysis and Visualization of Genetic Variation *EMBNew. news* 4, 14.
- Nicholls,A., Bharadwaj,R., and Honig,B. (1993). Grasp - Graphical Representation and Analysis of Surface-Properties. *Biophysical Journal* 64, A166.
- Noel,J.P., Hamm,H.E., and Sigler,P.B. (1993). The 2.2 Å crystal structure of transducin- α complexed with GTP γ S. *Nature* 366, 654-663.
- Oehler,S., Amouyal,M., Kolkhof,P., Wilcken-Bergmann,B., and Muller-Hill,B. (1994). Quality and position of the three lac operators of *E. coli* define efficiency of repression. *EMBO J* 13, 3348-3355.
- Ogle,J.M., Carter,A.P., and Ramakrishnan,V. (2003). Insights into the decoding mechanism from recent ribosome structures. *Trends Biochem. Sci.* 28, 259-266.
- Ohtsuka,T., Shimizu,K., Yamamori,B., Kuroda,S., and Takai,Y. (1996). Activation of brain B-Raf protein kinase by Rap1B small GTP-binding protein. *J Biol. Chem.* 271, 1258-1261.
- Okada,S., Matsuda,M., Anafi,M., Pawson,T., and Pessin,J.E. (1998). Insulin regulates the dynamic balance between Ras and Rap1 signaling by coordinating the assembly states of the Grb2-SOS and CrkII-C3G complexes. *EMBO J* 17, 2554-2565.
- Pacold,M.E., Suire,S., Perisic,O., Lara-Gonzalez,S., Davis,C.T., Walker,E.H., Hawkins,P.T., Stephens,L., Eccleston,J.F., and Williams,R.L. (2000). Crystal structure and functional analysis of Ras binding to its effector phosphoinositide 3-kinase γ . *Cell* 103, 931-943.
- Pak,D.T. and Sheng,M. (2003). Targeted protein degradation and synapse remodeling by an inducible protein kinase. *Science* 302, 1368-1373.
- Pak,D.T., Yang,S., Rudolph-Correia,S., Kim,E., and Sheng,M. (2001). Regulation of dendritic spine morphology by SPAR, a PSD-95-associated RapGAP. *Neuron* 31, 289-303.
- Park,H.O., Chant,J., and Herskowitz,I. (1993). BUD2 encodes a GTPase-activating protein for Bud1/Rsr1 necessary for proper bud-site selection in yeast. *Nature* 365, 269-274.
- Park,H.O., Kang,P.J., and Rachfal,A.W. (2002). Localization of the Rsr1/Bud1 GTPase involved in selection of a proper growth site in yeast. *J Biol. Chem.* 277, 26721-26724.

- Pasqualato,S., Renault,L., and Cherfils,J. (2002). Arf, Arl, Arp and Sar proteins: a family of GTP-binding proteins with a structural device for 'front-back' communication. *EMBO Rep.* 3, 1035-1041.
- Pawel-Rammingen,U., Telepnev,M.V., Schmidt,G., Aktories,K., Wolf-Watz,H., and Rosqvist,R. (2000). GAP activity of the Yersinia YopE cytotoxin specifically targets the Rho pathway: a mechanism for disruption of actin microfilament structure. *Mol Microbiol.* 36, 737-748.
- Pawson,T. and Saxton,T.M. (1999). Signaling networks--do all roads lead to the same genes? *Cell* 97, 675-678.
- Pizon,V., Chardin,P., Lerosey,I., Olofsson,B., and Tavitian,A. (1988). Human cDNAs rap1 and rap2 homologous to the Drosophila gene Dras3 encode proteins closely related to ras in the 'effector' region. *Oncogene* 3, 201-204.
- Pizon,V., Desjardins,M., Bucci,C., Parton,R.G., and Zerial,M. (1994). Association of Rap1a and Rap1b proteins with late endocytic/phagocytic compartments and Rap2a with the Golgi complex. *J Cell Sci.* 107, 1661-1670.
- Polakis,P., Rubinfeld,B., and McCormick,F. (1992). Phosphorylation of rap1GAP in vivo and by cAMP-dependent kinase and the cell cycle p34cdc2 kinase in vitro. *J Biol. Chem.* 267, 10780-10785.
- Polakis,P.G., Rubinfeld,B., Evans,T., and McCormick,F. (1991). Purification of a plasma membrane-associated GTPase-activating protein specific for rap1/Krev-1 from HL60 cells. *Proc. Natl. Acad. Sci. U. S. A* 88, 239-243.
- Posern,G., Weber,C.K., Rapp,U.R., and Feller,S.M. (1998). Activity of Rap1 is regulated by bombesin, cell adhesion, and cell density in NIH3T3 fibroblasts. *J Biol. Chem.* 273, 24297-24300.
- Potter,C.J., Pedraza,L.G., and Xu,T. (2002). Akt regulates growth by directly phosphorylating Tsc2. *Nat Cell Biol.* 4, 658-665.
- Prakash,B., Praefcke,G.J., Renault,L., Wittinghofer,A., and Herrmann,C. (2000). Structure of human guanylate-binding protein 1 representing a unique class of GTP-binding proteins. *Nature* 403, 567-571.
- Prive,G.G., Milburn,M.V., Tong,L., de Vos,A.M., Yamaizumi,Z., Nishimura,S., and Kim,S.H. (1992). X-ray crystal structures of transforming p21 ras mutants suggest a transition-state stabilization mechanism for GTP hydrolysis. *Proc. Natl. Acad. Sci. U. S. A* 89, 3649-3653.
- Rak,A., Fedorov,R., Alexandrov,K., Albert,S., Goody,R.S., Gallwitz,D., and Scheidig,A.J. (2000). Crystal structure of the GAP domain of Gyp1p: first insights into interaction with Ypt/Rab proteins. *EMBO J* 19, 5105-5113.
- Redfield,A.G. and Papastavros,M.Z. (1990). NMR study of the phosphoryl binding loop in purine nucleotide proteins: evidence for strong hydrogen bonding in human N-ras p21. *Biochemistry* 29, 3509-3514.
- Reedquist,K.A., Ross,E., Koop,E.A., Wolthuis,R.M., Zwartkuis,F.J., van Kooyk,Y., Salmon,M., Buckley,C.D., and Bos,J.L. (2000). The small GTPase, Rap1, mediates CD31-induced integrin adhesion. *J Cell Biol.* 148, 1151-1158.
- Renault,L., Guibert,B., and Cherfils,J. (2003). Structural snapshots of the mechanism and inhibition of a guanine nucleotide exchange factor. *Nature* 426, 525-530.

- Rhodes, G. (2000). *Crystallography made crystal clear*. Academic Press.
- Rittinger, K., Taylor, W.R., Smerdon, S.J., and Gamblin, S.J. (1998). Support for shared ancestry of GAPs. *Nature* **392**, 448-449.
- Rittinger, K., Walker, P.A., Eccleston, J.F., Nurmahomed, K., Owen, D., Laue, E., Gamblin, S.J., and Smerdon, S.J. (1997a). Crystal structure of a small G protein in complex with the GTPase-activating protein rhoGAP. *Nature* **388**, 693-697.
- Rittinger, K., Walker, P.A., Eccleston, J.F., Smerdon, S.J., and Gamblin, S.J. (1997b). Structure at 1.65 Å of RhoA and its GTPase-activating protein in complex with a transition-state analogue. *Nature* **389**, 758-762.
- Roy, B.C., Kuroda, T., Mori, S., Kohu, K., Akiyama, T., and Senda, T. (1999). Localization of a novel GAP family protein SPAL in the rat esophagus and heart. *Med. Electron Microsc.* **32**, 20-24.
- Rubinfeld, B., Crosier, W.J., Albert, I., Conroy, L., Clark, R., McCormick, F., and Polakis, P. (1992). Localization of the rap1GAP catalytic domain and sites of phosphorylation by mutational analysis. *Mol Cell Biol.* **12**, 4634-4642.
- Rubinfeld, B., Munemitsu, S., Clark, R., Conroy, L., Watt, K., Crosier, W.J., McCormick, F., and Polakis, P. (1991). Molecular cloning of a GTPase activating protein specific for the Krev-1 protein p21^{rap1}. *Cell* **65**, 1033-1042.
- Sahoo, T., Johnson, E.W., Thomas, J.W., Kuehl, P.M., Jones, T.L., Dokken, C.G., Touchman, J.W., Gallione, C.J., Lee-Lin, S.Q., Kosofsky, B., Kurth, J.H., Louis, D.N., Mettler, G., Morrison, L., Gil-Nagel, A., Rich, S.S., Zabramski, J.M., Boguski, M.S., Green, E.D., and Marchuk, D.A. (1999). Mutations in the gene encoding KRIT1, a Krev-1/rap1a binding protein, cause cerebral cavernous malformations (CCM1). *Hum. Mol Genet.* **8**, 2325-2333.
- Sambrook, J. Fritsch E. F. Maniatis T. *Molecular Cloning. A Laboratory Manual*. 1989. Cold Spring Harbor Laboratory Press.
- Sanger, F., Nicklen, S., and Coulson, A.R. (1977). DNA sequencing with chain-terminating inhibitors. *Biotechnology* **24**, 104-108.
- Scheffzek, K., Ahmadian, M.R., Kabsch, W., Wiesmuller, L., Lautwein, A., Schmitz, F., and Wittinghofer, A. (1997). The Ras-RasGAP complex: structural basis for GTPase activation and its loss in oncogenic Ras mutants. *Science* **277**, 333-338.
- Scheffzek, K., Ahmadian, M.R., and Wittinghofer, A. (1998). GTPase-activating proteins: helping hands to complement an active site. *Trends Biochem. Sci.* **23**, 257-262.
- Scheffzek, K., Klebe, C., Fritz-Wolf, K., Kabsch, W., and Wittinghofer, A. (1995). Crystal structure of the nuclear Ras-related protein Ran in its GDP-bound form. *Nature* **374**, 378-381.
- Scheffzek, K., Lautwein, A., Kabsch, W., Ahmadian, M.R., and Wittinghofer, A. (1996). Crystal structure of the GTPase-activating domain of human p120GAP and implications for the interaction with Ras. *Nature* **384**, 591-596.
- Schindelin, H., Kisker, C., Schlessman, J.L., Howard, J.B., and Rees, D.C. (1997). Structure of ADP x AIF4(-)-stabilized nitrogenase complex and its implications for signal transduction. *Nature* **387**, 370-376.
- Schneider, T.R. and Sheldrick, G.M. (2002). Substructure solution with SHELXD. *Acta Crystallogr. D. Biol. Crystallogr* **58**, 1772-1779.

- Schweins,T., Geyer,M., Scheffzek,K., Warshel,A., Kalbitzer,H.R., and Wittinghofer,A. (1995). Substrate-assisted catalysis as a mechanism for GTP hydrolysis of p21ras and other GTP-binding proteins. *Nat Struct. Biol.* 2, 36-44.
- Schweins,T., Scheffzek,K., Assheuer,R., and Wittinghofer,A. (1997). The role of the metal ion in the p21ras catalysed GTP-hydrolysis: Mn²⁺ versus Mg²⁺. *J Mol Biol.* 266, 847-856.
- Sebzda,E., Bracke,M., Tugal,T., Hogg,N., and Cantrell,D.A. (2002). Rap1A positively regulates T cells via integrin activation rather than inhibiting lymphocyte signaling. *Nat Immunol* 3, 251-258.
- Seewald,M.J., Korner,C., Wittinghofer,A., and Vetter,I.R. (2002). RanGAP mediates GTP hydrolysis without an arginine finger. *Nature* 415, 662-666.
- Seewald,M.J., Kraemer,A., Farkasovsky,M., Korner,C., Wittinghofer,A., and Vetter,I.R. (2003). Biochemical characterization of the Ran-RanBP1-RanGAP system: are RanBP proteins and the acidic tail of RanGAP required for the Ran-RanGAP GTPase reaction? *Mol Cell Biol.* 23, 8124-8136.
- Shindyalov,I.N. and Bourne,P.E. (1998). Protein structure alignment by incremental combinatorial extension (CE) of the optimal path. *Protein Eng* 11, 739-747.
- Shirouzu,M., Morinaka,K., Koyama,S., Hu,C.D., Hori-Tamura,N., Okada,T., Kariya,K., Kataoka,T., Kikuchi,A., and Yokoyama,S. (1998). Interactions of the amino acid residue at position 31 of the c-Ha-Ras protein with Raf-1 and RalGDS. *J Biol. Chem.* 273, 7737-7742.
- Singh,L., Gao,Q., Kumar,A., Gotoh,T., Wazer,D.E., Band,H., Feig,L.A., and Band,V. (2003). The high-risk human papillomavirus type 16 E6 counters the GAP function of E6TP1 toward small Rap G proteins. *J Virol.* 77, 1614-1620.
- Sonenberg,N. and Dever,T.E. (2003). Eukaryotic translation initiation factors and regulators. *Curr. Opin. Struct. Biol.* 13, 56-63.
- Spang,A. (2002). ARF1 regulatory factors and COPI vesicle formation. *Curr. Opin. Cell Biol.* 14, 423-427.
- Sprang,S.R. (1997). G protein mechanisms: insights from structural analysis. *Annu. Rev. Biochem.* 66, 639-678.
- Stebbins,C.E. and Galan,J.E. (2000). Modulation of host signaling by a bacterial mimic: structure of the Salmonella effector SptP bound to Rac1. *Mol Cell* 6, 1449-1460.
- Su,L., Hattori,M., Moriyama,M., Murata,N., Harazaki,M., Kaibuchi,K., and Minato,N. (2003). AF-6 controls integrin-mediated cell adhesion by regulating Rap1 activation through the specific recruitment of Rap1GTP and SPA-1. *J Biol. Chem.* 278, 15232-15238.
- Takai,Y., Sasaki,T., and Matozaki,T. (2001). Small GTP-binding proteins. *Physiol Rev.* 81, 153-208.
- Tee,A.R., Fingar,D.C., Manning,B.D., Kwiatkowski,D.J., Cantley,L.C., and Blenis,J. (2002). Tuberous sclerosis complex-1 and -2 gene products function together to inhibit mammalian target of rapamycin (mTOR)-mediated downstream signaling. *Proc. Natl. Acad. Sci. U. S. A* 99, 13571-13576.
- Tee,A.R., Manning,B.D., Roux,P.P., Cantley,L.C., and Blenis,J. (2003). Tuberous sclerosis complex gene products, Tuberin and Hamartin, control mTOR signaling by acting as a GTPase-activating protein complex toward Rheb. *Curr. Biol.* 13, 1259-1268.

- Tesmer, J.J., Berman, D.M., Gilman, A.G., and Sprang, S.R. (1997). Structure of RGS4 bound to AlF₄--activated G(i alpha1): stabilization of the transition state for GTP hydrolysis. *Cell* 89, 251-261.
- Thompson, J.D., Higgins, D.G., and Gibson, T.J. (1994). CLUSTAL W: improving the sensitivity of progressive multiple sequence alignment through sequence weighting, position-specific gap penalties and weight matrix choice. *Nucleic Acids Res.* 22, 4673-4680.
- Tochio, H., Mok, Y.K., Zhang, Q., Kan, H.M., Bredt, D.S., and Zhang, M. (2000). Formation of nNOS/PSD-95 PDZ dimer requires a preformed beta-finger structure from the nNOS PDZ domain. *J Mol Biol.* 303, 359-370.
- Tochio, H., Zhang, Q., Mandal, P., Li, M., and Zhang, M. (1999). Solution structure of the extended neuronal nitric oxide synthase PDZ domain complexed with an associated peptide. *Nat Struct. Biol.* 6, 417-421.
- Trahey, M. and McCormick, F. (1987). A cytoplasmic protein stimulates normal N-ras p21 GTPase, but does not affect oncogenic mutants. *Science* 238, 542-545.
- Tsygankova, O.M., Feshchenko, E., Klein, P.S., and Meinkoth, J.L. (2004). Thyroid-stimulating Hormone/cAMP and Glycogen Synthase Kinase 3 β elicit Opposing Effects on Rap1GAP Stability. *J Biol. Chem.* 279, 5501-5507.
- Tuberous Sclerosis Consortium (1993). Identification and characterization of the tuberous sclerosis gene on chromosome 16. The European Chromosome 16 Tuberous Sclerosis Consortium. *Cell* 75, 1305-1315.
- Tucker, J., Sczakiel, G., Feuerstein, J., John, J., Goody, R.S., and Wittinghofer, A. (1986). Expression of p21 proteins in *Escherichia coli* and stereochemistry of the nucleotide-binding site. *EMBO J* 5, 1351-1358.
- Urrutia, R., Henley, J.R., Cook, T., and McNiven, M.A. (1997). The dynamins: redundant or distinct functions for an expanding family of related GTPases? *Proc. Natl. Acad. Sci. U. S. A* 94, 377-384.
- Uthaiyah, R.C., Praefcke, G.J., Howard, J.C., and Herrmann, C. (2003). IIGP1, an interferon-gamma-inducible 47-kDa GTPase of the mouse, showing cooperative enzymatic activity and GTP-dependent multimerization. *J Biol. Chem.* 278, 29336-29343.
- Van Duyne, G.D., Standaert, R.F., Karplus, P.A., Schreiber, S.L., and Clardy, J. (1993). Atomic structures of the human immunophilin FKBP-12 complexes with FK506 and rapamycin. *J Mol Biol.* 229, 105-124.
- van Slegtenhorst, M., Nellist, M., Nagelkerken, B., Cheadle, J., Snell, R., van den, O.A., Reuser, A., Sampson, J., Halley, D., and van der, S.P. (1998). Interaction between hamartin and tuberlin, the TSC1 and TSC2 gene products. *Hum. Mol Genet.* 7, 1053-1057.
- Vetter, I.R., Linnemann, T., Wohlgemuth, S., Geyer, M., Kalbitzer, H.R., Herrmann, C., and Wittinghofer, A. (1999). Structural and biochemical analysis of Ras-effector signaling via RaIGDS. *FEBS Lett.* 451, 175-180.
- Vetter, I.R. and Wittinghofer, A. (1999). Nucleoside triphosphate-binding proteins: different scaffolds to achieve phosphoryl transfer. *Q. Rev. Biophys.* 32, 1-56.
- Vetter, I.R. and Wittinghofer, A. (2001). The guanine nucleotide-binding switch in three dimensions. *Science* 294, 1299-1304.

- Vogele, L., Palm, G.J., Mesters, J.R., and Hilgenfeld, R. (2001). Conformational change of elongation factor Tu (EF-Tu) induced by antibiotic binding. Crystal structure of the complex between EF-Tu.GDP and aurodox. *J Biol. Chem.* 276, 17149-17155.
- Vossler, M.R., Yao, H., York, R.D., Pan, M.G., Rim, C.S., and Stork, P.J. (1997). cAMP activates MAP kinase and Elk-1 through a B-Raf- and Rap1-dependent pathway. *Cell* 89, 73-82.
- Wallace, A.C., Laskowski, R.A., and Thornton, J.M. (1995). LIGPLOT: a program to generate schematic diagrams of protein-ligand interactions. *Protein Eng* 8, 127-134.
- Weiss, A. and Littman, D.R. (1994). Signal transduction by lymphocyte antigen receptors. *Cell* 76, 263-274.
- Wienecke, R., Konig, A., and DeClue, J.E. (1995). Identification of tuberin, the tuberous sclerosis-2 product. Tuberin possesses specific Rap1GAP activity. *J Biol. Chem.* 270, 16409-16414.
- Winn, M.D., Murshudov, G.N., and Papiz, M.Z. (2003). Macromolecular TLS refinement in REFMAC at moderate resolutions. *Methods Enzymol.* 374, 300-321.
- Wittinghofer, A. and Waldmann, H. (2000). Ras - A molecular switch involved in tumor formation [Review]. *Angewandte Chemie-International Edition* 39, 4193-4214.
- Wurtele, M., Wolf, E., Pederson, K.J., Buchwald, G., Ahmadian, M.R., Barbieri, J.T., and Wittinghofer, A. (2001). How the *Pseudomonas aeruginosa* ExoS toxin downregulates Rac. *Nat Struct. Biol.* 8, 23-26.
- Xiao, G.H., Shoarinejad, F., Jin, F., Golemis, E.A., and Yeung, R.S. (1997). The tuberous sclerosis 2 gene product, tuberin, functions as a Rab5 GTPase activating protein (GAP) in modulating endocytosis. *J Biol. Chem.* 272, 6097-6100.
- Xu, X., Wang, Y., Barry, D.C., Chanock, S.J., and Bokoch, G.M. (1997). Guanine nucleotide binding properties of Rac2 mutant proteins and analysis of the responsiveness to guanine nucleotide dissociation stimulator. *Biochemistry* 36, 626-632.
- York, R.D., Yao, H., Dillon, T., Ellig, C.L., Eckert, S.P., McCleskey, E.W., and Stork, P.J. (1998). Rap1 mediates sustained MAP kinase activation induced by nerve growth factor. *Nature* 392, 622-626.
- Yoshihisa, T., Barlowe, C., and Schekman, R. (1993). Requirement for a GTPase-activating protein in vesicle budding from the endoplasmic reticulum. *Science* 259, 1466-1468.
- Zeidler, W., Egle, C., Ribeiro, S., Wagner, A., Katunin, V., Kreutzer, R., Rodnina, M., Wintermeyer, W., and Sprinzl, M. (1995). Site-directed mutagenesis of *Thermus thermophilus* elongation factor Tu. Replacement of His85, Asp81 and Arg300. *Eur. J Biochem.* 229, 596-604.
- Zhang, M. and Wang, W. (2003). Organization of signaling complexes by PDZ-domain scaffold proteins. *Acc. Chem. Res.* 36, 530-538.
- Zhang, Y., Gao, X., Saucedo, L.J., Ru, B., Edgar, B.A., and Pan, D. (2003). Rheb is a direct target of the tuberous sclerosis tumour suppressor proteins. *Nat Cell Biol.* 5, 578-581.
- Zwartkruis, F.J., Wolthuis, R.M., Nabben, N.M., Franke, B., and Bos, J.L. (1998). Extracellular signal-regulated activation of Rap1 fails to interfere in Ras effector signalling. *EMBO J* 17, 5905-5912.

7 Appendix

7.1 Abbreviations

Å	Ångström (0.1 nm)
AU	Asymmetric unit
Da	Dalton
DNA	Deoxyribonucleic acid
DTE	1,4-dithioerythritol
EDTA	Ehtylendiamintetraacetat
E. coli	Escherichia coli
F_{calc} , F_{obs}	Structure factor amplitudes (calc: calculated, obs: observed)
GAP	GTPase Activating Protein
GDP	Guanosin diphosphate
GEF	Guanine nucleotide exchange factor
GMP	Guanosin monophosphate
GNBP	Guanine Nucleotide Binding Protein
GSH	Reduced glutathione
GST	Glutathione-S-transferase
GTP	Guanosin triphosphate
HEPES	4-(2-Hydroxyethyl)-piperazin-1-ethan-sulfonic acid
IAEDANS	(5-(((2-iodoacetyl) amino) ethyl) amino) naphthalin-1-sulfonic acid)
IPTG	Isopropyl- β -D-1-thiogalactopyranosid
kD	kilo Dalton
λ	wavelength
LRR	leucine rich repeat
MME	Mono-Methyl-Esther
MPD	2-Methyl-2,4-Pentandiol
NCS	Non-crystallographic symmetry
NMR	Nuclear magnetic resonance
OD ₆₀₀	Optical density at 600 nm
PEG	Polyethylene glykol
PMSF	Phenylmethylsulfonylfluoride
RBD	Ras binding domain

rmsd	Root-mean-square deviation
SAD	Single wavelength with anomalous dispersion
SDS-PAGE	Sodium dodecyl sulfate polyacrylamide gel electrophoresis
SIMBI	signal recognition particle, MinD and BioD
SeMet	Seleno-L-Methionine
SIRAS	Single isomorphous replacement with anomalous scattering
TCA	Trichloric acid
TLS	translation, libration, screw-rotation displacement
TRIS	Tris-(hydroxymethyl)-aminomethane
TRAFAC	Translation factor related

For amino acids, the one and three letter code was used

A	Ala	alanine	I	Ile	isoleucine	R	Arg	arginine
C	Cys	cysteine	K	Lys	lysine	S	Ser	serine
D	Asp	aspartate	L	Leu	leucine	T	Thr	threonine
E	Glu	glutamate	M	Met	methionine	V	Val	valine
F	Phe	phenylalanine	N	Asn	asparagine	W	Trp	tryptophane
G	Gly	glycine	P	Pro	proline	Y	Tyr	tyrosine
H	His	histidine	Q	Gln	glutamine	x		any amino acid

7.2 Deduction of equations

7.2.1 Determination of k_{on} and k_{off} via k_{obs}

The interaction of two proteins A and B in dynamic equilibrium is described in Figure 48.

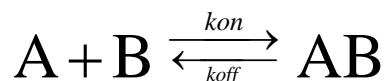


Figure 48. Two interacting proteins A and B in dynamic equilibrium.

The differential change in concentration [AB] is described by Equation 11.

$$\frac{d[AB]}{dt} = k_{on} \cdot [A] \cdot [B] - k_{off} \cdot [AB] \quad \text{Equation 11}$$

Concentration [A] is described by $[A_0] - [AB]$. If $[B_0] \gg [A_0]$, [B] is ~ equal to $[B_0]$ (pseudo first order kinetics). Substituting these values in Equation 11 leads to Equation 12.

$$\frac{d[AB]}{dt} = k_{on} \cdot ([A_0] - [AB]) \cdot [B_0] - k_{off} \cdot [AB] = k_{on} [A_0] \cdot [B_0] - [AB] \cdot (k_{on} \cdot [B_0] + k_{off})$$

Equation 12

or

$$\frac{d[AB]}{dt} + (k_{on} \cdot [B_0] + k_{off}) \cdot [AB] = k_{on} \cdot [A_0] \cdot [B_0] \quad \text{Equation 13}$$

To solve the inhomogeneous differential Equation 13, the associated homogeneous differential Equation 14 has to be solved first.

$$\frac{d[AB]}{dt} + (k_{on} \cdot [B_0] + k_{off}) \cdot [AB] = 0 \quad \text{Equation 14}$$

Rearranging variables in Equation 14 leads to Equation 15.

$$\frac{d[AB]}{[AB]} = -(k_{on} \cdot [B_0] + k_{off}) dt \quad \text{Equation 15}$$

Integration of Equation 15 leads to Equation 16.

$$\ln[AB] = -(k_{on} \cdot [B_0] + k_{off}) \cdot t + \alpha \quad \text{Equation 16}$$

or

$$[AB] = e^{-(k_{on} \cdot [B_0] + k_{off}) \cdot t + \alpha} = e^{-(k_{on} \cdot [B_0] + k_{off}) \cdot t} \cdot e^{\alpha} = \beta \cdot e^{-(k_{on} \cdot [B_0] + k_{off}) \cdot t}$$

$$\text{Equation 17}$$

in which $\beta = e^{\alpha}$.

Equation 17 is one solution of Equation 14. To make it also the solution for Equation 13, [AB] in Equation 13 has to be replaced by Equation 18.

$$\frac{d}{dt} \beta \cdot e^{-(k_{on} \cdot [B_0] + k_{off}) \cdot t} + (k_{on} \cdot [B_0] + k_{off}) \cdot \beta \cdot e^{-(k_{on} \cdot [B_0] + k_{off}) \cdot t} = k_{off} \cdot [A_0] \cdot [B_0] \quad \text{Equation 18}$$

With $\omega = k_{on} \cdot [B_0] + k_{off}$, Equation 18 can be simplified to Equation 19.

$$\frac{d}{dt} \beta \cdot e^{-\omega t} = k_{off} \cdot [A_0] \cdot [B_0] - \omega \cdot \beta \cdot e^{-\omega t} \quad \text{Equation 19}$$

$$\frac{d\beta}{dt} e^{-\omega t} + \beta \cdot (-\omega) e^{-\omega t} = k_{off} \cdot [A_0] \cdot [B_0] - \omega \cdot \beta \cdot e^{-\omega t} \quad \text{Equation 20}$$

$$\frac{d\beta}{dt} e^{-\omega t} = k_{off} \cdot [A_0] \cdot [B_0] \quad \text{Equation 21}$$

$$d\beta = k_{off} \cdot [A_0] \cdot [B_0] \cdot e^{+\omega t} dt \quad \text{Equation 22}$$

Integration of Equation 22 leads to Equation 23.

$$\beta = \frac{1}{\omega} \cdot k_{off} \cdot [A_0] \cdot [B_0] \cdot e^{+\omega t} + c \quad \text{Equation 23}$$

Equation 23 can be substituted in Equation 17.

$$[AB] = \left(\frac{1}{\omega} \cdot k_{off} \cdot [A_0] \cdot [B_0] \cdot e^{+\omega t} + c \right) \cdot e^{-\omega t}$$

$$[AB] = \frac{k_{off} \cdot [A_0] \cdot [B_0]}{\omega} + c \cdot e^{-\omega t} \quad \text{Equation 24}$$

c can be determined from the starting conditions ($t=0$, $[AB]=0$)

$$0 = \frac{k_{off} \cdot [A_0] \cdot [B_0]}{\varpi} + c \quad \text{Equation 25}$$

c from Equation 25 can be substituted in Equation 24.

$$[AB] = \frac{k_{off} \cdot [A_0] \cdot [B_0]}{\varpi} - \frac{k_{off} \cdot [A_0] \cdot [B_0]}{\varpi} \cdot e^{-\varpi t} = \frac{k_{off} \cdot [A_0] \cdot [B_0]}{\varpi} \cdot (1 - e^{-\varpi t}) \quad \text{Equation 26}$$

This expression for $[AB]$ can be used to express $[A]$ as

$$[A] = [A_0] - [AB] = [A_0] - \frac{k_{off} \cdot [A_0] \cdot [B_0]}{\varpi} \cdot (1 - e^{-\varpi t}) \quad \text{Equation 27}$$

If only species AB and A are fluorescent, the observed fluorescence Γ can be described as in Equation 28.

$$\Gamma = \lambda \cdot [A] + \nu \cdot [AB] = \lambda \cdot [A_0] + (\nu - \lambda) \cdot \frac{k_{off} \cdot B_0 \cdot A_0}{\varpi} - (\nu - \lambda) \cdot \frac{k_{off} \cdot B_0 \cdot A_0}{\varpi} \cdot e^{-\varpi t} = X - Y \cdot e^{-\varpi t}$$

Equation 28

in which λ is the fluorescence coefficient of species A and ν is the fluorescence coefficient of species AB. Thus,

$$k_{obs} = \varpi = k_{on} \cdot [B_0] + k_{off} \quad \text{Equation 29}$$

7.2.2 Fluorescence titration

In equilibrium as described in Figure 48, K_D can be described as

$$K_D = \frac{k_{off}}{k_{on}} = \frac{[A] \cdot [B]}{[AB]} \quad \text{Equation 30}$$

Substituting $[A]$ with $([A_0] - [AB])$ and $[B]$ with $([B_0] - [AB])$ and rearranging variables leads to Equation 31.

$$[A \cdot B]^2 - ([A_0] + [B_0] + K_D) \cdot [A \cdot B] + [A_0] \cdot [B_0] = 0 \quad \text{Equation 31}$$

The meaningful solution of Equation 31 is Equation 32.

$$[AB] = \frac{[A_0] + [B_0] + K_D}{2} - \sqrt{\left(\frac{[A_0] + [B_0] + K_D}{2}\right)^2 - [A_0] \cdot [B_0]} \quad \text{Equation 32}$$

The observed fluorescence Γ can be described as in Equation 33.

$$\Gamma = \lambda \cdot [A] + \nu \cdot [AB] = \lambda \cdot ([A_0] - [AB]) + \nu \cdot [AB] = \lambda \cdot [A_0] + [\nu - \lambda] \cdot [AB]$$

Equation 33

in which λ is the fluorescent coefficient of species A and ν the fluorescent coefficient of species AB.

If the fluorescence of species A is smaller than the fluorescence of species AB, then $\lambda \cdot [A_0]$ is equal to the minimum fluorescence Γ_{\min} and $\nu \cdot [A_0]$ is equal to the maximum fluorescence Γ_{\max} . Substituting $[AB]$ from Equation 32 and factoring out $[A_0]$ leads to Equation 34.

$$\Gamma = \Gamma_{\min} + (\Gamma_{\max} - \Gamma_{\min}) \cdot \frac{\frac{[A_0] + [B_0] + K_D}{2} - \sqrt{\left(\frac{[A_0] + [B_0] + K_D}{2}\right)^2 - [A_0] \cdot [B_0]}}{A_0}$$

Equation 34

This formula can be non-linearly fitted to obtain Γ_{\min} , Γ_{\max} and K_D .

8 Zusammenfassung

Rap1GAP ist das Gründungsmitglied einer Familie GTPase-aktivierender Proteine (GAPs) für das kleine Guaninnukleotid-bindende Proteinen (GNBP) Rap1. Diese Familie besitzt keine Sequenzgemeinsamkeit zu GAPs anderer GNBNPs. Im Gegensatz zu fast allen anderen kleinen GNBNPs hat Rap1 keinen katalytischen Glutaminrest, der sonst essentiell für die intrinsische und GAP vermittelte GTP-Hydrolyse ist. In dieser Arbeit wurde die Struktur und der Reaktionsmechanismus von Rap1GAP untersucht.

Die meisten GAPs stellen dem GNBP ein katalytisches Arginin zur Verfügung. In Rap1GAP konnte jedoch durch Mutationsanalyse kein katalytischer Argininrest identifiziert werden. Daraufhin wurde die Struktur eines katalytischen Fragments von Rap1GAP durch Röntgenstrukturanalyse bis zu einer maximalen Auflösung von 2,9 Å aufgeklärt. Das Phasenproblem wurde durch Selenomethionin-substituierte Kristalle und ein SIRAS-Phasierungsprotokoll gelöst. Ein molekulares Modell wurde erstellt und bis zu einem R_{crist} -Wert von 23,4% und einem R_{free} -Wert von 27,5% verfeinert.

In vorangegangenen Gelfiltrations-Experimenten wurde Dimerisierung von Rap1GAP beobachtet, und zwei Rap1GAP-Dimere befanden sich in der asymmetrischen Einheit des Kristalls. Ein Rap1GAP-Molekül ist aus zwei Domänen aufgebaut, die Dimerisierungs- und katalytische Domäne genannt wurden. Sie bestehen jeweils aus einem zentralen β -Faltblatt mit umgebenden α -Helices. Die katalytische Domäne zeigt überraschend strukturelle Ähnlichkeit zur G-Domäne der kleinen GNBNPs. Dies deutet auf einen gemeinsamen evolutionären Ursprung von Rap1GAP und den GNBNPs hin. Zu GAPs anderer Familien konnte keine strukturelle Ähnlichkeit entdeckt werden.

Durch Mutationsanalysen wurde gezeigt, dass die Dimerisierung von Rap1GAP für die Katalyse nicht erforderlich ist, aber beide Domänen benötigt werden. Eine Helix in der katalytischen Domäne, deren Sequenz in der Rap1GAP-Familie hochkonserviert ist, wurde als Interaktionshelix für Rap1 identifiziert. Mutationen in dieser Helix und in ihrer unmittelbaren Nähe führen zu starkem GAP-Aktivitätsverlust.

Mit Hilfe einer fluoreszenzbasierten Nachweisreaktion konnte eindeutig gezeigt werden, dass Rap1GAP ein katalytisches Asparagin aus der Interaktionshelix für die Katalyse bereitstellt. Eine Mutation dieses Restes zu Alanin inaktiviert Rap1GAP,

ohne die Bindung von Rap1•GTP zu beeinflussen. Im Gegensatz zum Wildtyp-Protein kann die Asparagin-Mutante nicht mit einem Übergangszustands-Analogen der Rap1-GTP-Hydrolyse assoziieren. Dies ist das erste Beispiel eines GAPs, das ein katalytisches Asparagin zur Katalyse bereitstellt. Mit Hilfe dieses Befundes und weiterer Mutationsanalysen wurde ein Interaktionsmodell für Rap1GAP mit Rap1 erstellt.

Diese Ergebnisse dieser Arbeit sind für die Krankheit Tuberöse Sklerose relevant, die durch inaktivierende Punkt-Mutationen im Rap1GAP-Homologen Tuberin ausgelöst werden kann. Die Ursachen des Funktionsverlusts können durch die strukturellen und biochemischen Befunde dieser Arbeit besser verstanden werden.

Danksagung

Ich möchte mich zunächst herzlich bei Professor A. Wittinghofer für die Unterstützung in den letzten drei Jahren, das spannende Thema und viele Dinge, die ich von ihm gelernt habe, bedanken.

Bei Professor H.W. Klein und Professor J. Howard möchte ich mich für die Übernahme des Gutachtens und für viele Diskussionen in den letzten Jahren bedanken, ich werde auch in Zukunft noch mit dem größten Vergnügen das eine oder andere Mal in Köln vorbeischaun.

Dr. M. Weyand gilt mein grosser Dank. Ohne seinen Enthusiasmus, seine Begeisterung, sein Wissen und seine Hilfe wäre diese Arbeit nicht in dieser Form entstanden.

Bei Dr. Ö. Yildiz muss ich mich herzlich für stunden- und tagelange Hilfe bei jeglichen Computerproblemen und viele Diskussionen bedanken.

Für seine unermüdliche Diskussionsbereitschaft, unzählige Computertipps und viele Dinge mehr möchte ich mich bei Dr. R. Gail bedanken.

Herzlichen Dank an D. Kühlmann für zahlreiche Tipps im Labor und für ihre grosse Hilfe im Klonieren.

Auch bei P. Stege und Dr. R. Ahmadian möchte ich mich für ihre Hilfe sehr bedanken.

Vielen Dank an Dr. A. Krämer für den tollen Fluoreszenzassay, die Einführung in die Stopped-flow-Technik und für die vielen Proteine, die sie mir überlassen hat.

Bei P. Chakrabarti möchte ich mich für drei gemeinsame Jahre in der Rap1GAP-Forschung, zahlreiche Diskussionen und den Austausch zahlreicher Proteine bedanken.

Bei A. Scrima möchte ich mich für drei Jahre als Nachbar an der Laborbank und viele gemeinsame Stunden am Computer bedanken.

Herzlichen Dank an Dr. A. Gosh für die Hilfe beim Kristallisieren und seinen fast unermüdlichen Optimismus.

Ein besonderes Dankeschön an Dr. H. Rehmann und L. Hemsath für die Hilfe bei den Fluoreszenzmessungen, für viele Diskussionen und für die Hilfe bei der Herleitung der benutzen Formeln.

Dr. I. Vetter gilt mein Dank für ihre Hilfe in der Kristallographie und die hervorragende Wartung aller X-ray Programme.

Ein herzliches Dankeschön an Dr. I. Schlichting, Dr. W. Blankenfeldt, Dr. E. Wolf, Dr. A. Rak, Dr. A. Scheidig, Dr. L. Pylypenko und Dr. R. Fedorov für viele gesammelte Datensätze, für zahlreiche Tipps beim Kristallisieren und bei der Prozessierung der Daten.

Bei Dr. M. Seewald, Dr. J. Tränkle, Dr. A. Shimada und Dr. M. Saric möchte ich mich für zahlreiche Diskussionen, Unterstützung und eine schöne Woche im Schnee bedanken.

Herzlichen Dank an O. Rocks, A. Berndt, R. Wagner, Dr. A. Wolf, A. Henkel für drei Jahre gemeinsame Forschung.

Herzlichen Dank an R. Schebaum, U. Kudus, W. Poguntke, R. Redlingshoefer und R. Anders für drei Jahre Unterstützung.

Herzlichen Dank an L.C. Polte und M. Rossbach für ihren grossen Einsatz.

Ein Dankeschön an Dr. T. Brinkmann für das Rap1GAP-Reinigungsprotokoll.

Herzlichen Dank an alle jetzigen und ehemaligen Mitgliedern der AG Wittinghofer, AG Ahmadian, AG Kuhlmann, AG Müller, AG Wolf, AG Herrmann und die X-ray community für drei Jahre gute Diskussionen und die sehr angenehme Atmosphäre.

Herzlichen Dank an die zentralen Einheiten und die Verwaltung für die immer unkomplizierte Hilfe.

Einen ganz herzlichen Dank an alle Mitarbeiter des Boehringer Ingelheim Fonds für die tolle Unterstützung während der Entstehung dieser Arbeit.

Zuletzt möchte ich mich bei meiner Familie und A. Poikane für die Unterstützung in den letzten drei Jahren ganz herzlich bedanken.

Teilpublikationen dieser Arbeit

Brinkmann, T., Daumke, O., Herbrand, U., Kuhlmann, D., Stege, P., Ahmadian, M.R., and Wittinghofer, A. (2002). Rap-specific GTPase activating protein follows an alternative mechanism. *J. Biol. Chem.* **277**, 12525-12531.

Daumke, O., Wittinghofer, A., and Weyand, M. (2004). The purification, crystallisation and preliminary structural characterisation of human Rap1GAP. *Acta Crystallogr. D.* **60**, 752-754

Daumke, O., Weyand, M., Chakrabarti P.P., Vetter I., Wittinghofer A. (2004) The GTPase-activating protein Rap1GAP uses a catalytic asparagine. *Nature* **429**, 197-201.

Erklärung

Ich versichere, daß ich die von mir vorgelegte Dissertation selbständig angefertigt, die benutzten Quellen und Hilfsmittel vollständig angegeben und die Stellen der Arbeit - einschließlich Tabellen, Karten und Abbildungen -, die anderen Werken im Wortlaut oder dem Sinn nach entnommen sind, in jedem Einzelfall als Entlehnung kenntlich gemacht habe; daß diese Dissertation noch keiner anderen Fakultät oder Universität zur Prüfung vorgelegen hat; daß sie - abgesehen von unten angegebenen Teilpublikationen - noch nicht veröffentlicht worden ist sowie, daß ich eine solche Veröffentlichung vor Abschluß des Promotionsverfahrens nicht vornehmen werde. Die Bestimmungen dieser Promotionsordnung sind mir bekannt. Die von mir vorgelegte Dissertation ist von Professor Dr. A. Wittinghofer und Professor Dr. H.W. Klein betreut worden.

Dortmund, März 2004

Oliver Daumke

Lebenslauf

Persönliche Daten:	Oliver Daumke Baroper Bahnhofstr.11 44225 Dortmund geb. am 18.9.1974 in Freiburg im Breisgau Staatsangehörigkeit: deutsch Familienstatus: ledig
1984 – 1994	Gymnasialausbildung am Kolleg St. Sebastian Abschluss: Allgemeine Hochschulreife
1994 – 1995	Zivildienst an der Uniklinik Freiburg
1995 – 1997	Grundstudium in Biologie an der Universität Freiburg Abschluss: Vordiplom
1997 – 1998	Austauschjahr an der University of Sussex / England
1998 – 2000	Hauptstudium in Biologie an der Universität zu Köln Abschluss: Diplom
2001 – 2004	Promotionsarbeit am Max-Planck-Institut für molekulare Physiologie / Dortmund mit dem Ziel der Promotion an der Universität zu Köln